AN ENERGY METHOD FOR SEISMIC DESIGN

by

Kent Richard Estes

A Dissertation Presented to the
FACULTY OF THE GRADUATE SCHOOL
UNIVERSITY OF SOUTHERN CALIFORNIA
In Partial Fulfillment of the
Requirements for the Degree
DOCTOR OF PHILOSOPHY
(CIVIL ENGINEERING)

May 2003

Copyright 2003   Kent Richard Estes

UMI Number: 3103885

Copyright 2003 by

Estes, Kent Richard

All rights reserved.

UMI®

UMI Microform 3103885

Copyright 2003 by ProQuest Information and Learning Company.

All rights reserved. This microform edition is protected against

unauthorized copying under Title 17, United States Code.

ProQuest Information and Learning Company
300 North Zeeb Road
P.O. Box 1346
Ann Arbor, MI 48106-1346

UNIVERSITY OF SOUTHERN CALIFORNIA
THE GRADUATE SCHOOL
UNIVERSITY PARK
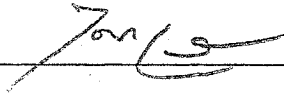#### LOS ANGELES, CALIFORNIA 90089-1695

This dissertation, written by

Kent Richard Estes
_____

under the direction of h is dissertation committee, and
approved by all its members, has been presented to and
accepted by the Director of Graduate and Professional
Programs, in partial fulfillment of the requirements for the
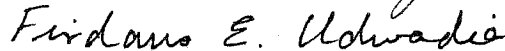*degree of*

DOCTOR OF PHILOSOPHY

_____
Director

Date **May 16, 2003**

Dissertation Committee

_____
Chair

_____

_____

_____

Dedication

To my wife, Dana, and my three boys, Matthew, Jonathan, and Daniel, who were forced to spend many hours leaving Dad alone so he could work on this dissertation.

Acknowledgements

I must express my appreciation to my principal advisor, Professor James Anderson, with whom I spent many individual hours pouring over the ideas contained in this document. Also, I would like to recognize those who participated in my Qualifying and Dissertation committee: Professors Vincent Lee, Geoffrey Martin, Firdaus Udwadia and Carter Wellford. Their support and encouragement were definitely felt and appreciated.

iii

Table of Contents

iv

List of Tables

List of Figures

viii

x

Abstract

This study presents a design methodology for multistory steel moment framed buildings for the effects of earthquakes that is energy based. After past work in the area is discussed, fundamentals of plastic analysis are presented. The central thesis of the proposed method is to establish energy demands and size members in steel moment frames, limiting plastic rotations to specified levels. An initial example of a two story building is presented. The broader case study buildings used in this effort are three story, nine story and twenty story steel structures designed as part of the SAC Steel Program. Nonlinear dynamic time history analyses are conducted for an ensemble of earthquake ground motions that are representative of earthquakes having a 10% probability of exceedance in 50 years and those for so-called Near Fault records. The distribution of hysteretic energy over the heights of each building is presented. The energy design procedure is demonstrated for the three case study buildings and verified by nonlinear time history analyses. Finally, the hysteretic energy obtained from the multistory analyses is also compared with the results from an equivalent generalized single degree of freedom analysis for each building type to demonstrate its applicability.

xi

Chapter 1: Introduction

The current state of building design for earthquake loads is in a state of flux and change. The 1997 Uniform Building Code (ICBO 1997) and subsequently the 2000 International Building Code (IBC 2000) have come out in recent years and have changed the method of calculating code mandated earthquake forces dramatically. Dynamic analysis is more common and even non-linear "pushover" analyses are increasing in usage. "Performance based design" is a phrase widely used today which, in a good sense, seeks to bring some uniformity and standardization to the development of earthquake ground motion input and design of building frames. However, none of these consider explicitly such important elements as duration and input energy. Building codes do try to consider energy dissipation in general terms and many detailing requirements attempt to mandate ductile details with the intention of preventing collapse mechanisms. It seems that the quantity most often focused on in building codes remains the peak ground acceleration. Complying with a single parameter, such as peak acceleration, can satisfy that single parameter, but may not provide for a prudent or safe design. In the words of Uang and Bertero, "It looks as if any attempt to base seismic design of structures on a design earthquake developed by only one engineering parameter is doomed to fail" (Uang and Bertero 1988). Probably the single most ignored quantity in earthquake design today is the issue of duration, which relates directly to input

1

energy. The aim of this present work is to examine the role of energy in seismic design and establish a design method incorporating energy concepts.

The organization of this dissertation is as follows: After a discussion of past literature on seismic energy and a review of energy terms, plastic analysis of frames is discussed with a suggested method to explicitly incorporate energy into the design process. A simple example for a two story building frame is discussed. Three, nine, and twenty story prototype building frames are then analyzed for a suite of ground motions. A design procedure is then presented discussing each frame type with confirming nonlinear computer analyses. Supporting data and discussions of important design considerations are presented at each stage, ending with conclusions and recommendations.

2

Chapter 2: Literature and Historical Background

In the past, there have been remarkably few published works in the area of energy based seismic design. Two very early papers that were truly prophetic relative to the subject of earthquake energy are "The Physical Evaluation of Seismic Destructiveness" by Hugo Benioff (Benioff 1934) and "A Mechanical Analyzer for the Prediction of Earthquake Stresses" by M. A. Biot (Biot 1940). Benioff was apparently one of the first to publish a concept that links the area under a response vs. frequency curve (i.e. energy) to the destructiveness of earthquakes. Biot's paper describes the mechanical process of developing such curves or spectra. Biot makes some far reaching statements, well ahead of his time, about the use of these curves, the presence of soft first stories and the lengthening of the period of a building that are considered in base-isolated buildings today. However, probably the foundational paper in this area of energy-based design is "Limit Design of Structures to Resist Earthquakes" by George Housner (Housner 1956). In it Housner describes the fundamental methodology that has been used in seismic design for the past 40+ years. To quote from the abstract, "Structures having small amounts of damping may develop stresses, when subjected to strong earthquake ground motion, that correspond to relatively large lateral loads, 50%g to 100%g having been observed. If plastic deformations are accepted, a safe design much less strong than required for 50%g can be made. The proposed method of limit-design is based on energy input into a structure by recorded strong ground motions." In these simple statements, Housner has set the standard that buildings are still designed for up to this day.

3

Simply put, it is not considered viable to design buildings to resist the maximum possible earthquakes elastically. This is judged to be economically and politically too extreme. It is a matter of the amount of risk that society is willing to accept as initial costs versus future damage. If building structures can be allowed to enter into the plastic range, while preserving life safety and preventing collapse, the construction cost will be reduced. This philosophy has been the basis of the Structural Engineers Association of California (SEAOC) Blue Book (SEAOC 1999) over many years that has been, in turn, the basis for the seismic provisions for the Uniform Building Code.

The critical question is how does one maintain elastic response for more frequent earthquakes, yet insure against catastrophic collapse for extreme earthquakes? In allowing buildings to experience plastic deformation, many other factors must be considered. Considerations such as ductility, strain hardening, strength degradation, damping, stress reversals and energy become important. As recently as 1997, George Housner has said that the energy approach described in his early paper "was clearly an appropriate direction in which to go, because the energy dissipated by inelastic deformation is the key item in preventing a structure from failing. People have tried to follow up on energy design, but it has not yet gotten into the code design process because of the unknown properties that many structures have. Designers now recognize the significance of inelastic deformation and energy loss, but we have not yet reached the point where energy dissipation is explicitly incorporated into the code." (EERI 1997). In a similar vein, Fajfar and Krawinkler

4

state in their preface "to this day, energy concepts have been ignored in earthquake resistant design because of apparent complexities in the quantification of energy demands and capacities and their implementation in the design process" (Fajfar and Krawinkler 1992).

Others have done some limited work in this area of energy-based design (Arya 1974, Berg and Thomaides 1960, Gluck 1974, McKeritt 1979, Muse 1960, Soni 1977). John Blume wrote on the subject in a 1960 paper (Blume 1960). George Housner even followed up his initial energy paper at the Second U.S. Conference on Earthquake Engineering (Housner 1960). It seems, however, that most are using a ductility factor concept to account for inelastic deformation. Usually displacement ductility is considered. The considerations seem to either create inelastic response spectra by means of the ductility factor or consider a ratio of yield to maximum forces through the ductility factor. In other words, energy seems to be mentioned in passing, but is not explicitly utilized.

One of the important works in the area of energy design is "Earthquake Resistant Limit-State Design for Buildings" by Hiroshi Akiyama (Akiyama 1985). It is undoubtedly the most rigorous treatment of the subject. He goes into great depth of the analysis and treatment of hysteretic damping in order to achieve estimates of energy. Two companion papers by Uang and Bertero (Uang and Bertero 1988) are also very important in this area. The first discusses the implications of recent ground motions studies and the other specifically discusses the use of energy in the area of earthquake design. There is a discussion of a shake table simulation to consider

5

multidegree of freedom systems, but again the presentation is somewhat general. A collection of papers for a workshop in nonlinear analysis of concrete buildings addresses the use of energy in design (Fajfar and Krawinkler 1992). Recent papers by Leelataviwat et al (Leelataviwat, Goel, and Stojadinovic 1999, 2002) attempt to develop a design procedure based on energy. At the more recent Seventh U.S. Conference on Earthquake Engineering (2002) several papers were presented on the subject of seismic energy. Two papers described procedures for developing energy spectra (Riddell and Garcia 2002, Chou and Uang 2002) for use in design. Although there seems to be an increase in interest regarding this subject, viable design methodologies are still waiting to be developed and thus the motivation for this present work.

6

Chapter 3: Energy Considerations in Seismic Design

In considering energy in relation to design, it is important to study each term in the equations of motion and to try and evaluate its meaning and significance to the design process. The basic equation of motion for a single degree of freedom system subjected to base excitation is well known:

$$m\ddot{x} + c\dot{x} + kx = -m\ddot{g} \qquad (3.1)$$

The means of obtaining the energy terms are, for each time step, to integrate each term with respect to x.

$$\int m\ddot{x}\,dx + \int c\dot{x}\,dx + \int kx\,dx = -\int m\ddot{g}\,dx \qquad (3.2)$$

Uang and Bertero (Uang and Bertero 1988) discuss in some detail the use of the terms "relative energy" and "absolute energy." If one uses the "absolute" displacement, the resulting energy is the "absolute energy." Conversely, if one uses the "relative" displacement, the resulting energy is the "relative energy." As Uang and Bertero explained, past researchers have been a bit remiss in using undefined terms. The displacement in the above equation produces different values of energy if it is the total absolute displacement versus the relative displacement between the floor level and the ground. The two differences are in the kinetic energy term and the input energy term, which are discussed below to be small. As will be discussed, the focus of the proposed design procedure is on the inelastic or hysteretic energy and is not affected by the above distinction.

7

The terms in the above Equation 3.2 form the basis for the energy analysis. While it is relatively straightforward to program the summation of each energy term for each time step in a numerical analysis, the summing of the terms and the generation of plots; a proper understanding of the meaning and significance of each term merits some scrutiny. The energy of an inelastic single degree of freedom system is made of five terms - the kinetic energy, the damping energy, the strain energy plus the hysteretic energy, and the input energy. Each of these terms relates to Equation 3.2 above. The kinetic energy is the energy generated by inertial forces displacing as the frame moves, the first term in the equation. The damping energy is the damping force multiplied by the displacement at each time step, the second term. The strain energy is the elastic energy stored in an elastic resistance produced in a spring ($\frac{1}{2}kx^2$). Related to the spring term is the hysteretic energy or the inelastic energy generated by a nonlinear resistance experiencing inelastic deformation. These last two are embodied in the third term on the left side of Equation 3.2. The input energy on the right side of the equation is the base shear times the ground displacement. Theoretically, the input energy is the sum of the other four terms. The four energy terms on the left side of the equation can be considered in two groups. The kinetic plus strain energy terms are termed the stored energy. The damping plus hysteretic energy terms are termed the dissipated energy. Therefore, the stored energy plus the dissipated energy equals the total input energy.

A central question is, "How does each of these energy terms enter into the design process?" Specifically, what part of these energy terms must be dissipated by

8

the building frame? Housner states "at any instant the sum of the kinetic energy plus strain energy plus energy dissipated through normal damping plus energy dissipated through permanent deformation will be equal to the total energy input" (Housner 1956). However, later Housner states that the energy resisted by the building frame must be equal to the elastic energy plus the plastic energy. Akiyama follows suit in considering only the elastic plus plastic energy (Akiyama 1985). What becomes clear is that in designing a frame to resist a given earthquake input, the inertial and damping energies are not specifically resisted by the building frame. Kinetic energy is produced by the inertial forces undergoing displacements. Damping energy is generated by elements in a building that tend to dampen out free vibration, such as office partitions, slip of connections, the exterior window wall, etc. These energies are independent of member sizes and the building frame does not dissipate nor store them. The elastic and inelastic strain energies are therefore the energies relevant to design of the building frame. Figure 3.1 shows a typical plot of energy versus time. Today several commercial software programs can generate plots such as this. One can see the distribution of plastic energy between stories of a building. In reviewing plots like this, several things are clear. One is that the kinetic and strain energies are almost negligible. Therefore, it seems entirely appropriate that these two terms are not significant in energy based design. Conversely, the two terms that contain the vast majority of the energy are the damping and hysteretic energy. Therefore, researchers from Akiyama to Goel (Akiyama 1985, Leelataviwat et al 1999) seem to agree that the central term relevant to the design process is the hysteretic energy.

9

This is the term that the building frame must be able to dissipate through inelastic deformation and should therefore be central to the design methodology.

ENERGY PLOT FOR TWO STORY BUILDING
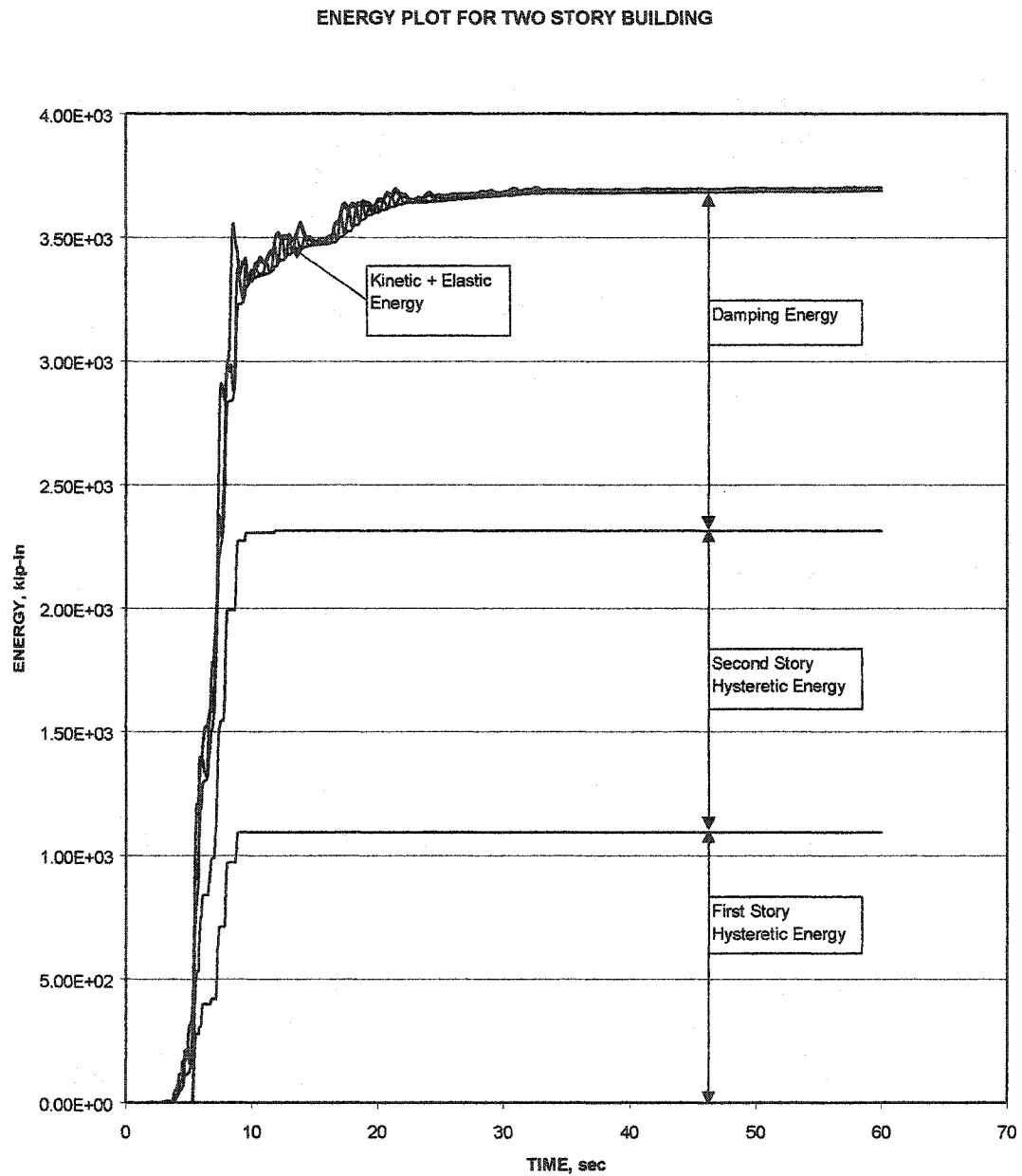
Figure 3.1 Typical Energy Plot

10

The above discussion has been focused on a single degree of freedom system. The extension to a multidegree of freedom system is fairly straightforward. The terms in the equations of motion become matrices and the energy equation becomes:

$$\int [M]\ddot{x}\,dx + \int [C]\dot{x}\,dx + \int [K]x\,dx = -\int \left(\sum [M]\ddot{g} \right) dx \qquad (3.3)$$

11

Chapter 4: Plastic Analysis and an Energy Design Method

4.1 Introduction to Plastic Analysis

Plastic analysis of frames seems to be going through a bit of a renaissance. What was once a rather isolated field of academic structural analysis has recently emerged as a very relevant tool in designing for earthquakes. It is believed that this shift parallels the shift from considering the design process in an elastic manner to considering it with a strength design orientation. The quantum shift in the 1997 Uniform Building Code was the transformation of the equivalent static loads from a "working stress" design level to an "ultimate strength" design level. Even when the code mandated static analysis was not used, elastic dynamic analyses were traditionally used. In recent years there has been a corresponding shift in the analysis tools used in engineering offices. Nonlinear static and dynamic analyses are becoming more common, especially in the analysis of existing buildings. As our engineering knowledge and codes have developed, our analysis tools have become more sophisticated. While these tools have been present in universities for many years, they are only relatively recently emerging into design practice. It seems that the analysis of existing buildings is the driving force behind these more sophisticated forms of analysis largely because of economic considerations. With each earthquake that occurs the level of design forces tends to escalate in the minds of those responsible for writing codes. Businesses with large real estate holdings or critical facilities such as fire, police or even utility providers correctly conclude that they are at risk and their buildings should be evaluated and possibly seismically upgraded.

12

To upgrade a large holding of buildings to comply with the full current code level forces can be cost prohibitive. It is, therefore, attractive to consider more site-specific geotechnical data instead of a rote application of code level forces, plus to consider the limit state of a building frame versus an elastic analysis. Likewise, commercially available programs are now available which can accommodate these more sophisticated analyses. Even more fundamentally, it is now getting clearer in the mind of the practicing engineer that building response in a major earthquake is a dynamic event and will most certainly push the building frame into the inelastic range. It is very appropriate to view the limit state of a steel frame for seismic design in light of its ultimate capacity, the formulation of hinges, and energy dissipation. The design of reinforced concrete has used a strength design approach for many years. Steel is transitioning over to strength design (or load and resistance factor design), as is masonry. Therefore, since the forces and allowable capacities of materials are being considered at a limit state, it seems appropriate that plastic analysis could become a tool for design practice.

4.2 Review of Plastic Analysis Fundamentals

As a brief review of plastic analysis methods, the limit state behavior of a simple fixed-fixed beam will first be considered. As Figure 4.1 shows, a clamped beam with a concentrated load at midspan can be analyzed by the method of virtual work. The total external work is the factored load, P_u, times the distance it travels, δ. The internal work done is the plastic moment capacities times the plastic rotations at

13
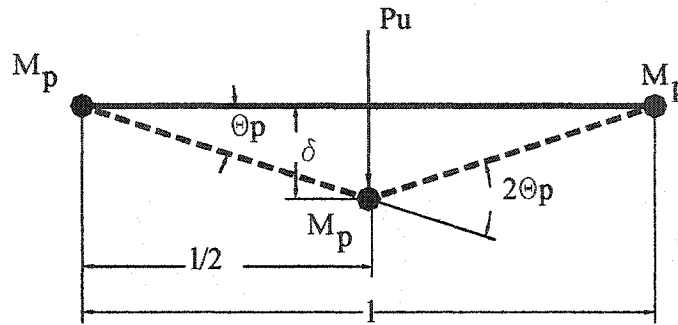
Figure 4.1 Beam Mechanism

each hinge. Since internal work equals external work,

$$P_u * \delta = M_p * \theta_p + M_p * 2\theta_p + M_p * \theta_p = 4 * M_p \theta_p \qquad (4.1)$$

And, therefore, one can solve for the required M_p,

$$M_p = P_u * \delta / 4 * \theta_p \qquad (4.2)$$

Since $\delta = l / 2 * \theta_p$ (for small θ_p),

$$M_p = P_u * l / 8 \qquad (4.3)$$

Consider a simple one story frame as shown in Figure 4.2. It is assumed for this illustration that the beam and columns have the same plastic moment capacity. A horizontal load V is assumed with no vertical loads. The external work is again $V * \Delta$, Δ being the horizontal drift in this case. For the sway mechanism shown, the internal work is $4 * M_p * \theta_p$. Therefore, again $V * \Delta = 4 * M_p \theta_p$. However, in this case, $\Delta = h * \theta_p$. Therefore,

14

$$M_p = V * h / 4 \tag{4.4}$$

It is desirable to introduce the energy demand into this process. Up to this point, for a fixed-fixed beam or a simple one story moment frame, the required plastic moment capacity of the members can be determined knowing the ultimate factored or limit load. Conversely, one could solve for the limit load knowing the plastic moment capacity of the members. In deriving these expressions, work considerations were used. The external work was equated to the external load times the distance it traveled. Also, the internal work was equal to the sum of the plastic moment capacities multiplied by the plastic rotations of the beams and columns. In a frame, it is assumed that a prudent and safe design will comply with the strong column-weak beam philosophy that attempts to restrict plastic hinging to the beams rather than the more vulnerable columns. If a column hinge appears, it is desirable that it should appear at the base as collapse is not necessarily induced. A key element of this present work is to establish a design input energy and equate that to the internal or external work capacities of the frame members. A suitable acceptance criterion could be established in order to solve for the required member sizes (Allahabadi 1987, Uang and Bertero 1988). As has been alluded to previously, this is proposed to be the hysteretic energy. For a one story frame (or single degree of freedom system), the process is greatly simplified. One can use either the external work or internal work and equate this to the energy demand. Since the goal of the design process is to establish the required member sizes, the internal work or plastic moments times plastic rotation restraints seems more appropriate.

15
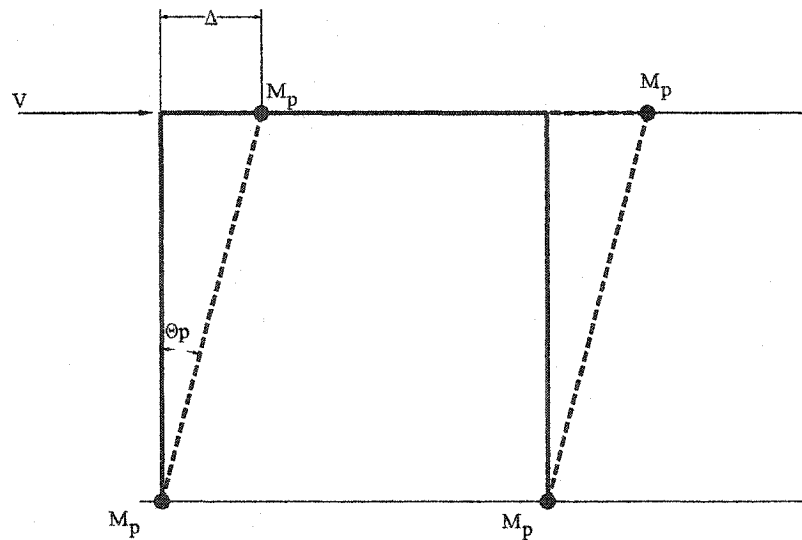
Figure 4.2 Frame Mechanism

4.3 Multistory Building – Storywise Optimization

The next logical case to consider would be a multistory building frame. The optimum design of large multistory frames becomes overly cumbersome with many collapse mechanisms possible and many constraints feasible. A safe method of piecewise design of such structures is therefore desirable and will be demonstrated after Ridha and Wright (Ridha and Wright 1967). One story at a time is considered starting with the uppermost story. The forces considered in the design of each story include the story loads, the lateral loads for the upper stories, the column axial loads from the upper columns, and moments equal to the plastic moment capacities of the column directly above the story. A short part of the column above is included to represent the existence of that column at its base joint, and to express the applied

16

(a) The Whole Frame   (a) A Story Considered Alone
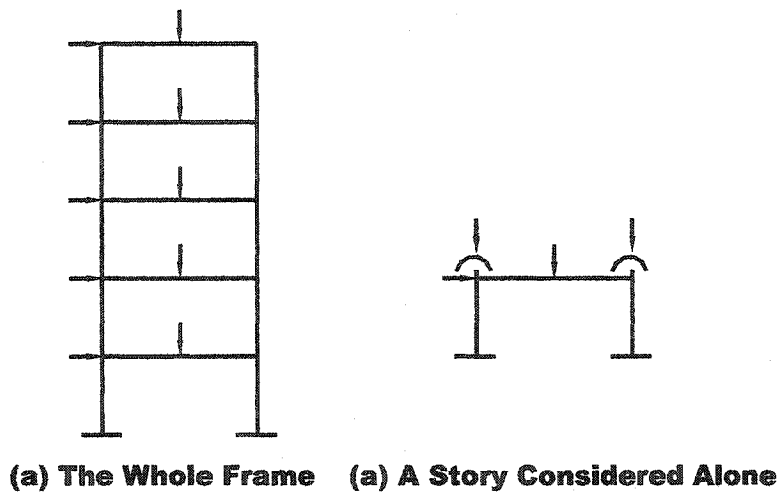
Figure 4.3 Multistory Frame and Isolated Story

moments by couples. The geometry and the loading considered for each story are shown in Figure 4.3. The basic and combined mechanisms for the single story are shown in Figure 4.4.

The safety of the resulting design is demonstrated by comparing the mechanisms in the whole frame and the similar ones for a single story, and showing that the internal work for the single story does not exceed that of the whole frame, and, likewise, that the external work for the whole frame does not exceed that of the single story.

The beam mechanisms of the considered story are shown in Figure 4.4a and Figure 4.4b for the entire frame and single story. The internal work and external work are identical for the two mechanisms.

17
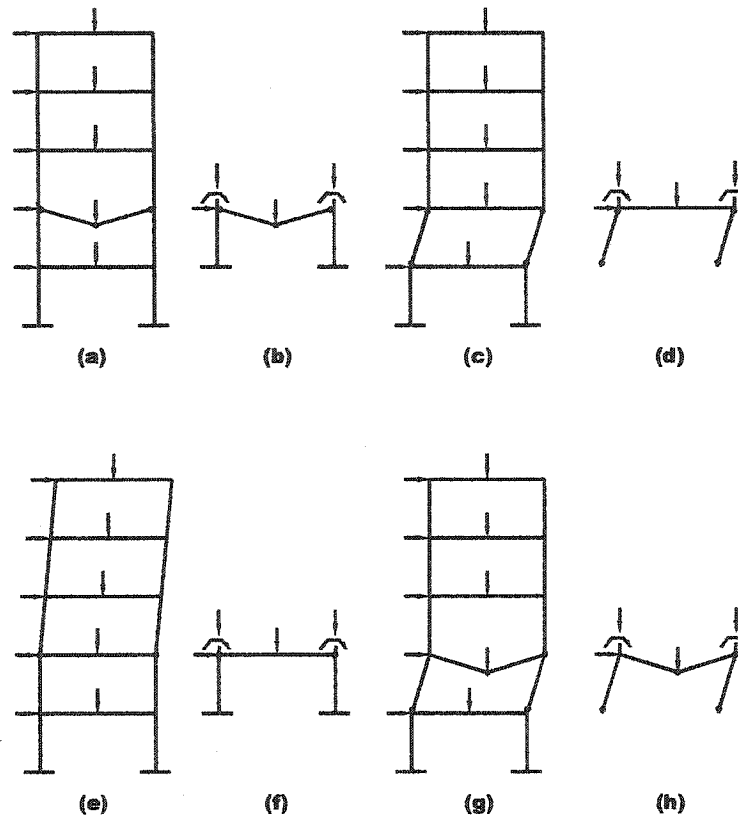
Figure 4.4 Mechanisms for Whole Frame and Single Story

The sway of the single story is shown in Figure 4.4c and 4.4d. The internal work and the external work are identical for the two mechanisms.

The sway of all the stories above the story being considered is shown in Figure 4.4e and 4.4f. It will be shown that the design is safe against failure by the mechanism shown in Figure 4.5.

1. The design of the top story, shown in Figure 4.5 satisfies

$$P_{roof} * h_1 * \theta_p = 2 * M_p (roof\ beam) * \theta_p + 2 * M_p (col2) * \theta_p \qquad (4.6)$$

18

in which $2 * M_p (roof\ beam) * \theta_p$ represents the internal work of the roof beam,

$2 * M_p (col2) * \theta_p$ represents the internal work of the columns, *col2* meaning the

second story column, *col1* later meaning the first story column. It is important to

note that a strong column-weak beam mechanism has been assumed. The term

above that contains the beam plastic moment capacity could be the plastic moment of

the top of the column.

TOP STORY
MECHANISM

LOWER STORY
MECHANISM
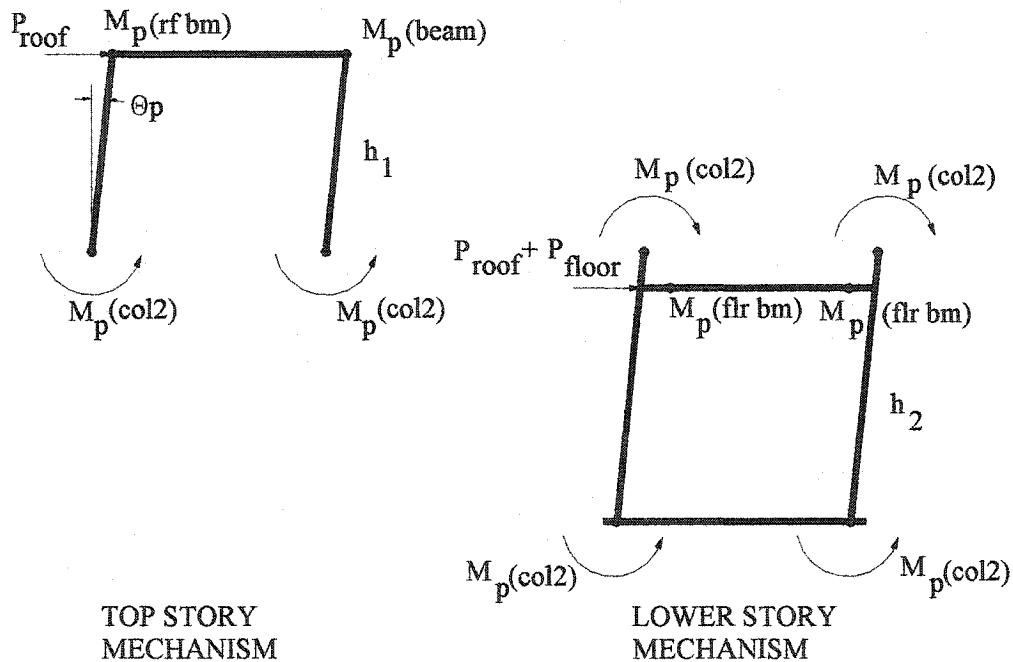
Figure 4.5 Separated Story Mechanisms

2. The design of the second story from the top, shown in Figure 4.5, satisfies

$$(P_{roof} + P_{2nd}) * h_2 * \theta_p + 2 * M_p (col2) * \theta_p = 2 * M_p (2nd\ flr\ beam) * \theta_p$$

$$+ 2 * M_p (col1) * \theta_p \qquad (4.7)$$

This equation can be rewritten as:

19

$$(P_{roof} + P_{2nd}) * h_2 * \theta_p = 2 * M_p(2nd \; flr \; beam) * \theta_p + 2 * M_p(col1) * \theta_p$$

$$-2 * M_p(col2) * \theta_p \tag{4.8}$$

3. Adding equations 4.6 and 4.8 gives

$$P_{roof} * (h_1 + h_2) * \theta_p + P_{2nd} * h_2 * \theta_p = 2 * M_p(rf \; bm) * \theta_p + 2 * M_p(2nd) * \theta_p$$

$$+ 2 * M_p(col1) * \theta_p \tag{4.9}$$

Equation 4.9 relates the internal work and the external work of the mechanism shown in Figure 4.5. Thus the frame is safe against failure by the mechanism represented by the sway of both stories.

4. By continuation of the above process it may be shown that the design resulting from the storywise optimization is safe against failure by the mechanism shown in Figure 4.4e or any mechanism involving the sway of a group of stories.

The interaction between adjacent stories is considered to provide a closer representation of the conditions in the whole frame. Two stories are considered in each step. The check for the upper story becomes that obtained from the optimum solution with the story below. However, the lower story is combined with the story below it and its design altered as the new pair of stories is optimized. The geometry and the loading for each pair are determined as in the single story optimization.

Two further considerations are important at this juncture. Figure 4.6 shows the similar mechanisms of a multistory, multispan building frame. The same logic can be followed for a multispan frame with the piecewise story optimization. Secondly, from Equation 4.9 the external work and internal work are separated on

20

each side of the equation. Either side can be equated with the story hysteretic energy

demand to solve for the plastic moment capacities. More will be discussed relative

to the optimization of the required column and beam plastic moments.
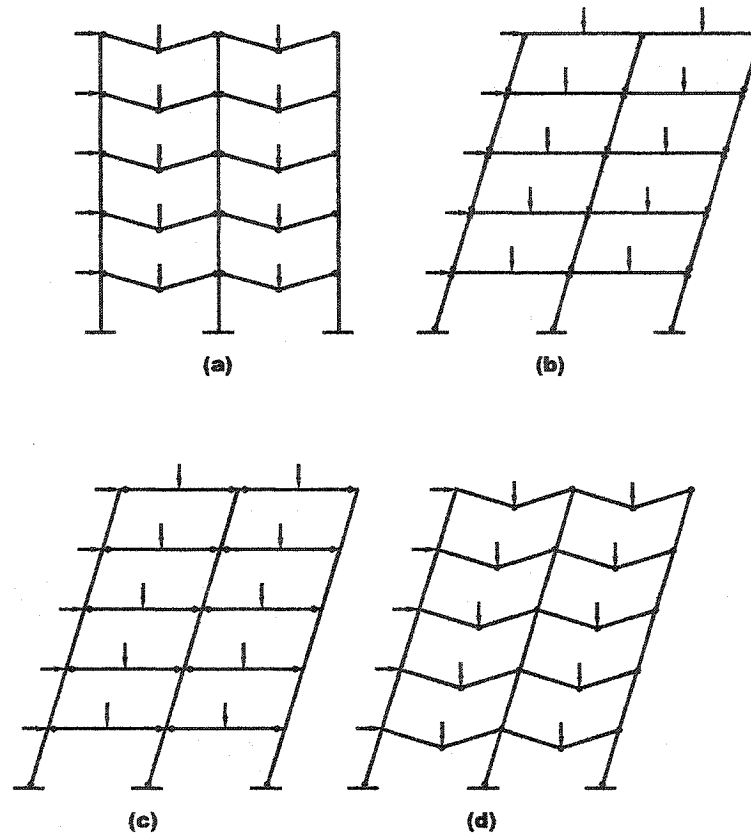
Figure 4.6 Multispan, Multistory Building Frame Mechanisms

4.4 Damping and Hysteresis

One important distinction should be made relative to internal work and

energy. The procedure for simple plastic analysis is a static, monotonic process.

The procedure that has been selected here to establish the hysteretic energy demand

21

is to perform a DRAIN2D+ inelastic time history analysis for a given earthquake record or series of records. DRAIN2D+ is an enhanced version of the DRAIN2D program. "The enhancement made in the DRAIN2D+ program includes capabilities of performing constant stiffness implicit-explicit integration, static nonlinear analysis, energy, mode shapes and periods, and structure section force computations" (Tsai and Li 1994). Contrary to even later versions of DRAIN2D, DRAIN2D+ allows the user to assign the elements into energy groups. It is believed that this is the only program currently available with this capability. This enhanced capability may be the key in quantifying the energy demands that Housner and earlier researchers have described as difficult to establish. The cumulative inelastic energy is summed at each time step. Therefore, it is possible to group the columns and beams in a building frame to obtain the story hysteretic energy. If the story energy demand can be established, the internal work for that story can be compared in order to solve for the required member sizes.

DRAIN2D+ is a two dimensional analysis program that can perform inelastic time history analysis. Since this analysis can incorporate real earthquake records and subject a given building frame to them, the energy developed is a result of random oscillatory motion which includes many load reversals. Therefore, the totality of hysteretic behavior is accounted for. On the other hand, a static plastic analysis will only include the static, monotonic energy. It became obvious in the course of this work that an adjustment needed to be made to correlate the static, monotonic energy with the full dynamic energy. This is illustrated in Figure 4.7 for a simplistic, highly

22

idealized hysteresis loop showing plastic moment capacity versus plastic rotations.
The shaded area represents the static pushover case. The initial, inclined and top
horizontal lines represent an elastic perfectly plastic bilinear representation of a static
pushover analysis. The shaded area represents the energy generated by that analysis.
However, the total enclosed area represents the total energy for a full cycle dynamic
analysis. Clearly, comparing the two energies must account for this difference and
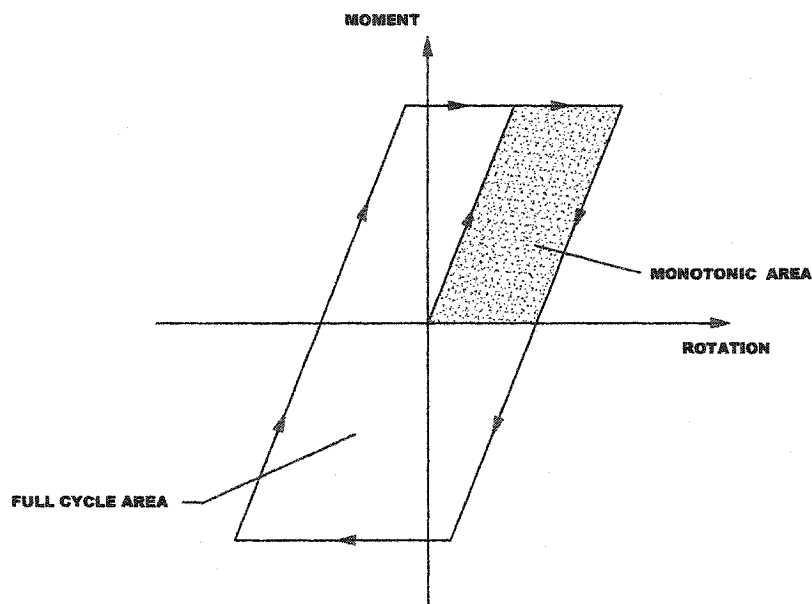
Figure 4.7 Hysteresis Loop

for the purposes of this work, a factor of 4 was taken to account for the ratio of these
areas i.e. energies. There is some disagreement in the literature regarding this factor.
One group has followed the method suggested by Newmark in relating an elastic
system to an inelastic system (Leelataviwat et al 1999). Both systems are assumed to
deflect to the same deflection and the plastic energy is equated to the equivalent
linear energy. This seems somewhat dated and simplistic. Akiyama and Kato argue

23

through examination of a typical hysteresis loop that the ratio of the monotonic to full cycle energy is two (Akiyama and Kato 1982). This seemed a bit counterintuitive. Perhaps the best discussion on this subject was found in ATC 40 for the analysis of existing concrete buildings (ATC 1996). There is an analysis of points on a typical hysteresis loop using a factor of four to relate monotonic to full cycle areas. Although the methodology in ATC 40 is used in establishing inelastic response spectra, the methodology of their argument seems the most reasonable that was encountered. Then based on the assumed ductility of the existing structure, factors to simulate the pinching of the hysteresis loops are proposed. The factors for different types of building categories fall into a typical range of .75, .67, etc. to provide an estimate of reduction in area or pinching of the hysteretic loops due to less ductile frame components. FEMA 273 contains recommendations for the analysis of existing buildings and also proposes a factor to account for pinching of hysteresis loops based on performance category and framing type (FEMA-273 1997). The thrust of this present work is ductile steel moment frames and it is concluded that the factor of four for well designed frames is appropriate. In fact, in the application of the proposed design procedure the four factor produced reasonable and consistent results that were confirmed by nonlinear dynamic analyses. Other values were analyzed and found to give inconsistent results. It is also certainly possible that in the analysis of existing buildings or other types of materials, that the ATC 40 or FEMA 273 reduction factors could be considered.

24

It should be said in passing that DRAIN-2D+ can incorporate strain hardening and 2% was used in the present analysis. No strength degradation was considered.

From the previous discussion, damping and hysteretic energy are the two key energy demand terms. Therefore, establishing the damping accurately is key to this process. DRAIN2D+ uses Rayleigh proportional damping, which is generally perceived to be the best mathematical model for representing building damping. For this method, $[C] = \alpha[M] + \beta[K]$, the damping matrix $[C]$ uses proportions of the mass $[M]$ and stiffness $[K]$ matrices. A preliminary data checking run is first made with the percent of critical damping input for two periods. The result of the first run gives the α and β factors which are then input for the full analysis. For the purposes of this analysis of very regular essentially square buildings, 5% damping was used in the first two modes to establish the α and β factors.

An excellent study of the energy dissipation of different damping models has been made by Leger and Dussault (Leger and Dussault 1992). The effects of viscous damping on seismic response are studied by varying the mathematical model selected for its representation. They considered a damping representation using mass-proportional, stiffness-proportional, or Rayleigh damping computed from either the initial elastic or the tangent inelastic system properties. Various heights of buildings were analyzed using records from the 1940 El Centro earthquake record, the 1952 Taft record and the 1962 Parkfield record. The ratio of hysteretic versus input energy was plotted by building height for various analyses. These analyses

25

held certain parameters constant while varying other parameters such as damping ratio and strain hardening to study the effect of their influence on energy dissipation. Among their conclusions are that for periods less than .5 seconds, Rayleigh damping should be used. For periods between .5 seconds and 1.5 seconds, Rayleigh proportional damping using damping factors based on initial elastic properties is recommended. The use of a tangent damping model is discussed in this range, although this model is difficult to implement and typically not used in practice. For building periods greater than 1.5 seconds, the seismic response is not affected by the type of Rayleigh damping model used. Therefore, Rayleigh proportional damping is verified to be the best model for the energy dissipation characteristics of damping and this model has been used for the present study.

From the work of SAC (a consortium of the Structural Engineers Association of California, the Applied Technology Council, and the California Universities for Research in Earthquake Engineering) and the work of many researchers on full scale test components after the Northridge earthquake, it seems that a value of .025 to .030 radians is a consensus for the maximum allowed plastic rotation (FEMA Interim Advisory No. 1 1997). In subsequent years, these figures have been modified. In FEMA 350 the drift angle is used which is the vertical deflection in a test divided by the length of the test beam piece. The drift angle is equated to the plastic rotation by subtracting .01 from the drift angle. The interstory drift angle is affected by an uncertainty factor, a variability factor, the performance level required, the type of moment frame, and confidence level desired. For example, the allowable plastic

26

rotations calculated based on FEMA 350 for the SAC three, nine, and twenty story buildings discussed later in this document are .039, .038 and .017 radians, respectively. This assumes a Collapse Prevention level of performance, a Special Moment frame, a 95% confidence level, analyzed by a nonlinear dynamic procedure. In this present work, a target plastic rotation of .030 radians has been used.

4.5 Minimum Weight Considerations

Previously it was discussed how one might consider a single story frame and perform a design check based on energy. The procedure for a one bay, one story building frame is relatively simple. It is desired to consider a multi story, multi-bay building frame. When there are several unknown variables i.e. beams, columns at the ends of the frame, columns interior to the frame; a minimum weight methodology is proposed. Minimum weight design establishes a weight function and minimizes it subject to constraint equations. The constraint equations are established according to the possible collapse mechanisms. It is assumed, and it was verified in this work, that vertical load mechanisms are not significant when considering earthquake forces. However, in the top stories of multi-story building frames, vertical load mechanisms should be checked versus the required moment capacity from the lateral analysis. It was found that beyond the top story or two, the required plastic beam moments for vertical load mechanisms are smaller than the energy based moment demands. In fact, it was found that for the frames studied in this work that were designed to the Uniform Building Code (UBC) that the vertical load demand moments never required an increase in the beam sizes. Frames

27

designed to the UBC are generally limited by drift requirements, in addition to some

practical considerations grouping columns and beams for several stories and,

consequently, vertical load mechanisms never governed for beam or column sizes.

For a typical story in a multi-story building, collapse mechanisms must be

prevented. For lateral sway mechanisms, equations can be written for each assumed

mechanism – hinges in columns, hinges in beams. These equations become the

constraint equations. Then a weight function is established based on the dimensions

of the frame members. The weight function for a given member can be assumed to

be proportional to its plastic section modulus multiplied by the length of the member.

Therefore the total weight function for a story is the sum of the plastic section

moduli times the lengths of the respective members (Foulkes 1953).

Minimizing (or maximizing) a function subject to constraints is a well known

mathematical problem. In its most general form, the function f is such that,

$$f = c_1 x_1 + \ldots\ldots c_n x_n \tag{4.10}$$

subject to the constraints,

$$a_{11} x_1 + \ldots\ldots + a_{1n} x_n = b_1$$

$$a_{21} x_1 + \ldots\ldots + a_{2n} x_n = b_2$$

$$\ldots\ldots\ldots\ldots\ldots\ldots\ldots\ldots\ldots$$

$$a_{n1} x_1 + \ldots\ldots + a_{mn} x_n = b_m \tag{4.11}$$

$$x_i \geq 0 \qquad (i = 1, \ldots\ldots, n)$$

28

In this general form, f is the objective function, x_i's are the design variables, and b_j's are the constants. For our problem, f is the weight function and the x_i's are the plastic moments required. This is a Linear Programming problem that is readily programmed into a computer. Three approaches to the solution will be demonstrated. For finding the optimal solution of this problem, Basic Feasible Solutions are the only solutions that need be considered. An n-tuple $(x_1, \ldots\ldots, x_n)$ that satisfies all the constraints is called a feasible point or feasible solution. A feasible solution is called an optimal solution if its objective function becomes a maximum, compared with all values of f at all feasible solutions. Then a basic feasible solution is one for which at least $n - m$ of the variables $x_1, \ldots\ldots, x_n$ are zero.

In 1948 G. B. Dansig published an iterative method called the Simplex Method for solving this problem in a systematic way. In this method, one proceeds stepwise from one basic feasible solution to another in such a way that the objective function f always increases in value. The method begins with an initial operation in which a basic feasible solution is found and started with. Each further step consists of three operations:

Operation O_1: Test for optimality,

Operation O_2: Location of a better feasible solution,

Operation O_3: Transition to a better solution.

The method will be demonstrated with a simple example from an earlier paper (Rubenstein and Karagozian 1966). The first step is to establish any basic feasible solution. This is done by dividing the variables $x_1, \ldots\ldots, x_n$ into two classes

29

by selecting m variables as basic variables, and the other $n - m$ variables are those which must be zero at a basic feasible solution; these are called nonbasic variables. For the example problem, a one story frame is considered. The weight function is

$$f = 20M_b + 16M_c,$$ (4.12)

M_b being the required plastic moment capacity of the beam and M_c being the plastic moment capacity of the columns. From the Rubinstein paper, there are four constraint equations,

$$M_c \geq 6 \text{ k-ft}$$

$$M_b \geq 2.5 \text{ k-ft}$$

$$2M_b + M_c \geq 17$$

$$M_b + M_c \geq 12$$ (4.13)

Introduce variables x_3 and x_4 (sometimes called slack variables) into the bottom two equations listed above and consider them as basic variables. Make plastic moment quantities, M_b and M_c, the nonbasic variables. Therefore,

$$2M_b + M_c + x_3 = 17$$

$$M_b + M_c + x_4 = 12$$ (4.14)

Solve for x_3 and x_4,

$$x_3 = 17 - 2M_b - M_c$$

$$x_4 = 12 - M_b - M_c$$ (4.15)

In favorable cases such as these, values of the variables of a basic feasible solution are obtained by setting the variables on the right side of the above equations equal to

30

zero. Then , $x_3 = 17$, $x_4 = 12$ and $M_b = 0$, $M_c = 0$. This solution yields both moments equal to zero and is not satisfactory.

Operation O_1: Test for optimality. Find out whether all coefficients of f, expressed as a function of the present non-basic variables, are negative or zero. If this optimality criterion is satisfied, then the basic feasible solution is optimal. Then f cannot increase if positive values are assigned to the non-basic variables. For this example, f is expressed in terms of the non-basic variables M_b and M_c. Therefore,

$$f = 20M_b + 16M_c,$$

which is not optimal since 20 and 16 are both positive. The next operation is taken.

Operation O2: search for a better basic feasible solution. If the basic feasible solution just tested is not optimal, go to a neighboring basic feasible solution for which f is larger. To go to a neighboring basic feasible solution means to go to a point at which another x_i is zero; that is, to make an exchange. The variable x_i which will now be zero leaves the set of basic variables, and one other variable becomes a basic variable instead. Consider a non-basic variable x_R that has a positive coefficient in f. Keep the other non-basic variables at zero. Determine the largest increase Δx_R of x_R such that all the old basic variables are still nonnegative; also list the corresponding increase Δf of f. From the above equations, for M_b this looks as follows:

$$x_3 = 17 - 2\underline{M_b} - M_c \,; \; 0 = 17 - 2M_b \,; \; \Delta M_b = 8.5 \,; \; \Delta f = 170$$

$$x_4 = 12 - M_b - M_c \,; \; 0 = 12 - M_b \,; \; \Delta M_b = 6 \,; \; \Delta f = 240 \qquad (4.16)$$

31

Underline $x_R = M_b$ in the equation that blocks any further increase in x_R; i.e. the maximum numerical value of the coefficient on M_b. Do this for every non-basic variable x_R whose coefficient in f, expressed as a function of the non-basic variables, is positive. Therefore, also consider $x_R = M_c$, underlining as before:

$$x_3 = 17 - 2M_b - M_c\,; \; 0 = 17 - M_c\,; \; \Delta M_c = 17\,; \; \Delta f = 272$$

$$x_4 = 12 - M_b - \underline{M_c}\,; \; 0 = 12 - M_c\,; \; \Delta M_c = 12\,; \; \Delta f = 192 \qquad (4.17)$$

Operation O_3: Exchange variables. Isolate both equations above where a variable is underlined.

$$x_3 = 17 - 2\underline{M_b} - M_c\,; \; \Delta f = 170$$

$$x_4 = 12 - M_b - \underline{M_c}\,; \; \Delta f = 192 \qquad (4.18)$$

Exchange that non-basic variable x_R which gave the greatest Δf with the basic variable in the equation where x_R is underlined. So M_b and x_4 are exchanged, so that M_b becomes basic and x_4 non-basic. Solve the system for the new basic variables. Therefore, by solving Equation 4.18 above for M_c and inserting this M_c into the first equation above.

$$M_c = 12 - M_b - x_4$$

$$x_3 = 5 - M_b + x_4 \qquad (4.19)$$

Perform Operations O_1, O_2, and O_3 again. Substituting values above into the weight expression, Equation 4.12,

$$f = 192 + 4M_b - 16x_4 \qquad (4.20)$$

By the optimality criterion, the present basic feasible solution is not optimal because M_b has a positive coefficient. For Operation O_2, now consider $x_R = M_c$. From the above expressions for M_c and x_3,

$$M_c = 12 - M_b - x_4; \quad 0 = 12 - M_b; \quad \Delta M_b = 12; \Delta f = 240$$

$$x_3 = 5 - \underline{M_b} + x_4; \quad 0 = 5 - M_b; \quad \Delta M_b = 5; \quad \Delta f = 100 \tag{4.21}$$

x_4 need not be considered since it is negative in the last expression for f. Write expression for M_b in Equation 4.21,

$$M_b = 5 - x_3 + x_4 \tag{4.22}$$

and substitute into first equation above for M_c,

$$M_c = 7 + x_3 + 2x_4 \tag{4.23}$$

Then,

$$f = 20 M_b + 16 M_c = 20(5 - x_3 + x_4) + 16(7 + x_3 + 2x_4) = 212 - 4x_3 - 52x_4$$

Which yields the solution with x_3 and x_4 set equal to zero,

$$M_b = 5 \text{ k-ft}; \quad M_c = 7 \text{ k-ft}; \quad f = 212; f \text{ being the minimum weight of the}$$

function. Note that the other constraints are also satisfied by this solution, namely, $M_c \geq 6$ and $M_b \geq 2.5$.

This problem can also be presented and solved graphically, as in the following figure. The constraint equations are plotted on the graph. The shaded
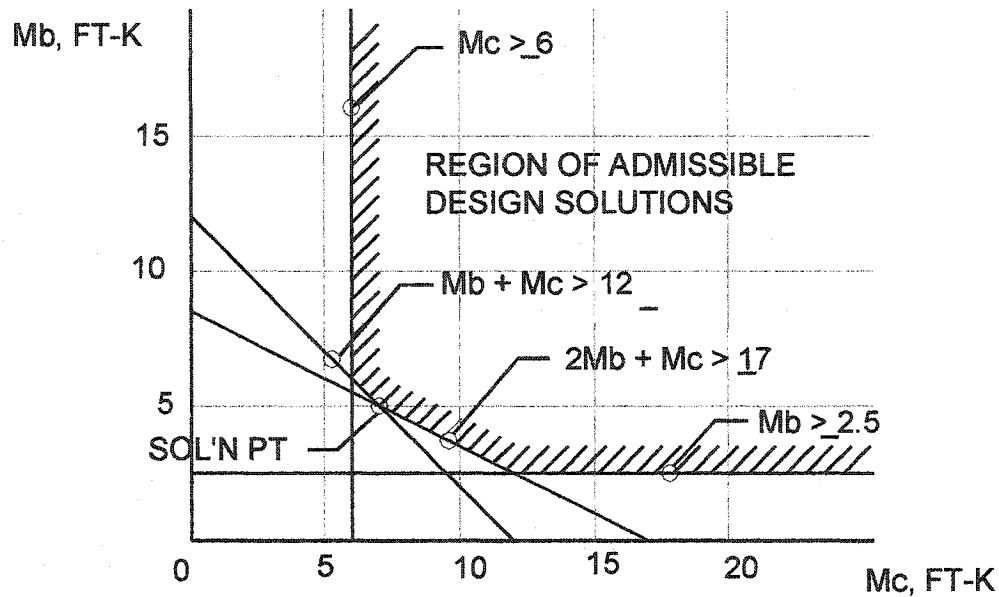
Figure 4.8 Minimum Weight Design Example Graph

area represents the region of permissible design solutions. Generally, a point at the lower left of this region is going to be a minimum weight solution. One could simply pick points off the graph and test for minimum weight. Three points could be selected,

$M_b = 6$; $M_c = 6$ and therefore $f = 20Mb + 16Mc = 216$ or

$M_b = 5$; $M_c = 7$; $f = 212$ or

$M_b = 2.5$; $M_c = 12$; $f = 242$.

Therefore, the middle point $M_b = 5$; $M_c = 7$; $f = 212$ is the solution which is in agreement with the mathematical treatment above.

A third method can be employed to solve minimum weight problems which employs the Simplex Method as proposed by Rubenstein and Karagozian and it is

34

required for more than two variables. The initial constraints are expressed as a series

of inequalities moving all terms over to the left side of the equations. Namely,

$$M_c \geq 6 \text{ k-ft} \qquad \text{becomes} \qquad M_c - 6 \geq 0$$

$$M_b \geq 2.5 \text{ k-ft} \qquad \text{becomes} \qquad M_b - 2.5 \geq 0$$

$$2M_b + M_c \geq 17 \qquad \text{becomes} \qquad 2M_b + M_c - 17 \geq 0$$

$$M_b + M_c \geq 12 \qquad \text{becomes} \qquad M_b + M_c - 12 \geq 0 \qquad (4.24)$$

which takes the form $[a]\begin{Bmatrix} M_b \\ M_c \end{Bmatrix} + \{r\} \geq 0$. So $[a] = \begin{bmatrix} 0 & 1 \\ 1 & 0 \\ 2 & 1 \\ 1 & 1 \end{bmatrix}$ and $\{r\} = \begin{Bmatrix} -6 \\ -2.5 \\ -17 \\ -12 \end{Bmatrix}$. The

following Figure 4.9 shows the procedure for the matrix solution using the Simplex

Method for this problem. The inequalities above are entered into the first four rows.

In rows 5 and 6, an identity matrix [b] of order 2 is stored (when n unknowns are

involved an identity matrix of order n is stored). Zeros are placed in the third or

indicator column to the right of the identity matrix. The position of these zeros will

contain M_b and M_c after the solution has been obtained. In the last row, the

coefficients of M_b and M_c in the weight function are recorded with zeros in the third

or indicator column. The position of this lower right zero in the matrix will contain

the minimum weight corresponding to the optimum solution. Therefore the matrix

takes the general form: $\begin{bmatrix} a_{ij} & r_j \\ b_{ij} & 0 \\ c_j & 0 \end{bmatrix}$, where $[a]$ and $\{r\}$ are as defined previously. $[b]$

35

is the identity matrix described above and $[c]$ contains the coefficient of the weight function. Then the initial matrix for the solution becomes the left matrix below.

$$\begin{bmatrix} 0 & 1 & -6 \\ 1 & 0 & -2.5 \\ \underline{2} & 1 & -17 \\ 1 & 1 & -12 \\ 1 & 0 & 0 \\ 0 & 1 & 0 \\ 20 & 16 & 0 \end{bmatrix} \qquad \begin{bmatrix} 0 & 1 & -6 \\ .5 & -.5 & 6 \\ 1 & 0 & 0 \\ .5 & \underline{-.5} & -3.5 \\ .5 & -.5 & 8.5 \\ 0 & 1 & 0 \\ 10 & 6 & 170 \end{bmatrix} \qquad \begin{bmatrix} -1 & 2 & 1 \\ 1 & -1 & 2.5 \\ 1 & 0 & 0 \\ 0 & 1 & 0 \\ 1 & -1 & 5 \\ -1 & 2 & 7 \\ 4 & 12 & 212 \end{bmatrix}$$

First iteration   Second iteration   Third iteration

Figure 4.9 Matrix Procedure – Minimum Weight Example

The steps for the solution by the Simplex Method are as follows:

1. Pick a row k with a negative number in the indicator column and compute the ratios c_j/a_{kj} if the row picked is in matrix $[a]$ or c_j/b_{kj} if it is in matrix $[b]$.

2. Find the smallest value of c_j/a_{kj} or c_j/b_{kj}. The corresponding element a_{kl} or b_{kl} is called the "pivot element." For example, in the initial matrix above and picking row 3, then $c_1/a_{31} = 20/2 = 10$, $c_2/a_{32} = 16/1 = 16$ and, therefore, a_{31} is a pivotal element (the value of 2 is underlined in the first column).

3. Divide each element of the first column in which the pivotal element a_{kl} is positioned by a_{kl}, and record this new column as the first column in a new table (column 1 in the second iteration matrix above). Use this column to reduce to zero all other elements of row k in the new table.

36

4. To record a zero in row k of any column n of the new table, multiply all the elements of column l of the new table by element a_{kn} and subtract from column n of the preceding table. For example, column 3 in the second iteration table above is obtained by multiplying each element of column 1 in the second table by (-17) and subtracting from column 3 of the initial table.

5. Repeat steps 1 to 4 with the second table to generate a third one. The solution is completed when no negative numbers appear in the indicator column.

Therefore, in the third column of the last table it can be seen that the two values opposite the initial b identity matrix in column 3 are 5 and 7. The value in the lower right corner of the table is 212. These are the moment values and minimum weight given in the previous results. It can be seen that the matrix operations mirror the naming of basic and non-basic variables, the method of exchange and the test for optimality that were performed in the more mathematical method. It can also be seen that when 3 or 4 or 5 variables are sought, the mathematical solution can be quite cumbersome. However, the matrix method can be readily programmed and handle many variables.

This is precisely what was done to facilitate the design methodology using energy for multistory buildings. The details of how the energy for each story is obtained will be demonstrated in following pages, but the principle follows the plastic design procedures and the Simplex procedure presented in this chapter.

Microsoft Excel was used to generate a spreadsheet that automatically performs the above mentioned matrix operations. A sample of this spreadsheet is presented below in Figure 4.11 with a flow chart of its use in Figure 4.10. It was believed that Excel allows great flexibility for interactive design, while at the same time providing a great degree of sophistication in programming. Each cell in the spreadsheet contains a large amount of logical evaluation operations based on the pivot element entered from the previous step. An evaluation matrix is between each iteration to determine the pivot element. The steps in the analysis are exactly the same as listed above for the simple example. However, the division by the weight function coefficients (c_j/a_{kj} or c_j/b_{kj}) is performed automatically in the intermediate matrix. The pivot element value and location are entered interactively in the space listed after the evaluation matrix. The next matrix is computed automatically and the next evaluation matrix is examined. The next pivot element value and location is entered after the next evaluation matrix and so on until the values in the last indicator column are positive, again as indicated in the steps for the example above. The Excel spreadsheet has a capacity of five constraint equations and three unknowns. This can obviously be expanded, but the amount of information in each cell in the spreadsheet must be altered with care as each cell address must be accurate. The procedure follows the same steps as the previous example; the weight in the lower right cell must increase with each new matrix. Capacity is allowed for six iterations or new matricies. This capacity was not exceeded for up to a twenty story building examined in this effort. Further, the text of a typical cell of one of the derived Simplex matrices (matrix 2,

38

matrix 3, etc.) is shown in Figure 4.12 to show the complexity of the logical operations performed by the minimum weight subroutine. For each cell, there is a test to evaluate the location of the pivot element; if the cell under consideration is the pivot cell there is one set of calculations and others if not. This spreadsheet allows for great flexibility in reviewing interactively the entire process in evaluating the desired moments, the pivot elements and the minimum weight values.

39
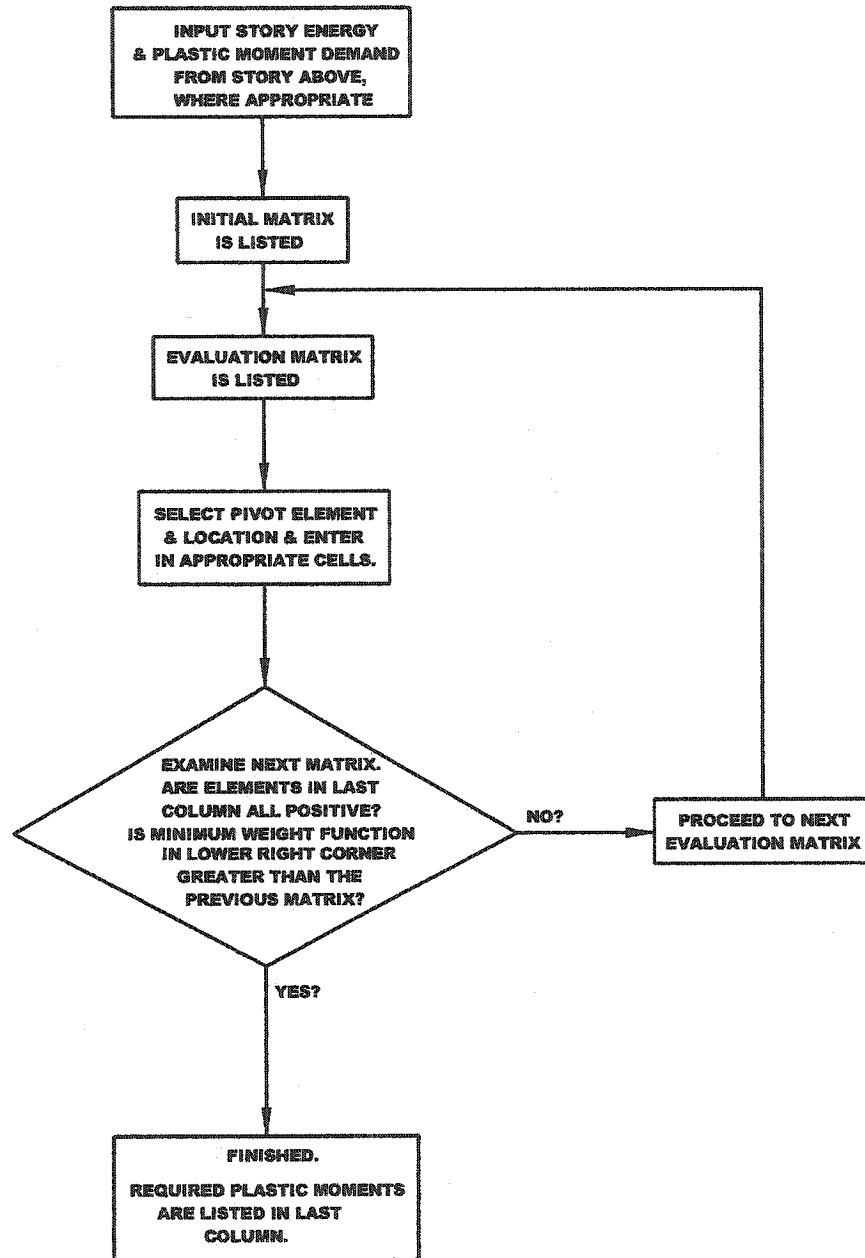
Figure 4.10 Flow Chart of Minimum Weight Subroutine

40

Subroutine for Minimum Weight Design by Story

Enter Story Energy =	7331	Enter Mp(ext. col. Above) =	508	Enter Mp(int. col. Above) =	1017

Initial Matrix

					Find 1st Pivot Element			
2	1	0	-2543.743		26	26	#DIV/0!	Enter Column of Pivot
2	1	5	-5087.486		26	26	24	3
0	1	-1	0		#DIV/0!	26	-120	Enter Row of Pivot
-0.5	1	0	0		-104	26	-120	2
0	1	-1	0		#DIV/0!	26	-120	Enter Value of Pivot
1	0	0	0		52	#DIV/0!	#DIV/0!	5
0	1	0	0		#DIV/0!	26	#DIV/0!	
0	0	1	0		#DIV/0!	#DIV/0!	120	
52	26	120	0		1	1	1	

Second Matrix

					Find 2nd Pivot Element			
2	1	0	-2543.743		2	2	#DIV/0!	Enter Column of Pivot
0	0	1	0		#DIV/0!	#DIV/0!	24	2
0.4	1.2	-0.2	-1017.497		10	1.666667	-120	Enter Row of Pivot
-0.5	1	0	0		-8	2	#DIV/0!	3
0.4	1.2	-0.2	-1017.497		10	1.666667	-120	Enter Value of Pivot
1	0	0	0		4	#DIV/0!	#DIV/0!	1.2
0	1	0	0		#DIV/0!	2	#DIV/0!	
-0.4	-0.2	0.2	1017.497		-10	-10	120	
4	2	24	122099.7		1	1	1	

Figure 4.11 Excel Minimum Weight Subroutine – First Two Matrices

41

=SUM(IF(J8=1,A7/PIVOT1,0), IF(AND(J8=2,J10=1),

-N7*A7+A7,IF(AND(J8=2,J10=2),-N7*A8+A7,IF(AND(J8=2,J10=3),

-N7*A9+A7,IF(AND(J8=2,J10=4),-N7*A10+A7,IF(AND(J8=2,J10=5),

-N7*A11+A7,0))))), IF(AND(J8=2,J10=6),

-N7*A12+A7,IF(AND(J8=2,J10=7),-N7*A13+A7,IF(AND(J8=2,J10=8),

-N7*A14+A7,IF(AND(J8=2,J10=9),-N7*A15+A7,0)))),

IF(AND(J8=3,J10=1),-O7*A7+A7,IF(AND(J8=3,J10=2),

-O7*A8+A7,IF(AND(J8=3,J10=3),-O7*A9+A7,IF(AND(J8=3,J10=4),

-O7*A10+A7,IF(AND(J8=3,J10=5),-O7*A11+A7,0))))),

IF(AND(J8=3,J10=6),-O7*A12+A7,IF(AND(J8=3,J10=7),

-O7*A13+A7,IF(AND(J8=3,J10=8),-O7*A14+A7,IF(AND(J8=3,J10=9),

-O7*A15+A7,0)))))

Figure 4.12 Contents of Sample Cell in Simplex Matrix

4.6 Summary of the Proposed Method

The following is a general summary of the proposed procedure outlined in this chapter:

1. It is assumed that a code level analysis, or even a nonlinear pushover analysis, has been performed on a given frame and initial member sizes have been determined. If an existing building is the subject of study, then obviously one uses the existing member sizes.

42

2. An energy demand is established for the building frame as a whole and then distributed to each story such that there is a demand story by story. This will be examined in later chapters of this document.

3. The member sizes are then determined by a minimum weight subroutine limiting the plastic rotation to .03 radians.

Important issues to be explored and confirmed are the effect of vertical load, maintaining a "strong column-weak beam" configuration, limiting overall drift, and confirming if the resulting maximum plastic rotations are in fact less than .03 radians.

It could be noted that a possible starting point for the energy demand may be to utilize an Energy Spectrum for a given earthquake record or records. The elastic energy being $E = 1/2mS_v{}^2$, S_v being the spectral velocity and m being the mass of a single degree of freedom structure. After Housner, elastic energy can be considered as an upper bound of inelastic energy and has been used as such by several researchers. Energy spectra are commonly plotted in a normalized form as E/m versus period or frequency and could be easily adopted into this procedure.

43

Chapter 5: Example of a Two Story Moment Frame Building

In order to test the outlined procedure it was desired to first look at a simple example. A two story moment frame building was severely damaged by the Northridge earthquake. The building, located in Santa Clarita, California, has received considerable analysis and testing at USC (Anderson, Johnston, and Partridge 1995). It was a two story steel framed building with lateral resistance provided by single bay steel moment frames on each of its four sides. During the Northridge earthquake in 1994 this building did not collapse but experienced severe, irreparable damage. Several of its moment connections experienced the now well-known column flange cracking. As the building was torn down, key beam-column connections were cut out and brought to USC for full scale testing. A great deal of analysis, both elastic and inelastic, was performed on the building in conjunction with the full scale testing. Therefore, this building seemed a good test case to try this new method of analysis.

The first story of the lateral resisting frames of the building experienced the clear majority of the structural damage. The first story columns and beams underwent significant inelastic excursions while the top story almost moved as a rigid body. A representative building frame in the building was analyzed by inelastic time history analysis using DRAIN 2D. Even though there are later versions of this program, it was decided to utilize DRAIN 2D+ as modified by Tsai and Li at Taiwan National University (Tsai and Li 1994). The procedure outlined previously was followed. Starting with the "as designed" sizes, Frame #1 was analyzed.

44

Several different approaches are presented in what follows. First, the selected building frame was analyzed using the Uniform Building Code static force procedure in effect at the time the building was designed. In reconstructing this analysis, all of the stress ratios for all of the members were one or less. In other words, the building complied with the building code when it was designed. Additionally, a pushover analysis was performed using the FEMA 273 method as shown in Figure 5.1. The FEMA method establishes a target displacement. Using the program XLINEA (RAM XLINEA version 3.0), which uses DRAIN 2DX as its core solver with various postprocessing functions, the frame was pushed over to the target displacement. At the target displacement, all plastic rotations were within .03 radians with plastic hinges located in the beams. In other words, using a pushover analysis in addition to a static code analysis would seemingly deem this frame adequate.

Of interest, an elastic time history analysis was also performed using the Newhall Fire Station record utilizing the computer program ETABS with its STEELER postprocessor. Considering only lateral loads and checking the members with the LRFD specification of the AISC (a load factor of 1.0 was used with the time history), stress ratios of 4 to 5 resulted. This would seem to indicate that the member sizes would need to be increased dramatically. However, a nonlinear analysis can be utilized to produce a safe design.

45

a) Pushover Curve

**b) Resulting Plastic Rotations
at Perf. Pt. Displacement**
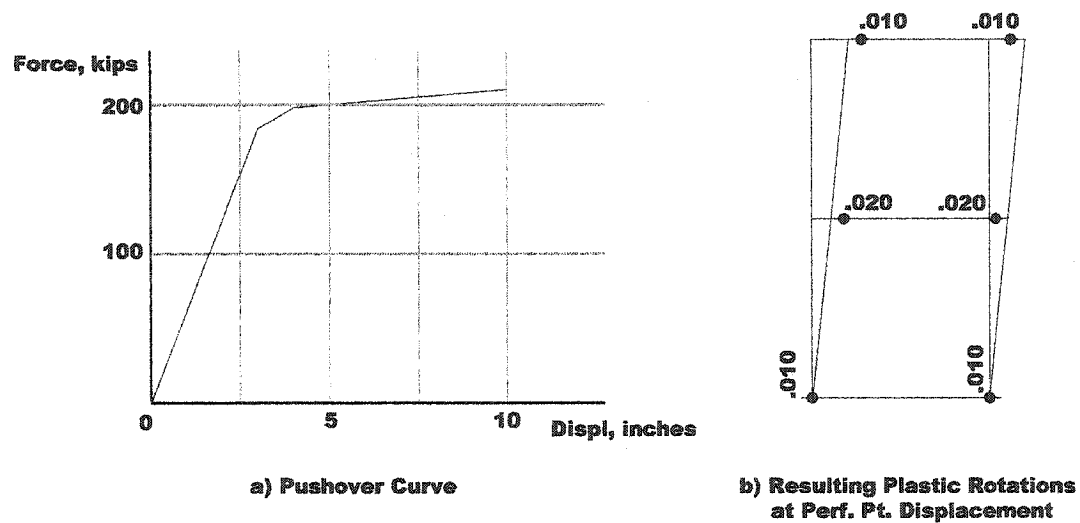
Figure 5.1 Two Story Building Analyzed with FEMA 273

Several inelastic analyses were performed on the building frame using the

Newhall Fire Station North record. The first presentation in what follows is to

perform a series of inelastic analyses in an iterative fashion to check the resulting

hysteretic energy for each story. The members are grouped into two energy story

groups. The energy demand is verified with each computer run. Secondly, the

building frame was analyzed for all twenty of the SAC records having a 10%

probability on exceedance in 50 years (10/50) (Somerville et all 1997). Then using

the mean plus one standard deviation hysteretic energy of the twenty records as the

energy demand, each story was checked and member sizes verified with the

minimum weight subroutine. The resulting frame sizes were checked by inelastic

analysis using records near the mean plus standard deviation energy. The resulting

maximum plastic rotations are presented. Finally, the building frame is designed to

46

the energy demand from the SAC Near Fault records (Somerville et all 1997) in a similar fashion. The results of the analyses of the 20 Near Fault SAC records for the building frame are presented. The frame is checked for the twenty near fault records to establish the mean hysteretic energy demand. The sizes are checked by the minimum weight procedure and verified by inelastic time history analysis.

5.1 Design Procedure for a Single Bay Moment Frame

First, an iterative methodology is used with successive DRAIN 2D+ runs and member sizes changing as indicated with each run.

Iteration #1: From the initial DRAIN 2D+ analysis with initial sizes, the hysteretic energy for the first story is calculated as 3545 kip-inches. For the second story, the resulting hysteretic energy is 667 kip-inches. Starting with the top story, the existing beam and columns are W24x62 and W14x132, respectively. Assuming a plastic sway mechanism for the second story similar to Figure 4.5, write an equation for the internal work and equate this to the hysteretic energy demand. Limit the plastic rotation to .03 radians.

$$\text{Hysteretic Energy} = 667 = [2M_p(col) + 2M_p(bm)]\theta_p * 4$$

$$667 = [2M_p(col) + 2M_p(bm)] * .03 * 4 \qquad (5.1)$$

The column plastic moment capacity will be made larger than the beam plastic moment capacity to assure a "strong column-weak beam" configuration, however, for this example assume one M_p for the story. Therefore, the expression in the

47
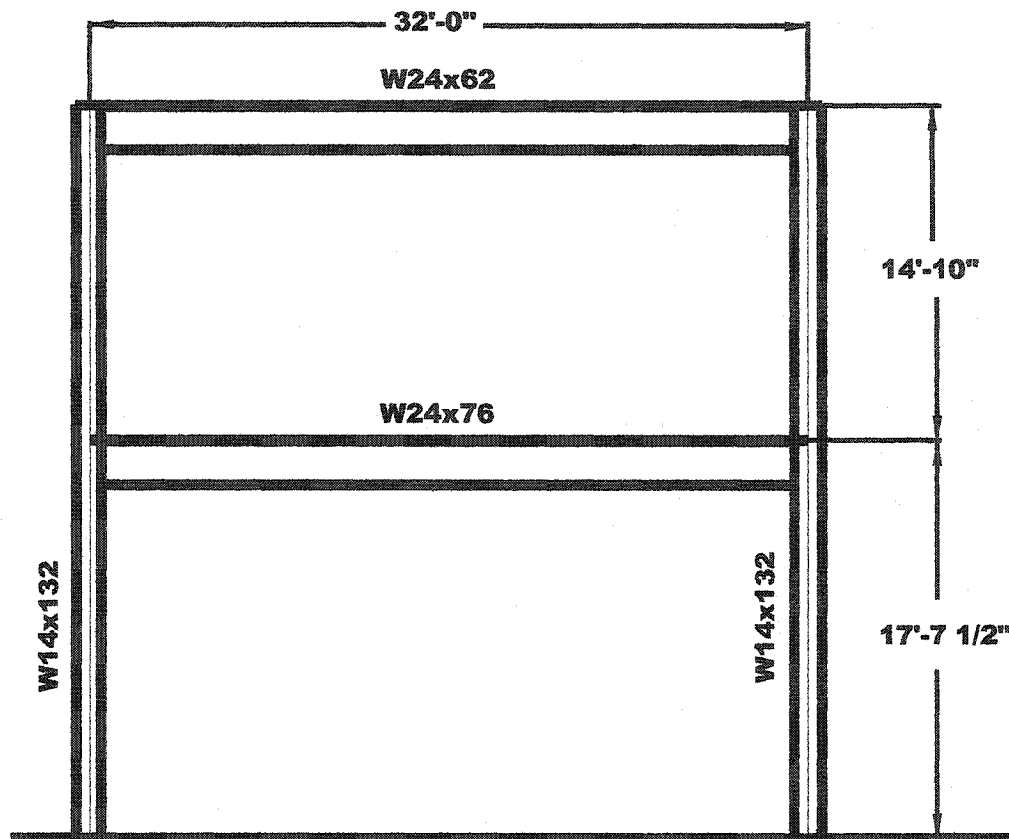
Figure 5.2 Two Story Moment Frame Building – Original Sizes

brackets above becomes $4M_p$.

$$\therefore M_p = \frac{667}{4 * 4 * .03} = 1390^{k-in} = 116^{k'} \tag{5.2}$$

This is a low figure. The W14x132 column and W24x62 roof beam will be

maintained.

For the first story, the column is a W14x132 and the beam is a W24x76.

Again, write an equation setting the hysteretic energy demand equal to the internal

48

work. The added complexity is that the column plastic moments from above will be included as external forces for this lower story consistent with the mechanism shown in Figure 4.5. The column plastic moment capacity from above is used:

$$HE = 3545 = [2M_p(col) + 2M_p(bm) - 2M_p(col\ above)] * 4 * .03$$

$$3545 = [4M_p - 2*116*12] * 4 * .03$$

$$3545 = .48M_p - 334$$

$$Mp = 8081^{k-in} = 673^{k'} \tag{5.3}$$

The factor of 12 is included to produce required moment capacities in kip-feet, as is commonly listed in the American Institute of Steel Construction Manual. Choose a W14x145 column and a W24x94 floor beam.

Note that the second story members have been maintained and the first story sizes have been increased.

Iteration #2 with revised sizes: From the second DRAIN 2D+ run, the hysteretic energy demand for first story is 3613 kip-inches; the second story hysteretic energy is 618 kip-inches. The 2nd story members are the same W14x132 column and W24x62 roof beam. Writing the same equations,

$$\text{Hysteretic Energy} = 618 = [2M_p(col) + 2M_p(bm)] * .03 * 4$$

$$\therefore M_p = \frac{618}{16*.03} = 1288^{k-in} = 107^{k'} \tag{5.4}$$

Maintain the same sizes of a W14x132 column and a W24x62 roof beam.

For the first story the member sizes have been revised to a W14x145 column and a W24x94 floor beam. Again, write an equation for the internal work and energy demand including the plastic column moments from above.

$$HE = 3613 = [2M_p(col) + 2M_p(bm) - 2M_p(col\ above)] * 4 * .03$$

$$3613 = [4M_p - 2*107*12] * 4 * .03$$

$$3613 = .48M_p - 308$$

$$Mp = 8169^{k-in} = 681^{k'} \tag{5.5}$$

Maintain a W14x145 column and a W24x94 floor beam.

Observation: This is an iterative process. Large changes in member sizes are not advised. The energy comes to equilibrium quickly. There must be a balance between limiting plastic rotation, hinging in undesirable column locations, and making the sizes practical. In Figure 5.5, the resulting maximum plastic rotations from an analysis of the original frame subjected to the Newhall Fire Station North record are presented. Figure 5.6 shows the resulting maximum plastic rotations for the revised sizes above subjected to the Newhall Fire Station North record.

The second approach to this building frame is to subject it to all twenty of the SAC 10/50 records. The energy distribution from these analyses is shown in Figure 5.3. The mean plus standard deviation hysteretic energy is used as the energy demand for each story. The hysteretic energy demand for the top story is 512 kip-inches. The energy demand for the bottom story is 3724 kip-inches. In order to use the minimum weight subroutine, constraint equations are formulated. For the top

story, first a sway mechanism assuming hinges in the top and bottom of the columns is used. For this case,

$$HystereticEnergy(HE) = [4Mp(col)] * .03 * 4$$

then, $$M_p(col) = HE/(.03 * 16 * 12) \qquad (5.6)$$

Therefore, with the energy demand of 512 kip-inches,

$$M_p(col) = 88.9$$

In order to put this in the form to use in the Simplex Method, the first constraint equation becomes,

$$M_p(col) - 88.9 \geq 0 \qquad (5.7)$$

Considering next the plastic mechanism in the top story with hinges at the bottom of the columns and the ends of the beams,

$$HystereticEnergy = [2Mp(col) + 2Mp(bm)] * .03 * 4$$

$$M_p(col) + M_p(bm) = HE/(.03 * 8 * 12) \qquad (5.8)$$

With the energy demand = 512 kip-inches, the right side of the equation becomes 177.8. Moving this to the left side and formulating this in the Simplex form,

$$M_p(col) + M_p(bm) - 177.8 \geq 0 \qquad (5.9)$$

There is another constraint equation that can be written and that is to insure that the column moment capacity is always greater than the beam plastic moment capacity. This is to produce a "strong column/weak beam" configuration to help prevent collapse. Therefore, it can be said,

$$M_p(col) \geq M_p(bm) \qquad (5.10)$$

51

or again in the Simplex form,

$$M_p(col) - M_p(bm) \geq 0 \qquad (5.11)$$

The weight function for the top story is the plastic moments multiplied by the lengths of the members. Therefore, for the top story, $f = 2*14.83'*M_{col} + 32'*M_{bm} = 29.67M_{col} + 32M_{bm}$. Consequently, for input into the Simplex algorithm, the initial matrix becomes:

$$\begin{bmatrix} 1 & 0 & -88.9 \\ 1 & 1 & -177.8 \\ 1 & 0 & 0 \\ 0 & 1 & 0 \\ 29.67 & 32 & 0 \end{bmatrix}$$

The required moment capacity from the Simplex subroutine is the same for both beam and column at 86 kip-feet. This is less than the capacity of the existing members, so no change is recommended.

For the bottom story and following Figure 4.5, an equation for hinges in the columns only becomes

$$HE = [4M_p(col) - 2M_p(col\ abv)]*.03*4$$

then, $$M_p(col) = HE/(16*.03*12) - .5M_p(col\ abv) \qquad (5.12)$$

Using HE = 3724 k-in and $M_p(col\ abv)$ = 86,

$$M_p(col) = 604$$

or $$M_p(col) - 604 \geq 0 \qquad (5.13)$$

52

For the second mechanism with hinges in the beams only,

$$HE = [2M_p(col) + 2M_p(bm) - 2M_p(col\ above)] * 4 * .03$$

$$M_p(col) + M_p(bm) = HE/(.03 * 8 * 12) + M_p(col\ above) \qquad (5.14)$$

then, $$M_p(col) + M_p(bm) = 1379$$

$$M_p(col) + M_p(bm) - 1379 \geq 0 \qquad (5.15)$$

Note that the calculated column plastic moment demand from above is used which is different than was used previously. In all examples that follow, the calculated column demand will be used, as opposed to that from the actual column size. With the same constraint that the column plastic moment be equal to or greater than the beam plastic moment, the input matrix into the Simplex algorithm becomes,

$$\begin{bmatrix} 1 & 0 & -604 \\ 1 & 1 & -1379 \\ 1 & 0 & 0 \\ 0 & 1 & 0 \\ 35.25 & 32 & 0 \end{bmatrix}$$

The weight function is slightly different due to the different story height. From the minimum weight subroutine, the required plastic moment for the beam and column is 690 kip-feet. Selecting a column slightly larger than the beam plastic moment capacity, use a W14x145 column and a W27x84 beam. Vertical loads are not considered in plastic mechanisms, but are included in the computer models as fixed end forces. With these sizes then selected, a DRAIN 2D+ run is made checking with the SAC records LA14 and LA16. These were records with approximately the same energy demand as the mean plus standard deviation used in this procedure. The

53

resulting maximum plastic rotations are shown in Figure 5.7, resulting in rotations equal to or less than .03 radians.

Finally, the proposed energy method was applied to this frame using the SAC Near Fault records to produce the energy demand. These records simulate a phenomenon that has received much attention in recent years, that of faults in close proximity to a given site that tend to possess a distinct "pulse." More will be discussed regarding these records later. The methodology is the same as above and the results of these analyses are presented in Figure 5.4, 5.7, and 5.8, including the inelastic time history runs for records near the mean energy. Note the mean energy demand was used for the Near Fault records.

In summary, for the several analyses that were performed on the two story building, the proposed energy design procedure has produced member sizes that satisfy the rotational constraint with reasonable and consistent results.
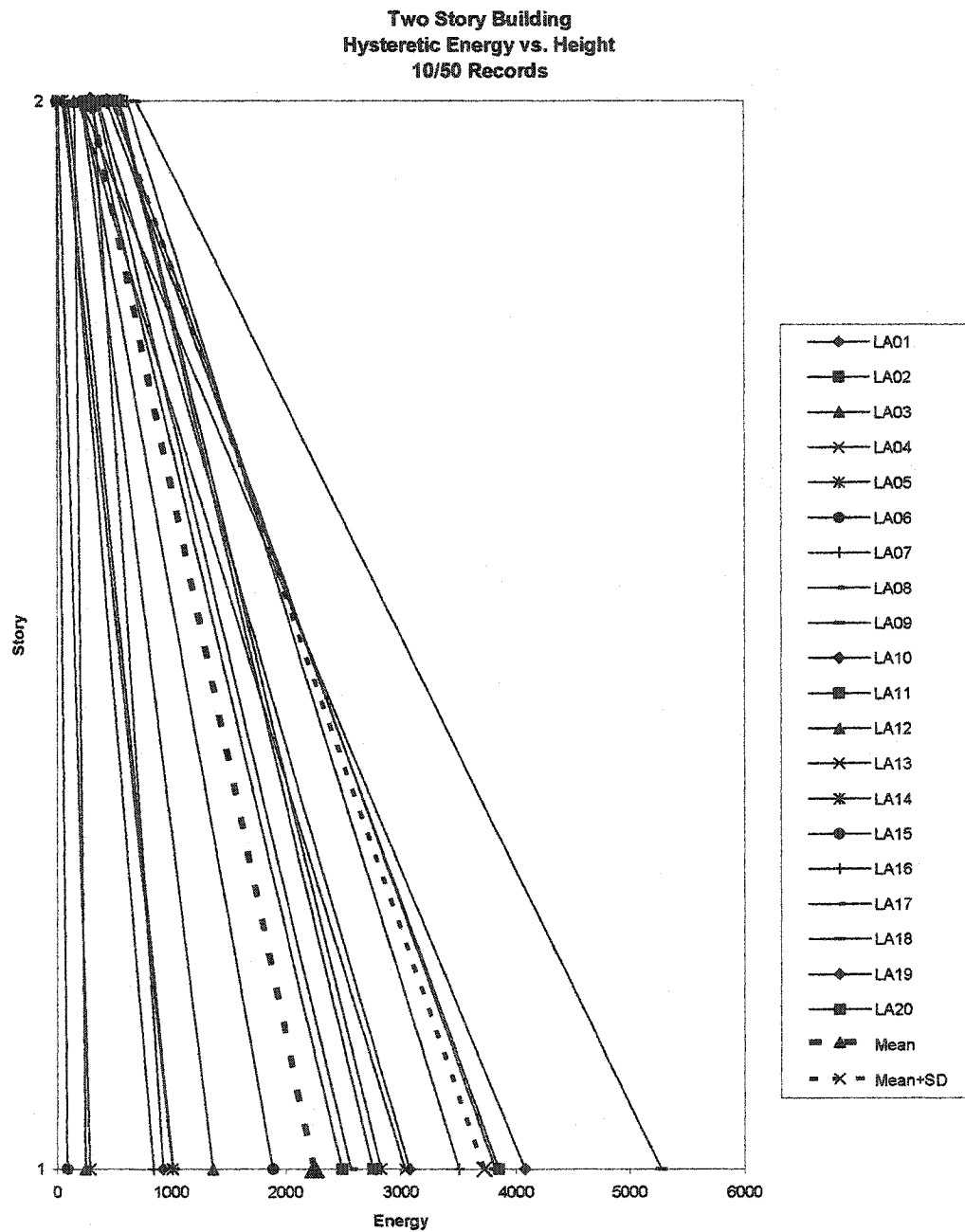
Figure 5.3 – Two Story Building SAC 10/50 Energies
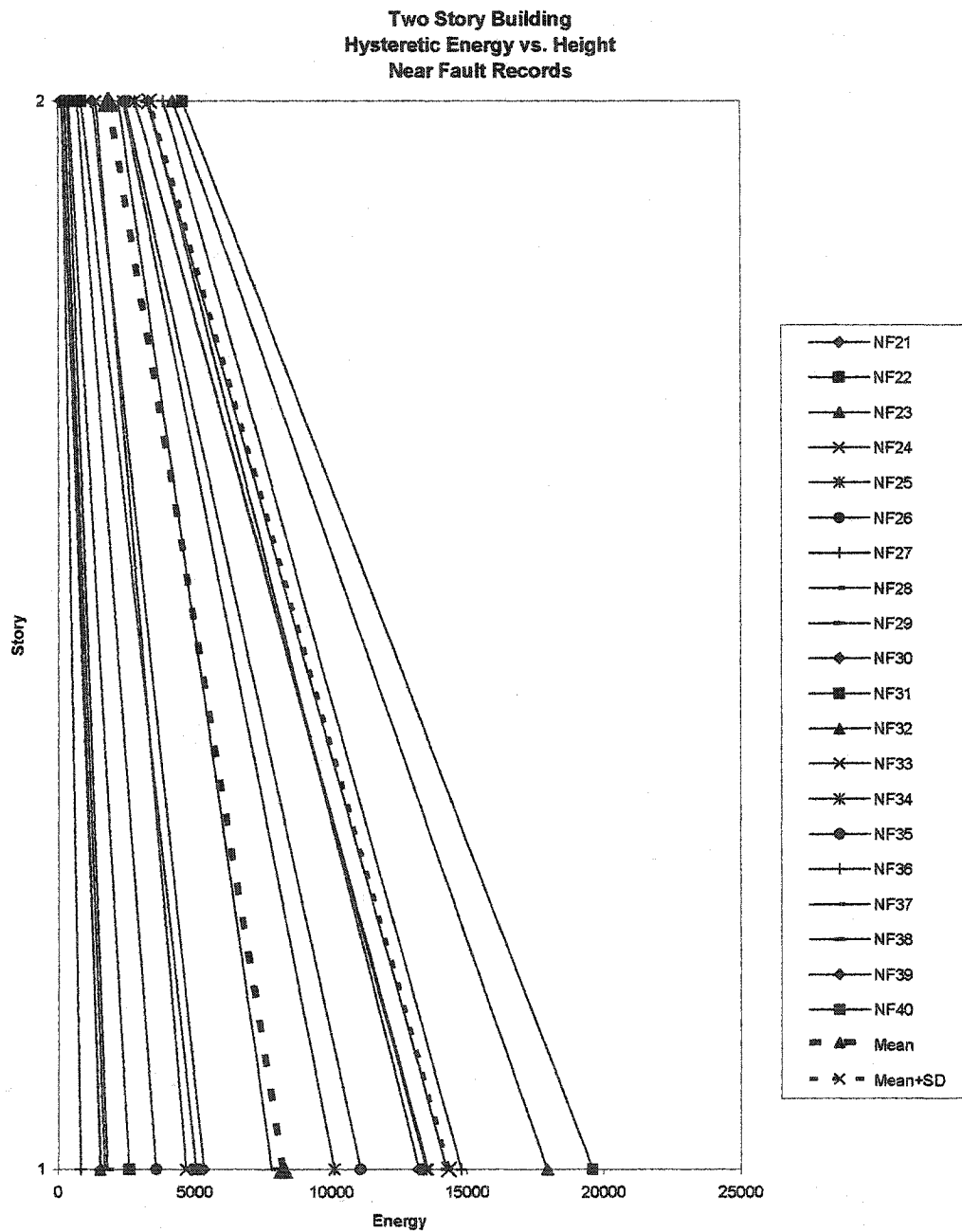
Figure 5.4 Two Story Building SAC Near Fault Energies

56

[ ] = RESULTING MAX. PLASTIC ROTATIONS
BASED ON NEWHALL FIRE STATION NORTH RECORD
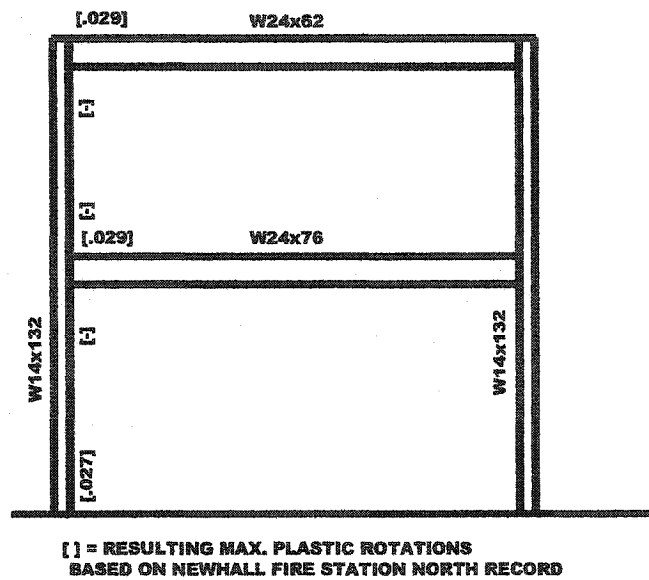
Figure 5.5 Two Story Building Original Sizes

[ ] = RESULTING MAX. PLASTIC ROTATIONS
BASED ON NEWHALL FIRE STATION NORTH RECORD

Figure 5.6 Two Story Building Revised Sizes from Iterative Procedure

57
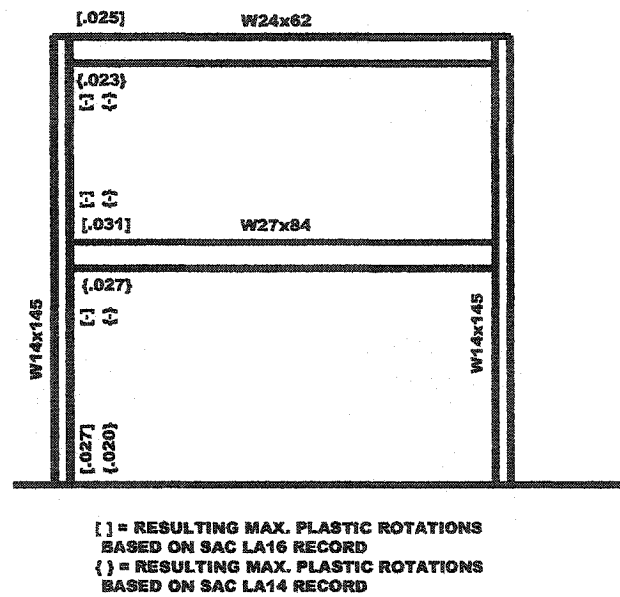
Figure 5.7 Two Story Building Revised Sizes from SAC 10/50 Records
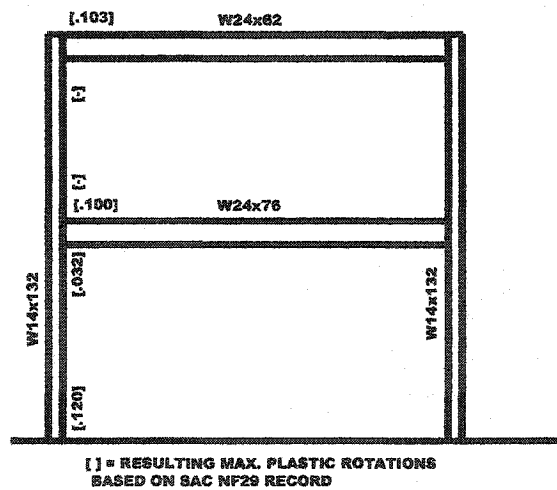
Figure 5.8 Two Story Building Original Sizes subjected to SAC Near Fault Record

58

[ ] = RESULTING MAX. PLASTIC ROTATIONS
BASED ON SAC NF29 RECORD
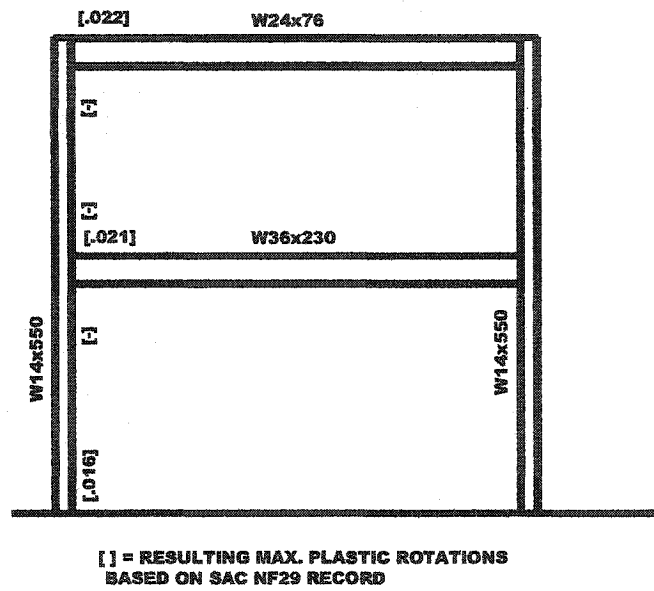
Figure 5.9 Two Story Building Revised Sizes from SAC Near Fault Records

59

Chapter 6: Energy Analysis of a Three, Nine and Twenty Story Building Frame

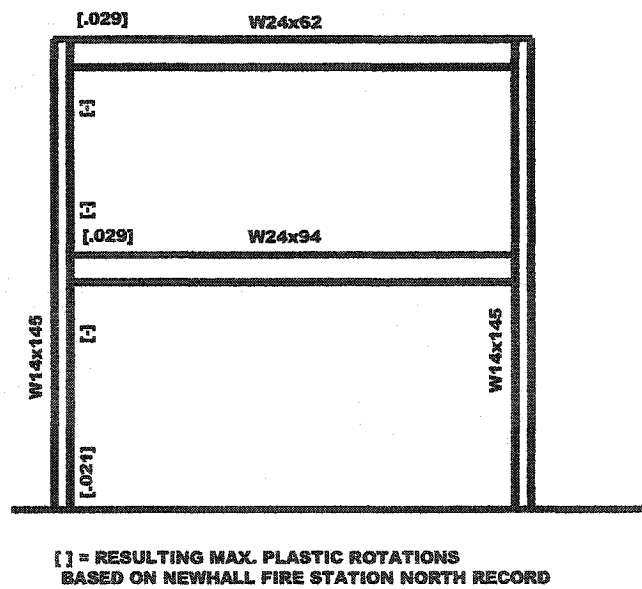The energy design method has been described in detail for a simple two story frame. It is desired to broaden the method to be applicable to a wide range of buildings. SAC has analyzed several prototype buildings with ground motions representative of Los Angeles. Three, nine, and twenty story buildings have been examined. SAC has also developed a suite of ground motions for the Los Angeles area based on scaled records of past earthquakes. The records have been scaled to provide an equivalent level of risk or type. Records used in this study are those with a 10% probability of exceedance in 50 years and for Near Fault sites. Other suites of ground motions have been developed for a 50% probability of exceedance in 50 years, a 2% probability of exceedance in 50 years and for Soft Soil sites. Other records with other values of risk or return period could obviously be used. The two cited above were judged to be of most interest in this study. A schematic picture of each building is shown in Figure 6.1. A single frame of each building was selected and analyzed in a two dimensional DRAIN 2D+ model and subjected to all 20 of the SAC time histories in each of the 10/50 and Near Fault categories. In this way, two areas could be studied. One is the effect of the different ground motions. Second is the variation of energy with the height of a building frame or by story. The hysteretic energy can be somewhat fluid, based on the loading, mass, stiffness and yielding properties of the frame members. It is intended to "envelope" the energies for the given ground motions and perform a design check based on this envelope.

60

The following pages show charts of hysteretic energies for each of the three building heights. The hysteretic energy for each story is plotted versus the height of the buildings. For each building, first the energy from the 10/50 records is shown, and then those for the Near Fault records. It is very interesting to note the distribution of energy as it "radiates" up the building frame. The three-story frame appears to be quite predictable. Starting with the nine-story frame, the energy is seen to be at a peak, not at the base, but somewhere several stories up. The twenty-story frame verifies this phenomenon. The energy lines for each earthquake record are shown, in addition to the mean and mean plus standard deviation (M+SD) shown in dotted lines. Also very important are the magnitudes of the hysteretic energy for each building type for the 10/50 records versus the Near Fault records. The hysteretic energy demand for the Near Fault records is approximately 5 times that for the 10/50 records. This is very interesting in light of the Near Fault Factors currently in the Uniform Building Code and International Building Code. These code factors vary from about 1.5 to 2.0. Although these are modifications on force, the significant energy increase suggests that they need to be reexamined based on these results.
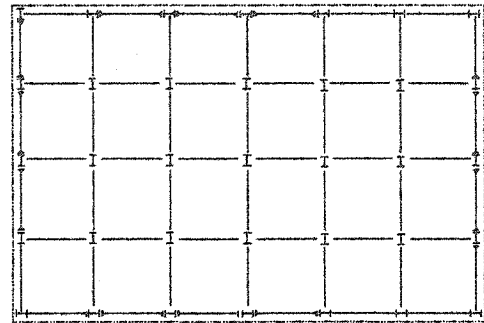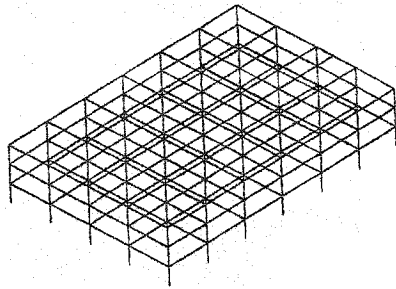
(a) Three Story Building
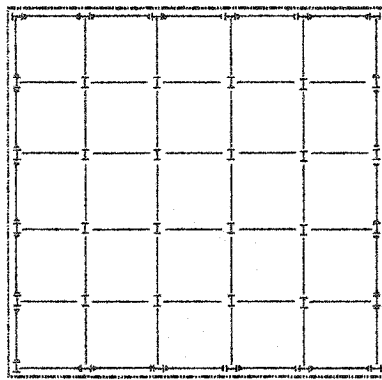
(b) Nine Story Building
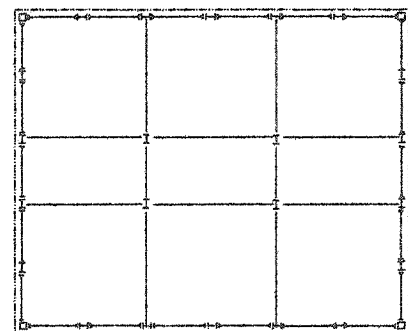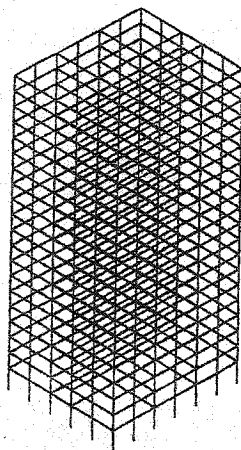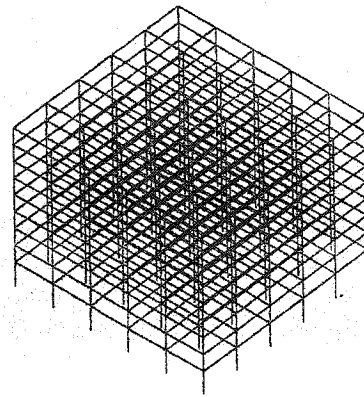
(c)Twenty Story Building

Figure 6.1 Typical Floor Plans and SAC Building Models

62

3 Story Building
Hysteretic Energy vs. Height
10/50 Records
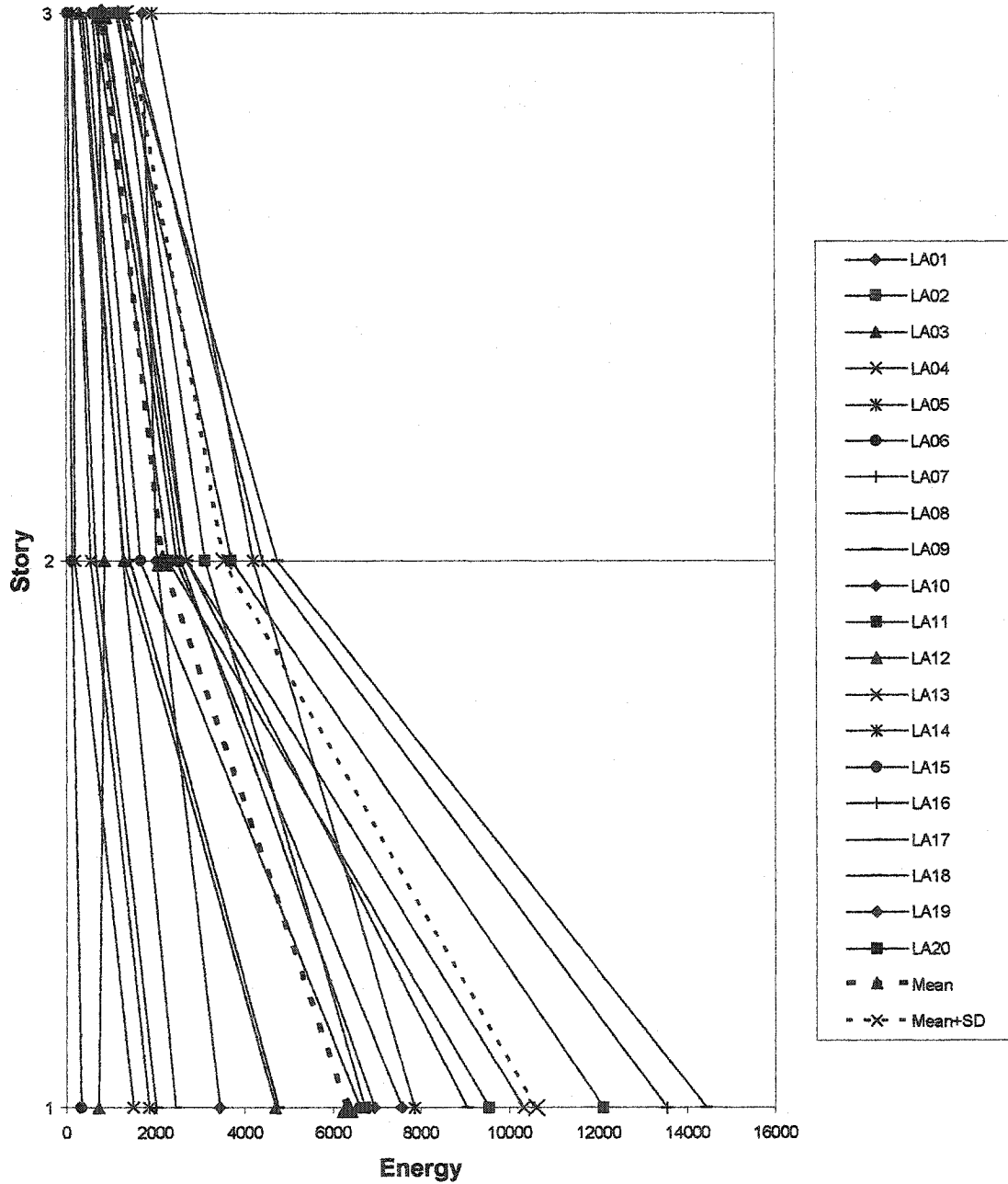
Figure 6.2 Three Story Building Energies from SAC 10/50 Records

63

3 Story Building
Hysteretic Energy vs. Height
Near Fault Records
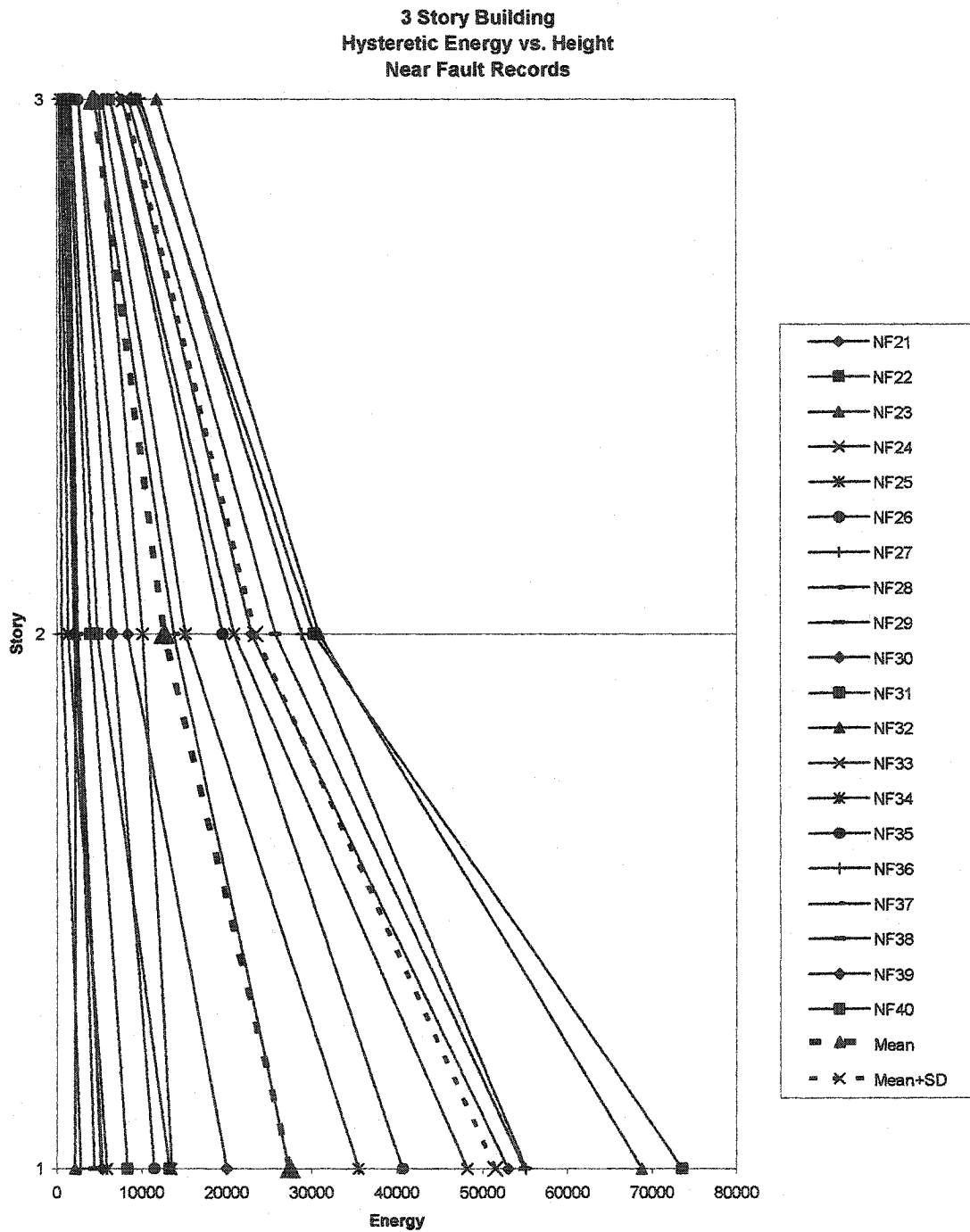
Figure 6.3 Three Story Building Energies from SAC Near Fault Records

64
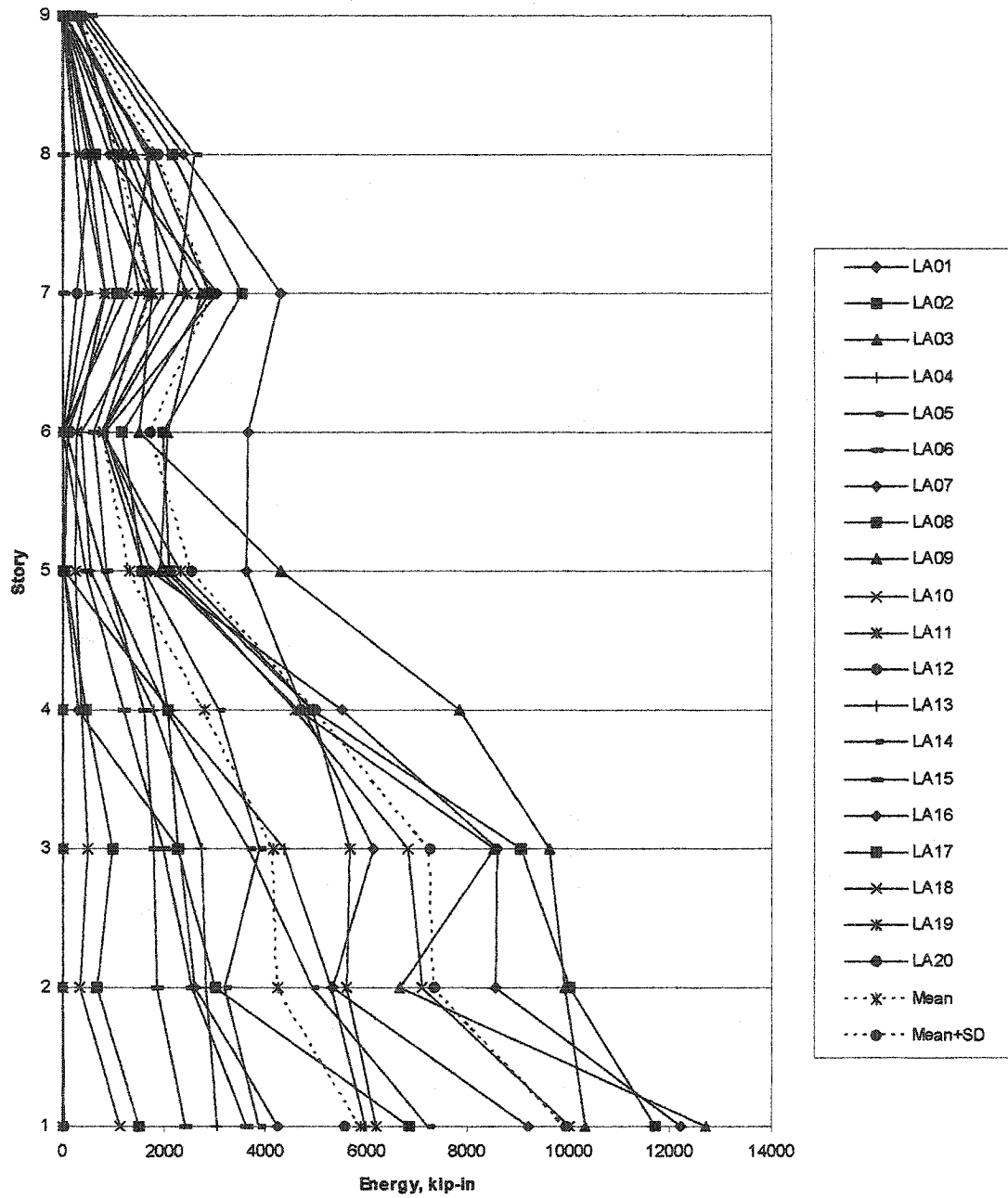
Figure 6.4 Nine Story Building Energies from SAC 10/50 Records

65

9 Story Building
Hysteretic Energy vs. Height
Near Fault Records

Legend: NF21, NF22, NF23, NF24, NF25, NF26, NF27, NF28, NF29, NF30, NF31, NF32, NF33, NF34, NF35, NF36, NF37, NF38, NF39, NF40, Mean, Mean+SD, Akiyama Dist

Y-axis: Story
X-axis: Energy, kip-in
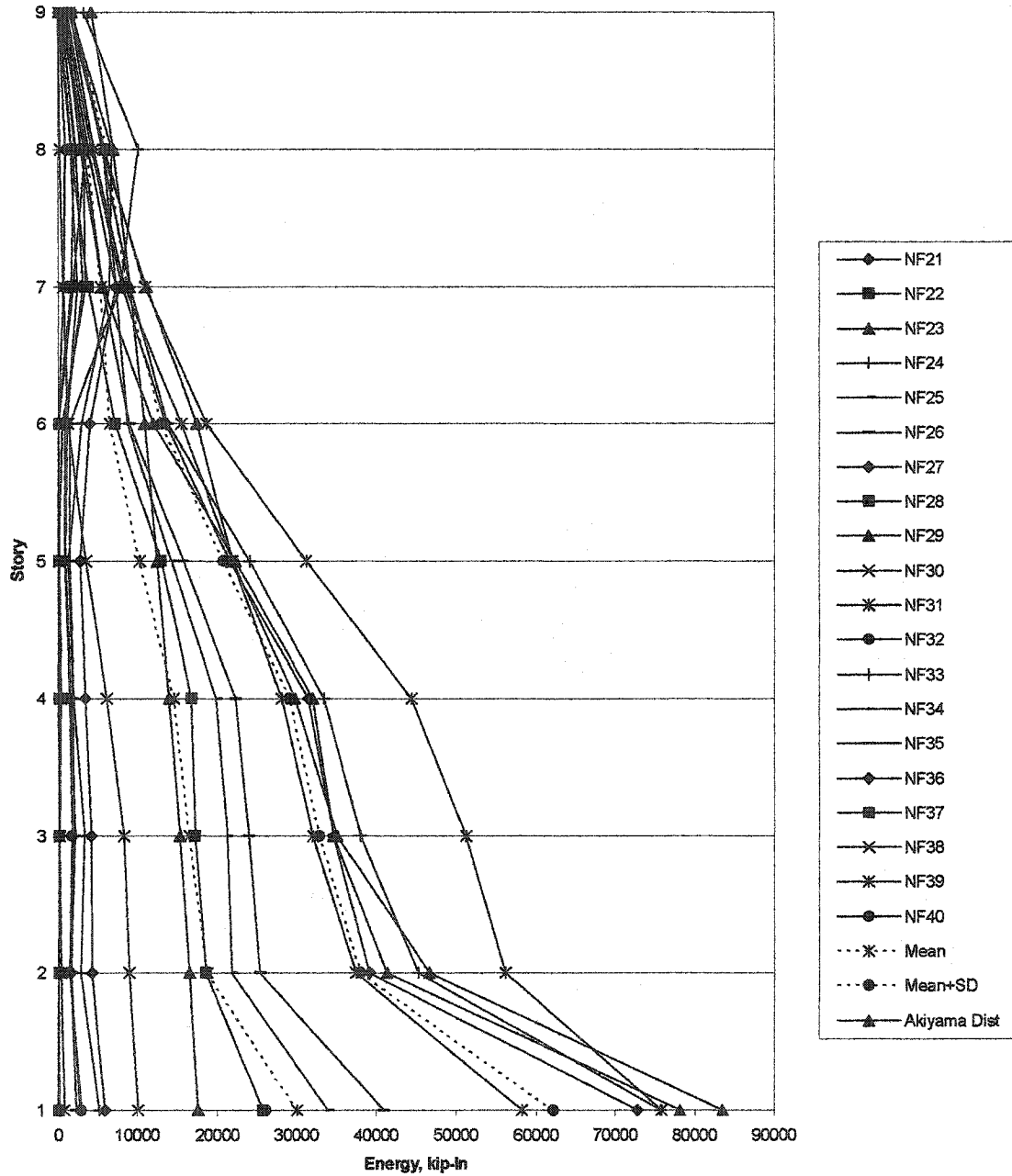
Figure 6.5 Nine Story Building Energies from SAC Near Fault Records

**20 Story Building
Hysteretic Energy vs. Height
10/50 Records**

Legend: LA01, LA02, LA03, LA04, LA05, LA06, LA07, LA08, LA09, LA10, LA11, LA12, LA13, LA14, LA15, LA16, LA17, LA18, LA19, LA20, Mean, Mean+SD
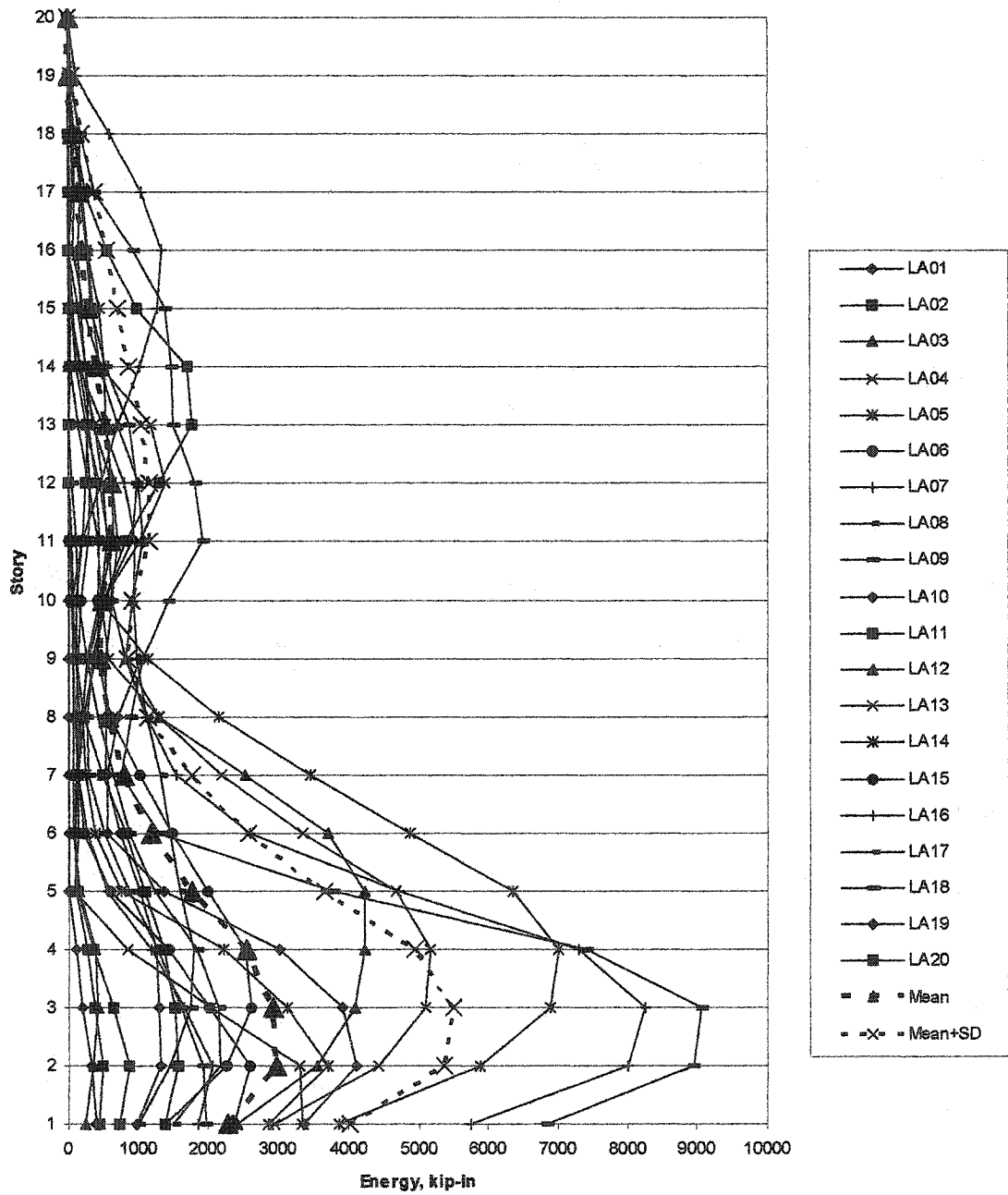
Figure 6.6 Twenty Story Building from SAC 10/50 Records

67

20 Story Building
Hysteretic Energy vs. Height
Near Fault Records
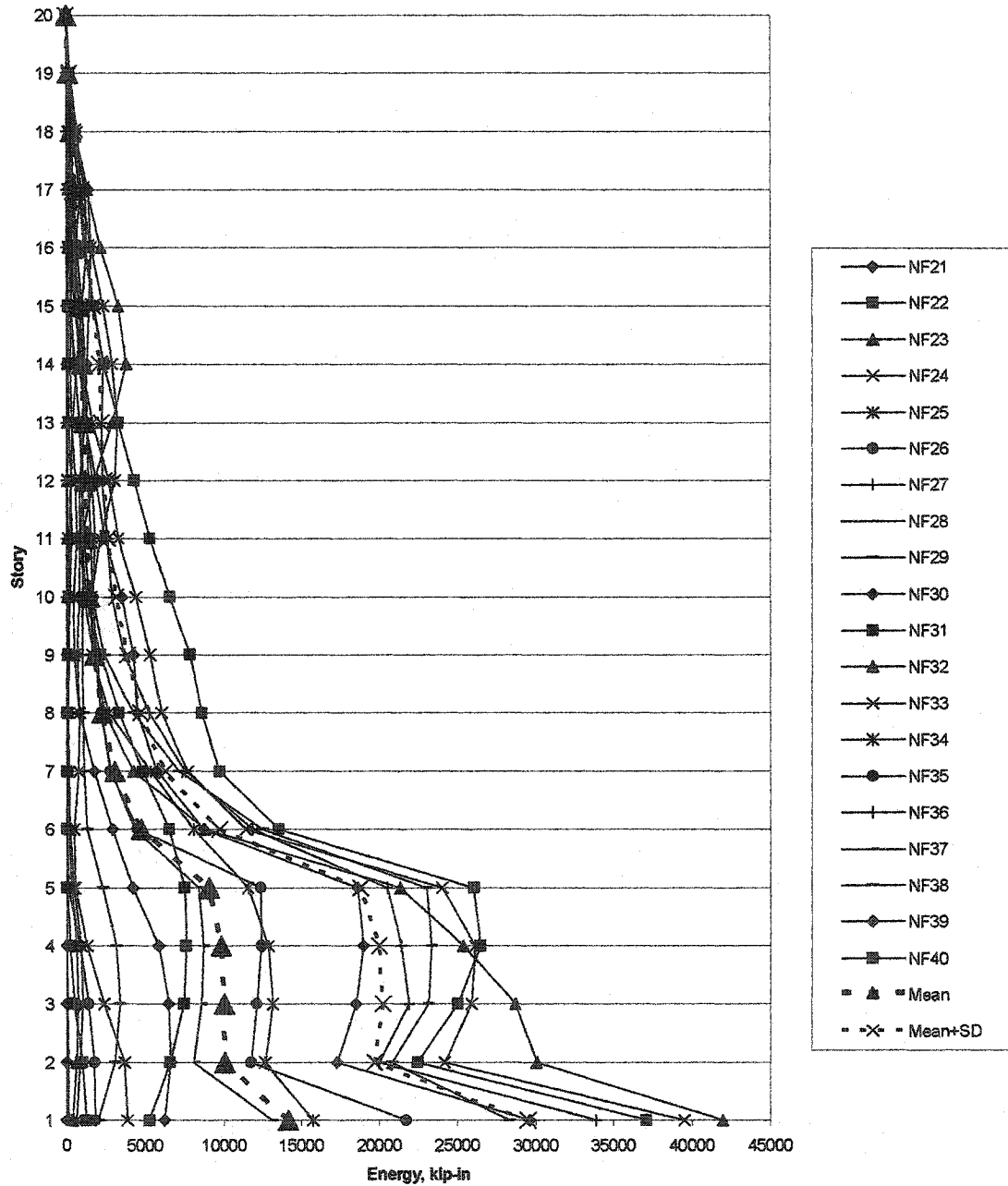
Figure 6.7 Twenty Story Building Energies from SAC Near Fault Records

68

Chapter 7: Design of a Three, Nine and Twenty Story Building Frame Using an Energy Method

The minimum weight design procedure will now be discussed as it applies to each of the prototype SAC buildings. For each building frame, an energy demand is taken from the preceding charts for the 10/50 SAC records and the Near Fault SAC records. Each building frame is designed according to the energy demand for each story and inelastic time histories are run in DRAIN 2D+ to verify the resulting maximum plastic rotations.

7.1 Consideration of Vertical Loads

It might be said in passing that the inclusion of vertical loads has a minimal effect on the hysteretic energy demands. DRAIN 2D+ runs were made with and without vertical loads and the difference between the resulting energies was on the order of a low single digit percentage.

However, to design a beam-column according to the American Institute of Steel Construction (AISC) Manual it is necessary to include vertical load and bending effects. To do this, the equations for beam-column interaction according to the AISC Load and Resistance Factor Design (LRFD) were used (AISC 1997). Similar equations appear in FEMA documents (FEMA 1997). The vertical loads for each building type were first calculated and applicable load factors imposed. The LRFD interaction equations depend upon $P_u/\varphi P_n$. For $P_u/\varphi P_n$ less than .2 and from Chapter H in the LRFD Manual,

69

$$\frac{P_u}{2\phi_c P_n} + \frac{M_u}{\phi_b M_n} \le 1.0 \qquad (7.1)$$

From Chapter E,

$$\phi_c = .85 \qquad P_n = A_g F_{cr} \qquad F_{cr} = (.658^{\lambda_c^2})F_y \qquad (7.2)$$

$$\lambda_c = \frac{kl}{r\pi}\sqrt{\frac{F_y}{E}} \qquad (7.3)$$

These factors obviously will vary with the section selected. λ_c is less than 1.5 in these equations. If one rearranges the initial Equation 7.1 above,

$$\frac{M_u}{\phi_b M_n} \le 1.0 - \frac{P_u}{2\phi_c P_n} \qquad (7.4)$$

$$M_n \ge \frac{M_u}{\phi_b (1.0 - \frac{P_u}{2\phi_c P_n})} \qquad (7.5)$$

The factor $\dfrac{1}{\phi_b(1.0 - \dfrac{P_u}{2\phi_c P_n})}$ becomes the increase factor on the required M_u to account

for the reduction in section capacity due to vertical loads.

Likewise, for $P_u/\phi P_n$ greater than .2,

$$\frac{P_u}{\phi_c P_n} + \frac{8}{9}\frac{M_u}{\phi_b M_n} \le 1.0 \qquad (7.6)$$

$$\frac{8}{9}\frac{M_u}{\phi_b M_n} \le 1.0 - \frac{P_u}{\phi_c P_n} \qquad (7.7)$$

70

$$M_n \geq \frac{\frac{8}{9}M_u}{\phi_b(1.0 - \frac{P_u}{\phi_c P_n})} \qquad (7.8)$$

Figures 7.1, 7.2, and 7.3 show the calculations to establish the modification factors to account for vertical load effects for the prototype SAC buildings. This also insures that the plastic moment capacity of the columns is larger than the beams to produce a "strong column/weak beam" configuration. The columns in the figures that indicate "Axial Load" are from the computer run for the record closest to the M+SD for each building. They include factored dead and live loads plus the axial load from the overturning due to the earthquake forces. The "increase factor" for columns is essentially 1.20 to 1.30 for the three story and nine story buildings and is fairly constant. The factors for these buildings were somewhat insensitive to the axial load. They were approximately the same just considering dead load plus live load. The effects of axial load become quite significant for the twenty story building. It can be seen in Figure 7.3 that the necessary increase in the beam plastic moments exceeds 2 and even 3 at the bottom stories. These factors rely on the magnitude of the axial load, however, when analyzed with a Near Fault record they did not change appreciably.

It is important to note that the prototype building frames are already designed for the effects of secondary moments from vertical loads (P-Δ analysis) as part of the SAC analysis.

Three Story SAC Building
Vertical Load Effects

Exterior Column of Frame

Story	Initial Col	ry	Area	Z	Axial Load	lambda	Fcr	phi*Pn	Factor
1	W14x257	4.13	75.6	487	348	0.499241	45.04683	2894.709	1.182171
2	W14x257	4.13	75.6	487	209	0.499241	45.04683	2894.709	1.152725
3	W14x257	4.13	75.6	487	72	0.499241	45.04683	2894.709	1.125103

Interior Column of Frame

Story	Initial Col	ry	Area	Z	Axial Load	lambda	Fcr	phi*Pn	Factor
1	W14x311	4.2	91.4	603	240	0.490921	45.20244	3511.777	1.150422
2	W14x311	4.2	91.4	603	147	0.490921	45.20244	3511.777	1.134863
3	W14x311	4.2	91.4	603	55	0.490921	45.20244	3511.777	1.119881

Figure 7.1 Three Story Building Vertical Load Effects from SAC 10/50 Record

72

Nine Story SAC Building
Vertical Load Effects

Exterior Column of Frame

Story	Initial Col	ry	Area	Z	Axial Load	lambda	Fcr	phi*Pn	Factor
1	W14x370	4.27	109	736	1212	0.668593	41.46808	3842.017	1.533875
2	W14x370	4.27	109	736	1031	0.482873	45.35095	4201.766	1.391416
3	W14x370	4.27	109	736	868	0.482873	45.35095	4201.766	1.323385
4	W14x283	4.17	83.3	542	735	0.494453	45.13664	3195.9	1.363605
5	W14x283	4.17	83.3	542	593	0.494453	45.13664	3195.9	1.289214
6	W14x257	4.13	75.6	487	440	0.499241	45.04683	2894.709	1.202502
7	W14x257	4.13	75.6	487	279	0.499241	45.04683	2894.709	1.167368
8	W14x233	4.1	68.5	436	163	0.502894	44.97786	2618.836	1.1468
9	W14x233	4.1	68.5	436	66	0.502894	44.97786	2618.836	1.125291

Interior Column of Frame

Story	Initial Col	ry	Area	Z	Axial Load	lambda	Fcr	phi*Pn	Factor
1	W14x500	4.43	147	1050	739	0.465433	45.66597	5705.963	1.188045
2	W14x455	4.38	134	936	643	0.470746	45.571	5190.537	1.184477
3	W14x455	4.38	134	936	560	0.470746	45.571	5190.537	1.174467
4	W14x370	4.27	109	736	480	0.482873	45.35095	4201.766	1.178421
5	W14x370	4.27	109	736	398	0.482873	45.35095	4201.766	1.166351
6	W14x283	4.17	83.3	542	312	0.494453	45.13664	3195.9	1.168131
7	W14x283	4.17	83.3	542	228	0.494453	45.13664	3195.9	1.152211
8	W14x257	4.13	75.6	487	147	0.499241	45.04683	2894.709	1.140059
9	W14x257	4.13	75.6	487	62	0.499241	45.04683	2894.709	1.123139

Figure 7.2 Nine Story Building Vertical Load Effects from SAC 10/50 Record

73

20 Story SAC Building
Vertical Load Effects

Exterior Column of Frame

Story	Initial Col	ry	Area	Z	Axial Load	lambda	Fcr	phi*Pn	Factor
1	2" Box	5.37	104	511	1985	0.531637	44.42154	3926.865	2.123324
2	1.25" Box	5.64	68.75	355.5	1868	0.365579	47.27986	2762.917	3.241712
3	1.25" Box	5.64	68.75	355.5	1747	0.365579	47.27986	2762.917	2.85561
4	1.25" Box	5.64	68.75	355.5	1621	0.365579	47.27986	2762.917	2.54052
5	1" Box	5.73	56	294.5	1492	0.359837	47.36236	2254.449	3.104696
6	1" Box	5.73	56	294.5	1357	0.359837	47.36236	2254.449	2.637668
7	1" Box	5.73	56	294.5	1228	0.359837	47.36236	2254.449	2.306176
8	1" Box	5.73	56	294.5	1102	0.359837	47.36236	2254.449	2.054036
9	1" Box	5.73	56	294.5	979	0.359837	47.36236	2254.449	1.855952
10	1" Box	5.73	56	294.5	858	0.359837	47.36236	2254.449	1.695137
11	1" Box	5.73	56	294.5	745	0.359837	47.36236	2254.449	1.568236
12	1" Box	5.73	56	294.5	658	0.359837	47.36236	2254.449	1.482773
13	1" Box	5.73	56	294.5	572	0.359837	47.36236	2254.449	1.40698
14	.75" Box	5.83	42.75	228.7	486	0.353665	47.44975	1724.205	1.462129
15	.75" Box	5.83	42.75	228.7	403	0.353665	47.44975	1724.205	1.370276
16	.75" Box	5.83	42.75	228.7	322	0.353665	47.44975	1724.205	1.29112
17	.75" Box	5.83	42.75	228.7	243	0.353665	47.44975	1724.205	1.222258
18	.75" Box	5.83	42.75	228.7	168	0.353665	47.44975	1724.205	1.163353
19	.75" Box	5.83	42.75	228.7	97	0.353665	47.44975	1724.205	1.14327
20	.50" Box	5.92	29	157.75	38	0.348288	47.52476	1171.485	1.129429

Figure 7.3 Twenty Story Building Vertical Load Effects from SAC 10/50 Record

74

20 Story SAC Building
Vertical Load Effects

Interior Column of Frame

Story	Initial Col	ry	Area	Z	Axial Load	lambda	Fcr	phi*Pn	Factor
1	W24x335	3.23	98.4	1020	1476	0.883868	36.05487	3015.63	2.056606
2	W24x335	3.23	98.4	1020	1431	0.638349	42.15984	3526.249	1.767122
3	W24x335	3.23	98.4	1020	1392	0.638349	42.15984	3526.249	1.734831
4	W24x335	3.23	98.4	1020	1353	0.638349	42.15984	3526.249	1.703699
5	W24x229	3.11	67.2	676	1312	0.66298	41.59801	2376.079	2.344641
6	W24x229	3.11	67.2	676	1263	0.66298	41.59801	2376.079	2.241425
7	W24x229	3.11	67.2	676	1208	0.66298	41.59801	2376.079	2.135886
8	W24x229	3.11	67.2	676	1134	0.66298	41.59801	2376.079	2.008635
9	W24x229	3.11	67.2	676	1031	0.66298	41.59801	2376.079	1.854823
10	W24x229	3.11	67.2	676	916	0.66298	41.59801	2376.079	1.708732
11	W24x192	3.07	56.3	559	808	0.671618	41.39778	1981.091	1.773218
12	W24x192	3.07	56.3	559	720	0.671618	41.39778	1981.091	1.649481
13	W24x192	3.07	56.3	559	650	0.671618	41.39778	1981.091	1.562737
14	W24x131	2.97	38.5	370	566	0.694231	40.86605	1337.341	1.820476
15	W24x131	2.97	38.5	370	466	0.694231	40.86605	1337.341	1.611548
16	W24x131	2.97	38.5	370	364	0.694231	40.86605	1337.341	1.442668
17	W24x117	2.94	34.4	327	270	0.701315	40.6973	1189.989	1.358156
18	W24x117	2.94	34.4	327	189	0.701315	40.6973	1189.989	1.206959
19	W24x117	2.94	34.4	327	108	0.701315	40.6973	1189.989	1.163929
20	W24x84	1.95	27.7	224	44	1.057368	31.31423	737.2934	1.145285

Figure 7.3 Twenty Story Building Vertical Load Effects from SAC 10/50 Record (Continued)

75

7.2 Design of a Three Story Building

Similar to what has been presented for the previous two story building, several constraint equations are formulated for use in the minimum weight subroutine. The original frame configuration is shown in Figure 7.4. The constraint equations are drawn from the mechanisms shown in the following Figures 7.5 and 7.7. First, as shown in
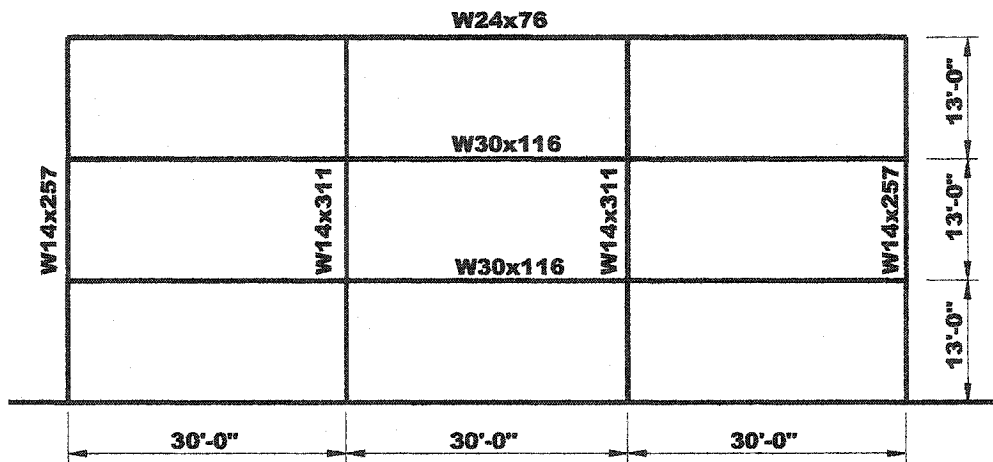
Figure 7.4 Three Story Building – Original Sizes

Figure 7.5 for the top story, the mechanism #1 is a sway mechanism with hinges in the columns. The equation for the hysteretic energy, limiting the plastic rotation to .03 radians is,

$$HE = (4M_{CI} + 4M_{CE}) * 4 * .03 \tag{7.9}$$

In this and the examples that follow, M_{CI} equals the interior column plastic moment capacity; that is, columns interior to the frame. M_{CE} equals the column plastic moment

76

capacity for the frame exterior column, usually the corner column. M_{BM} equals the plastic moment capacity of the beam at any given level. In the following examples
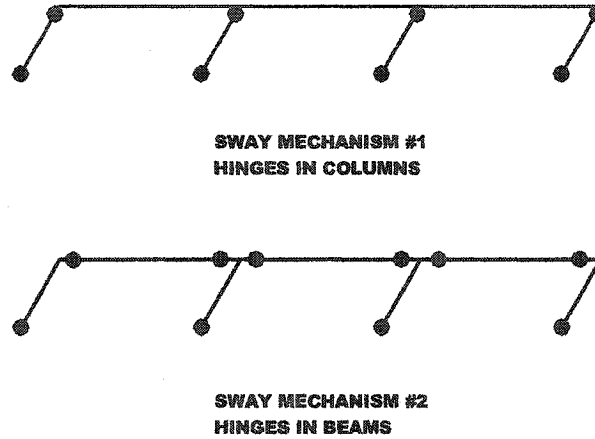
Figure 7.5 Three Story Top Story Mechanisms

col above or *(abv)* will be used to indicate the plastic column demand from the story above. Using the mean plus one standard deviation energy demand from the chart in Figure 6.2, for the top story the energy demand is 1377 kip-inches. Therfore,

$$M_{CI} + M_{CE} = HE/(16*.03*12) = 239 \ \text{kip-feet}$$

$$M_{CI} + M_{CE} - 239 \geq 0 \tag{7.10}$$

Mechanism #2 is a sway mechanism with hinges in the ends of the beams. So,

$$HE = (2M_{CI} + 2M_{CE} + 6M_{BM})*4*.03$$

$$M_{CI} + M_{CE} + 3M_{BM} = HE/(8*.03*12) = 478 \ \text{kip feet}$$

$$M_{CI} + M_{CE} + 3M_{BM} - 478 \geq 0 \tag{7.11}$$

77

Similar additional constraints are imposed as was done for the two story building. Namely, it is desired that the minimum column plastic moment capacity is greater than that for the beam. Also, an additional constraint is imposed that the exterior column plastic moment is at least half the interior column plastic moment for practical considerations. So these additional constraints become,

$$M_{CE} - M_{BM} \geq 0 \qquad (7.12)$$

$$M_{CE} - .50M_{CI} \geq 0 \qquad (7.13)$$

Finally, the weight function $f = 26M_{CI} + 26M_{CE} + 90M_{BM}$. Therefore, the initial input matrix for the Simplex minimum weight procedure becomes,

COEFFICIENTS FOR

M_{CI} M_{CE} M_{BM}

$$\begin{bmatrix} 1 & 1 & 0 & | & -239 \\ 1 & 1 & 3 & | & -478 \\ \hline 0 & 1 & -1 & | & 0 \\ -.5 & 1 & 0 & | & 0 \\ \hline 1 & 0 & 0 & | & 0 \\ 0 & 1 & 0 & | & 0 \\ 0 & 0 & 1 & | & 0 \\ \hline 26 & 26 & 90 & | & 0 \end{bmatrix}$$

---- WORK EQUATIONS

---- CONSTRAINT EQUATIONS

---- PLACEHOLDERS FOR UNKNOWNS
UNKNOWNS WILL APPEAR IN FINAL
MATRIX IN LAST COLUMN

---- WEIGHT FUNCTION
MIN WEIGHT APPEARS IN FINAL
MATRIX IN LAST COLUMN.

Figure 7.6 Formulation of Simplex Matrix for Three Story Building

78

The resulting required plastic moments are M_{CI} = 159 kip-feet; M_{CE} = M_{BM} = 80 k-ft.

The plastic moment capacities of the current beam and columns are all greater than

these values, therefore, no increase in member size is recommended. Note that for the

column required moments, the axial load factor should be applied.

The second story sway mechanisms are those shown in Figure 7.7. For

mechanism #1 with hinges all in the columns,

$$HE = (4M_{CI} + 4M_{CE} - 2M_{CI}(abv) - 2M_{CE}(abv)) * 4 * .03$$

$$M_{CI} + M_{CE} = HE/(16 * .03 * 12) + .5M_{CI}(abv) + .5M_{CE}(abv) \qquad (7.14)$$

For mechanism #2 with hinges in beams,

$$HE = (2M_{CI} + 2M_{CE} + 6M_{BM} - 2M_{CI}(abv) - 2M_{CE}(abv)) * 4 * .03$$

$$M_{CI} + M_{CE} + 3M_{BM} = HE/(8 * .03 * 12) + M_{CI}(abv) + M_{CE}(abv) \quad (7.15)$$

For a second story hysteretic energy demand of 3555 and the column plastic

moment demands from above, the initial matrix for the Simplex algorithm is:

$$\begin{bmatrix} 1 & 1 & 0 & -239 \\ 1 & 1 & 3 & -478 \\ 0 & 1 & -1 & 0 \\ -.5 & 1 & 0 & 0 \\ 1 & 0 & 0 & 0 \\ 0 & 1 & 0 & 0 \\ 0 & 0 & 1 & 0 \\ 26 & 26 & 90 & 0 \end{bmatrix}$$

From the Simplex algorithm, M_{CE} = M_{BM} = 246 kip-feet; M_{CE} = 491 k-ft. Original sizes

are adequate. Similarly, for the first story with a hysteretic energy demand of 10,601

kip-inches, M_{CE} = M_{BM} = 736 kip-feet; M_{CE} = 1473 k-ft. Likewise, with the increase

79

factor for columns (approximately 1.20), the original sizes appear adequate. Given that the original sizes appear to be adequate for the energy demand from the 10/50 SAC records, nonlinear time history analyses were performed for records closest to the Mean + Standard Deviation (M+SD) energy demand. The results of those analyses are presented in Figure 7.8. It is apparent that all plastic rotations are less than .03 radians.
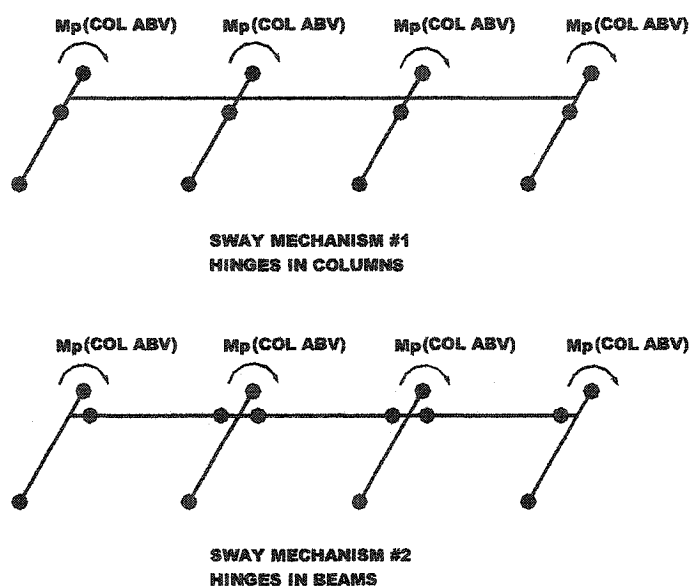
Figure 7.7 Three Story Building Typical Story Mechanisms

Similarly, the mean hysteretic energy from the Near Fault records is used as the demand for this building. The same procedure is followed to determine the required plastic moments for the beams and columns for each story. Then the records with the closest energy to this mean are used to make a nonlinear time history run to check the plastic rotations. The results of these analyses are shown in Figure 7.9 and 7.10. First, the frame is analyzed with the listed Near Fault records using the original frame sizes in

80

Figure 7.9. Then, the results of the energy based design sizes and resulting plastic

rotations are presented in Figure 7.10.

[ ] = RESULTING MAX. PLASTIC ROTATIONS BASED ON RECORD LA14
{ } = RESULTING MAX. PLASTIC ROTATIONS BASED ON RECORD LA13

THREE STORY BUILDING - ORIGINAL SIZES

**Figure 7.8 Three Story Building Plastic Rotations from 10/50 Records
with Original Sizes**

[ ] = RESULTING MAX. PLASTIC ROTATIONS BASED ON RECORD NF37
{ } = RESULTING MAX. PLASTIC ROTATIONS BASED ON RECORD NF21

THREE STORY BUILDING - ORIGINAL SIZES

**Figure 7.9 Three Story Building Plastic Rotations from Near Fault Records
with Original Sizes**

[.046]   [.051]   W30x99

{.022}   {.016}

[.050]   [.055]   W33x118

{.025}   {.021}

                                        W14x550   W14x311

[.050]   [.053]   W36x135

{.025}   {.022}

[.045] {.016}   {.046} {.016}

[ ] = RESULTING MAX. PLASTIC ROTATIONS BASED ON RECORD NF37
{ } = RESULTING MAX. PLASTIC ROTATIONS BASED ON RECORD NF21

THREE STORY BUILDING - REVISED SIZES

Figure 7.10 Three Story Building Plastic Rotations from Near Fault Records with Revised Sizes

It can be seen that the sizes have increased dramatically. Also for one record, the resulting plastic rotations are less than .03 radians and the sizes seem adequate. However, the resulting rotations for run NF37 are well over .03. More will be discussed about the Near Fault records.

7.3 Design of a Nine Story Building

The design for the nine story building proceeds in a similar fashion as for the three story building. The original building frame and sizes are shown in Figure 7.11. Constraint equations are written based on probable plastic collapse mechanisms. Hysteretic energy demands are established story by story and required plastic moments are determined by the Simplex minimum weight subroutine. Proceeding as before, but

82

not repeating the same level of detail, the assumed collapse mechanisms for the top

story of the nine story building are presented in Figure 7.12. Note that the right end of

the rightmost beam is not a moment connection at every level. Rather, wide flange

columns are at each corner of the building and on the weak axis of each corner column
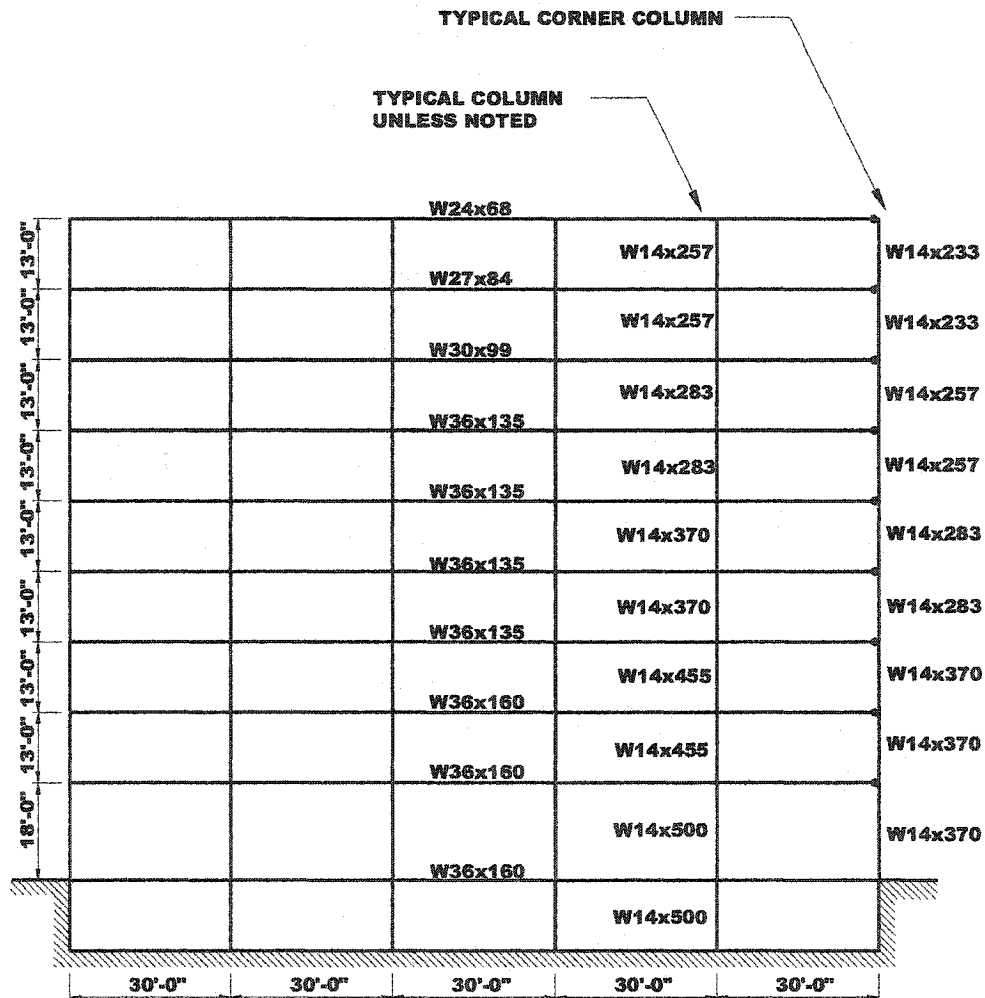
Figure 7.11 Nine Story Building – Original Sizes

SWAY MECHANISM #1
HINGES IN COLUMNS

SWAY MECHANISM #2
HINGES IN BEAMS
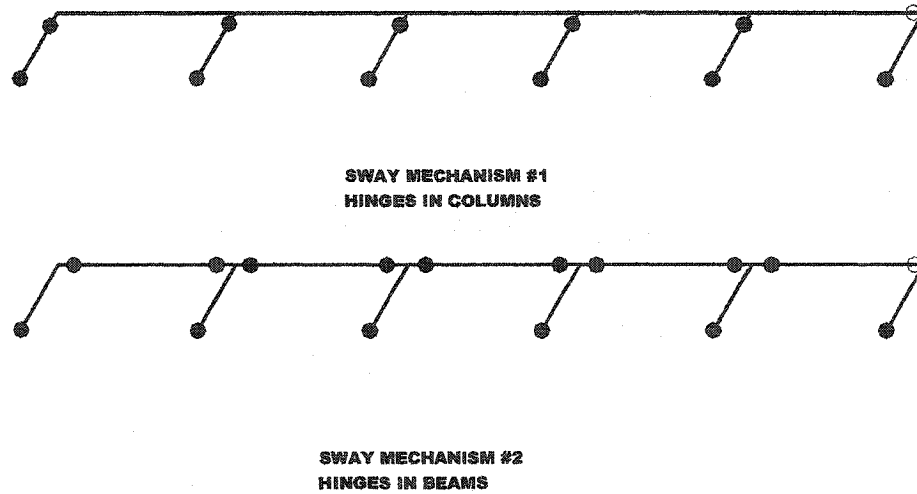
Figure 7.12 Nine Story Building Top Story Mechanisms

a standard non-moment connection is made. Each corner column is rotated 90 degrees from the adjacent corner columns and, in this way, the frames on each side of the building are the same stiffness.

Again, writing general constraint equations for each mechanism, mechanism #1 produces,

$$HE = (8M_{CI} + 3M_{CE}) * 4 * .03$$

$$8M_{CI} + 3M_{CE} = HE / (4 * .03 * 12)$$

$$4M_{CI} + 1.5M_{CE} - HE / (8 * .03 * 12) \geq 0 \qquad (7.16)$$

For mechanism #2 in Figure 7.12,

$$HE = (4M_{CI} + 2M_{CE} + 9M_{BM}) * 4 * .03$$

$$4M_{CI} + 2M_{CE} + 9M_{BM} = HE / (4 * .03 * 12)$$

$$2M_{CI} + M_{CE} + 4.5M_{BM} - HE / (8 * .03 * 12) \geq 0 \qquad (7.17)$$

84

SWAY MECHANISM #1
HINGES IN COLUMNS

SWAY MECHANISM #2
HINGES IN BEAMS
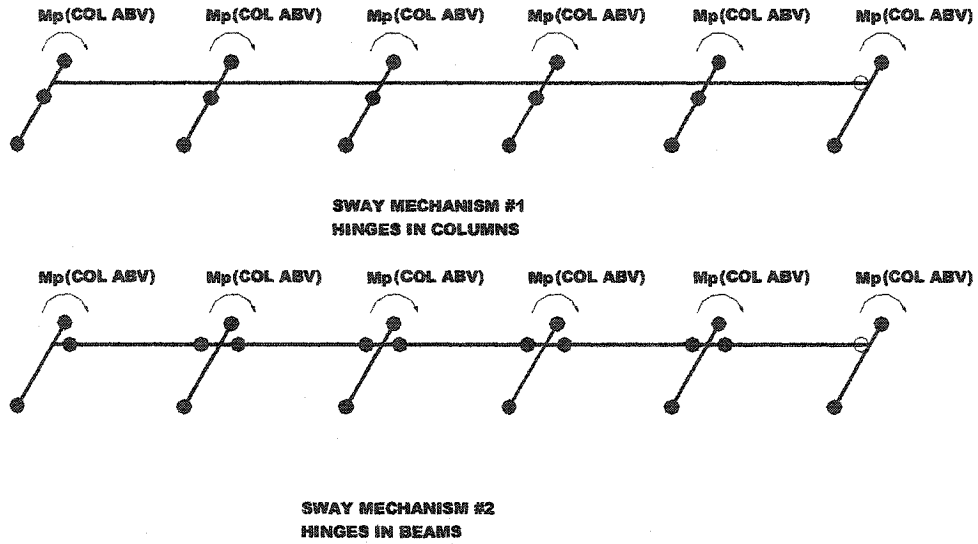
Figure 7.13 Nine Story Building Typical Story Mechanisms

For a typical floor shown in Figure 7.13 and considering first mechanism #1,

$$HE = (8M_{CI} + 3M_{CE} - 4M_{CI}(abv) - 2M_{CE}(abv)) * 4 * .03$$

$$4M_{CI} + 1.5M_{CE} = HE/(8*.03*12) + 2M_{CI}(abv) + M_{CE}(abv)$$

$$4M_{CI} + 1.5M_{CE} - HE/(8*.03*12) - 2M_{CI}(abv) - M_{CE}(abv) \geq 0 \quad (7.15)$$

For mechanism #2 for a typical floor,

$$HE = (4M_{CI} + 2M_{CE} + 9M_{BM} - 4M_{CI}(abv) - 2M_{CE}(abv)) * 4 * .03$$

$$2M_{CI} + M_{CE} + 4.5M_{BM} = HE/(8*.03*12) + 2M_{CI}(abv) + M_{CE}(abv);$$

$$2M_{CI} + M_{CE} + 4.5M_{BM} - HE/(8*.03*12)$$

$$- 2M_{CI}(abv) - M_{CE}(abv) \geq 0 \quad (7.18)$$

85

This procedure is followed story by story with the resulting required plastic moments determining the member sizes. Following the establishment of the new sizes, the building frame is reanalyzed by nonlinear time history with the records that are closest to the mean plus one standard deviation energy demand for the 10/50 records. The results of nonlinear analyses for the listed records for the original frame sizes are given in Figure 7.14. The results for the revised energy based sizes are shown in Figure 7.15. It is noteworthy to point out that the nine story building also seems adequate when examining the resulting plastic rotations from the analyses using the 10/50 earthquake records. It is very apparent that these SAC building frames have received a great deal of analysis from many researchers and subjected to many different types of analyses. For the sizes from the energy based sizes, the resulting plastic rotations are within the design criteria of .03 radians.

An important finding of this procedure must be highlighted at this point. Previous charts have shown the distribution of hysteretic energy with the height of the three, nine and twenty story prototype buildings (Figures 6.2 to 6.7). For the three story building, and even for the two story building, the mean plus one standard deviation energy was used as the energy demand for the energy design procedure. For these low rise buildings, this procedure produced very good results with plastic rotations less than .03 radians. However, for the nine story building (and later for the twenty story building) the distribution of energy reflected in the previous charts when used for design did not produce results with less than .03 radians maximum plastic rotations in a

86

[.002]   [-]   W24x68

Plastic Rotations		Beam	Column	Column
{.013} {.005} [.008] [.006]		W27x84	W14x257	W14x233
{.018} {.012} [.011] [.006]		W30x99	W14x257	W14x233
{.020} {.015} [.007] [.003]		W36x135	W14x283	W14x257
{.016} {.011} [.008] [.005]		W36x135	W14x283	W14x257
{.012} {.009} [.011] [.008]		W36x135	W14x370	W14x283
{.011} {.008} [.014] [.011]		W36x135	W14x370	W14x283
{.010} {.007} [.013] [.011]		W36x160	W14x455	W14x370
{.008} {.006} [.014] [.011]		W36x160	W14x455	W14x370
{.009} {.007}		W36x160	W14x500	W14x370
		W36x160	W14x500	

[ ] = RESULTING MAX. PLASTIC ROTATIONS BASED ON RECORD LA18
{ } = RESULTING MAX. PLASTIC ROTATIONS BASED ON RECORD LA09

NINE STORY BUILDING - ORIGINAL SIZES

Figure 7.14 Nine Story Building Plastic Rotations from 10/50 Records
With Original Sizes

consistent manner. It is very apparent that the distribution of hysteretic energy in a building frame is dependent on many factors, such as mass distribution, stiffness distribution, the manner in which the forces are applied, the specific record imposed, etc. It seems logical to distribute the energy to stories in a building by the resulting distributions established in the earlier part of this paper. However, caution is advised. The distribution represented by the charts developed earlier in this paper is essentially a

87

[-] [-] W24x68

Record LA09 / LA18		Beam	Interior Column	Exterior Column
{.002} [.020]	(-) [.011]	W27x84	W14x257	W14x233
{.008} [.023]	{.006} [.017]	W30x99	W14x257	W14x233
{.011} [.026]	{.006} [.021]	W36x135	W14x283	W14x257
{.007} [.027]	{.003} [.023]	W36x135	W14x283	W14x257
{.008} [.028]	{.005} [.023]	W36x135	W14x370	W14x283
{.011} [.021]	{.008} [.017]	W36x135	W14x370	W14x283
{.014} [.028]	{.011} [.023]	W36x260	W14x455	W14x370
{.013} [.021]	{.011} [.017]	W36x260	W14x730	W14x398
{.014}	{.011}	W36x260	W14x730	W14x398
			W14x730	

[ ] = RESULTING MAX. PLASTIC ROTATIONS BASED ON RECORD LA18
{ } = RESULTING MAX. PLASTIC ROTATIONS BASED ON RECORD LA09

NINE STORY BUILDING - REVISED SIZES

Figure 7.15 Nine Story Building Plastic Rotations from 10/50 Records With Revised Sizes

triangular one with the maximum energy at the base and decreasing with height. The result of imposing this energy distribution is that the lower stories receive the larger energy demand. The top stories consequently receive little energy demand. By applying the energy demand in this manner, the lower stories are strengthened. This means that the revised lower beams and columns will experience less inelastic behavior.

88

Therefore, yielding and consequently hysteretic energy is moved to upper stories. The result of energy demand moving up is that plastic rotations are increased in the upper stories of a building. This is, in fact, exactly what happened in numerous nonlinear time histories. What emerged as a key consideration is the proper energy distribution for the design phase of the energy analysis. Clearly, the energy demand needed to be increased in the upper stories while still maintaining a consistent energy demand in the lower stories. Through many nonlinear time history analyses, many different distributions of energy were tried with mixed results. Professor Akiyama proposed a triangular distribution based on a higher level polynomial (Akiyama and Kato 1986); a triangular distribution based on the first mode shape was tried. The distribution that produced the best and most consistent results was a simple one, namely a uniform distribution that applied the same energy to each story. Rather than pushing energy up from lower stories to upper stories, a uniform distribution applied the energy demand in a uniform way. So the total hysteretic energy demand for the building can simply be divided by the number of stories and applied equally to each. This is the recommended distribution for the proposed energy design procedure.

In keeping with previous building frames, the hysteretic energy demand for the SAC Near Fault records was imposed. Following the same procedure as above but using the Near Fault mean energy applied to each story equally, Figures 7.16 and 7.17 show the resulting member sizes and plastic rotations from nonlinear analyses based on records with energies close to the mean. Figure 7.16 shows member rotations for the

89

original sizes; Figure 7.17 shows the rotations for the energy based revised sizes.

Again, plastic rotations are within .03 for the revised sizes.

[.005]	[-]		W24x68		
{-} [.010]	{-} [.006]		W27x84	W14x257	W14x233
{.006} [.013]	{.010} [.011]		W30x99	W14x257	W14x233
{.011} [.019]	{.013} [.012]		W36x135	W14x283	W14x257
{.018} [.035]	{.017} [.030]		W36x135	W14x283	W14x257
{.028} [.046]	{.028} [.042]		W36x135	W14x370	W14x283
{.037} [.053]	{.037} [.050]		W36x135	W14x370	W14x283
{.044} [.051]	{.045} [.048]		W36x160	W14x455	W14x370
{.043} [.048]	{.044} [.045]		W36x160	W14x455	W14x370
{.039}	{.039}		W36x160	W14x500	W14x370
				W14x500	

[ ] = RESULTING MAX. PLASTIC ROTATIONS BASED ON RECORD NF40
{ } = RESULTING MAX. PLASTIC ROTATIONS BASED ON RECORD NF37
NINE STORY BUILDING - ORIGINAL SIZES

Figure 7.16 – Nine Story Building Plastic Rotations from Near Fault Records with Original Sizes

90

```
[-]          [-]                    W36x170

{.004}   {-}                                    W14x455              W14x342
[.005]   [.002]            W36x170

{.016}   {.012}                                 W14x455              W14x342
[-]      [-]               W36x393

{.008}   {-}                                    W36x485              W36x665
[.001]   [-]               W36x393

{.009}   {.006}                                 W36x485              W36x665
[-]      [-]               W36x485

{.012}   {.010}                                 W36x720              W36x527
[-]      [-]               W36x485

{.014}   {.014}                                 W36x720              W36x527
[-]      [-]               W36x650

{.015}   {.012}                                 W36x848              W36x720
[-]      [-]               W36x650

{.016}   {.015}                                 W36x848              W36x720
[-]      [-]               W36x720

{.015}   {.011}                                 W36x848              W36x848
                          W36x720

                                                W36x848
```

[ ] = RESULTING MAX. PLASTIC ROTATIONS BASED ON RECORD NF40
{ } = RESULTING MAX. PLASTIC ROTATIONS BASED ON RECORD NF37

NINE STORY BUILDING - REVISED SIZES

Figure 7.17 – Nine Story Building Plastic Rotations from Near Fault Records
with Revised Sizes

7.4 Design of a Twenty Story Building

The design check for the twenty story SAC building proceeds similarly. The original building frame and member sizes are shown in Figure 7.19.

Again, constraint equations are written for the top story for mechanism #1 shown in Figure 7.18.

SWAY MECHANISM #1
HINGES IN COLUMNS

SWAY MECHANISM #2
HINGES IN BEAMS
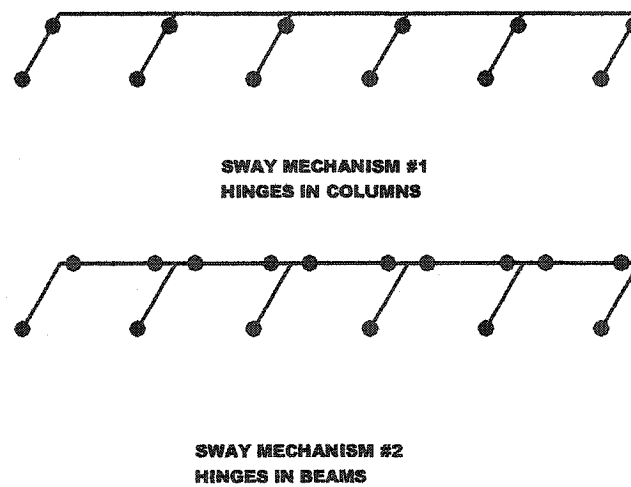
Figure 7.18 Twenty Story Building Top Story Mechanisms

This produces,

$$HE = (8M_{CI} + 4M_{CE}) * 4 * .03$$

$$8M_{CI} + 4M_{CE} = HE/(4 * .03 * 12)$$

$$2M_{CI} + M_{CE} - HE/(16 * .03 * 12) \geq 0 \tag{7.19}$$

92

Figure 7.19 Twenty Story Building Original Sizes

For mechanism #2 in Figure 7.18,

$$HE = (4M_{CI} + 2M_{CE} + 10M_{BM}) * 4 * .03$$

$$4M_{CI} + 2M_{CE} + 10M_{BM} = HE/(4*.03*12)$$

$$2M_{CI} + M_{CE} + 5M_{BM} - HE/(8*.03*12) \geq 0 \qquad (7.20)$$

For a typical floor shown in Figure 7.20 and considering first mechanism #1,

$$HE = (8M_{CI} + 4M_{CE} - 4M_{CI}(abv) - 2M_{CE}(abv)) * 4 * .03$$

$$4M_{CI} + 2M_{CE} = HE/(8*.03*12) + 2M_{CI}(abv) + M_{CE}(abv)$$

$$4M_{CI} + 2M_{CE} - HE/(8*.03*12) - 2M_{CI}(abv) - M_{CE}(abv) \geq 0 \qquad (7.21)$$

For mechanism #2 for a typical floor,

$$HE = (4M_{CI} + 2M_{CE} + 10M_{BM} - 4M_{CI}(abv) - 2M_{CE}(abv)) * 4 * .03$$

$$2M_{CI} + M_{CE} + 5M_{BM} = HE/(8*.03*12) + 2M_{CI}(abv) + M_{CE}(abv)$$

$$2M_{CI} + M_{CE} + 5M_{BM} - HE/(8*.03*12)$$

$$- 2M_{CI}(abv) - M_{CE}(abv) \geq 0 \qquad (7.22)$$

Results for the energy demands for the twenty story building for the 10/50 and Near Fault records are presented in Figures 7.21 and 7.22.

A comment in passing is that, for all buildings, the interstory drift indices (IDI) were checked and found to be with reasonable limits. Therefore, it appears that limiting the maximum plastic rotations also successfully limits the interstory drifts.
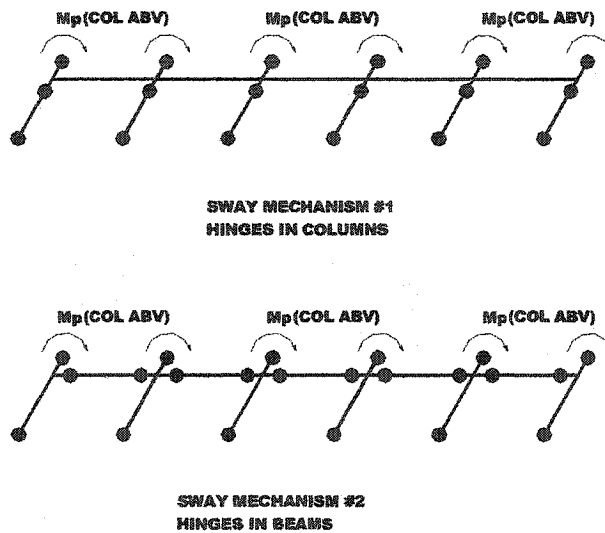
Figure 7.20 Twenty Story Building Typical Story Mechanisms

7.5 Note on Near Fault Records

It is appropriate to comment at this point about the results of the analyses for Near Fault (NF) records. At this stage, the energy based design procedure for the two story building, the three story, nine story, and twenty story SAC buildings seem to be working quite well for the 10/50 records. All plastic rotations are less than the required .03 radians when checking the resulting energy based member sizes by nonlinear time history. The nine story energy based design appears to be very adequate when checked for the Near Fault records. However, plastic rotations for the three story and twenty story buildings still result in plastic rotations of greater than .03 radians when analyzed for some of the Near Fault SAC records (see Figures 7.10 and 7.22).

Figure 7.21 Twenty Story Building Plastic Rotations from 10/50 Records

96

TYPICAL CORNER COLUMN

TYPICAL COLUMN
UNLESS NOTED

[-]	W21x50			
[.008]	W24x62		W24x84	15"□x.5"
[.008]	W27x84		W24x84	15"□x.5"
[.009]	W27x84		W24x117	15"□x.75"
[.009]	W30x99		W24x117	15"□x.75"
[.011]	W30x99		W24x131	15"□x.75"
[.012]	W30x99		W24x131	15"□x.75"
[.011]	W30x99		W24x131	15"□x.75"
[.007]	W30x99		W24x192	15"□x1"
[.008]	W30x99		W24x192	15"□x1"
[.011]	W30x109		W24x192	15"□x1"
[.014]	W30x109		W24x229	15"□x1"
[.017]	W30x109		W24x229	15"□x1"
[.022]	W30x109		W24x229	15"□x1"
[.027]	W30x109		W24x229	15"□x1"
[.036]	W30x109		W24x229	15"□x1"
[.060]	W30x99		W24x229	15"□x1"
[.057]	W30x99		W24x335	15"□x1.25"
[.051]	W30x99		W24x335	15"□x1.25"
[.043]	W30x99		W24x335	15"□X1.25"
	W30x99		W24x335	15"□X2"
	W21X44		W24x335	
			W24x335	

[ ] = RESULTING MAX. PLASTIC ROTATIONS
BASED ON RECORD NF037

TWENTY STORY BUILDING - ORIGINAL SIZES

Figure 7.22 Twenty Story Building Plastic Rotations from Near Fault Record

97

It can be noted that the scatter of the energies for the Near Fault records is quite large. In other words, there seems to be more variability in these records than the 10/50 records. Near Fault records seem, by nature, to be highly variable by the admission of some of the literature produced by the SAC Joint Venture (Sommerville 1997). It is important to note that these records are not actual records. They are scaled and some modification is performed on them. The following Tables 7.1 and 7.2 list available information relative to the 10/50 and Near Fault SAC records. In considering these records, an additional set of Near Fault records was examined as provided by the PEER (Pacific Earthquake Engineering Research) Center. These records are listed in Table 7.3. It is interesting to note that the PEER Center divides their Near Fault records into several categories – one sided pulses, two sided, and multiple sided pulses, in addition to soil and rock sites. Table 7.2 lists background information on the SAC Near Fault records. The first half contains records from all over the world, including those from Iran and Turkey. The second half are simulated records based on the Elysian Park and Palos Verdes faults. These simulated records are the ones that give the most trouble in the energy based design. One would have to question the use of records for areas such as Elysian Park and Palos Verdes, as they are not historically significant records. A representative group of the PEER records were used to check the energy based sizes for the three and twenty story SAC buildings. They are highlighted in bold in Table 7.3. The results of these analyses are presented in Figures 7.23 and 7.24. For the three story building, the only record that produces excessive plastic rotations is the record obtained at Takatori, Japan. For other records, plastic rotations are very close to the allowable

98

rotation of .03 radians. If one considers the allowable plastic rotations calculated previously from FEMA 350, the allowable rotation for the three story building is a larger value of .039 radians which would deem the frame adequate for three of the four records. Likewise, Figure 7.20 lists plastic beam rotations for the twenty story building on the left side of the figure. Column rotations are not critical. Again, it can be seen that the plastic rotations are much less critical for these actual records. Maximum rotations are present for the Los Gatos and James Road (El Centro) records. Los Gatos is especially known to be a very strong record with a great degree of input energy. Therefore, it appears that the plastic rotations for the twenty story building subjected to Near Fault records are within acceptable limits for two of these records and exceeded for two of the Near Fault records.

Another study was made at this point for the twenty story building. The plastic rotations due to the Near Fault (NF) records are indicated in Figures 7.22 and 7.24. However, the energy design procedure outlined previously did not result in an increase in member sizes using the NF uniform energy distribution at each story. Many distributions were tried for the twenty story building. While maintaining the same total hysteretic energy demand, various and different distributions with height were applied. Even step distributions were tried reflecting the distributions shown in the earlier charts indicating little energy demand in the upper ten stories of the building.

The only NF distribution that did result in an increase in member sizes was that from the chart in Figure 6.7 using the mean plus standard deviation energy values. However, applying this distribution and following the energy design procedure resulted

in excessive plastic rotation in the stories just above the strengthened stories. Several

design iterations were performed with the energy from the previous iteration considered

as the demand for the next iteration. Figure 7.25 shows the resulting energy

distributions from these iterations. The distribution from the calculated energy plot,

Figure 6.7, is shown as the NF Mean + Standard Deviation (M+SD). SAC Near Fault

record NF039 was used as the input record as distribution for it was very close to the

M+SD distribution. The resulting energy distribution for the original sizes subjected to

this record are listed in the chart as "Original Sizes." In the first iteration, the bottom

four floor beams were increased in size. The second iteration energy distribution from

the resulting change in sizes is shown in the figure as "Second Iteration." The energy

demand for this iteration increases dramatically at the fifth story, just above the

strengthened floor beams. This distribution resulted in an increase in floor beam sizes

for the bottom six floors. Corner columns were also increased in size extending the

larger box sections from below up several floors. In addition to the axial load factor

mentioned previously, a strain hardening factor was used for all the columns as

described in an earlier paper by Anderson and Gupta (Anderson 1972). It was

attempted to assure as much as possible that hinges formed in the beams and the use of

these two factors was quite effective. In all, five design iterations were performed

checking the energy at each step. It can be seen from Figure 7.25 that successive

iterations moved the energy up the frame. In fact, all but the top several stories

SAC Name	Record	Magnitude	Distance (km)	Scale Factor	Number of Points	DT (sec)	Duration (sec)	PGA (cm/sec^2)
LA01	Imperial Valley, 1940, El Centro	6.9	10	2.01	2674	0.02	39.38	452.03
LA02	Imperial Valley, 1940, El Centro	6.9	10	2.01	2674	0.02	39.38	662.88
LA03	Imperial Valley, 1979, Array #05	6.5	4.1	1.01	3939	0.01	39.38	386.04
LA04	Imperial Valley, 1979, Array #05	6.5	4.1	1.01	3939	0.01	39.38	478.65
LA05	Imperial Valley, 1979, Array #06	6.5	1.2	0.84	3909	0.01	39.08	295.69
LA06	Imperial Valley, 1979, Array #06	6.5	1.2	0.84	3909	0.01	39.08	230.08
LA07	Landers, 1992, Barstow	7.3	36	3.2	4000	0.02	79.98	412.98
LA08	Landers, 1992, Barstow	7.3	36	3.2	4000	0.02	79.98	417.49
LA09	Landers, 1992, Yermo	7.3	25	2.17	4000	0.02	79.98	509.7
LA10	Landers, 1992, Yermo	7.3	25	2.17	4000	0.02	79.98	353.35
LA11	Loma Prieta, 1989, Gilroy	7	12	1.79	2000	0.02	39.98	652.49
LA12	Loma Prieta, 1989, Gilroy	7	12	1.79	2000	0.02	39.98	950.93
LA13	Northridge, 1994, Newhall	6.7	6.7	1.03	3000	0.02	59.98	664.93
LA14	Northridge, 1994, Newhall	6.7	6.7	1.03	3000	0.02	59.98	644.49
LA15	Northridge, 1994, Rinaldi RS	6.7	7.5	0.79	2990	0.005	14.945	523.3
LA16	Northridge, 1994, Rinaldi RS	6.7	7.5	0.79	2990	0.005	14.945	568.58
LA17	Northridge, 1994, Sylmar	6.7	6.4	0.99	3000	0.02	59.98	558.43
LA18	Northridge, 1994, Sylmar	6.7	6.4	0.99	3000	0.02	59.98	801.44
LA19	North Palm Springs, 1986	6	6.7	2.97	3000	0.02	59.98	999.43
LA20	North Palm Springs, 1986	6	6.7	2.97	3000	0.02	59.98	967.61

Table 7.1 SAC 10/50 Records

101

SAC Near Fault Records						
Record	Earthquake	M_w	R - km	Site	Station	Comments
Recorded Records						
NF21	1978 Tabas	7.4	1.2	D	Tabas	Iran
NF22	1989 Loma Prieta	7	3.5	D_1	Los Gatos	steep topography
NF23	1989 Loma Prieta	7	6.3	D_1	Lex. Dam	dam abutment
NF24	1992 C. Mendocino	7.1	8.5	D_1	Petrolia	steep topography
NF25	1992 Erzincan	6.7	2	D	Erzincan	Turkey
NF26	1992 Landers	7.3	1.1	D_1	Lucerne	thin alluvium
NF27	1994 Northridge	6.7	7.5	D	Rinaldi	over hard rock
NF28	1994 Northridge	6.7	6.4	D	Olive View	
NF29	1995 Kobe	6.9	3.4	D_1	Kobe JMA	thin alluvium
NF30	1995 Kobe	6.9	4.3	D	Takatori	fairly soft soil
Simulated Records						
NF31	Elysian Park 1	7.1	17.5	D_1		Simulation
NF32	Elysian Park 2	7.1	10.7	D_1		Simulation
NF33	Elysian Park 3	7.1	11.2	D_1		Simulation
NF34	Elysian Park 4	7.1	13.2	D_1		Simulation
NF35	Elysian Park 5	7.1	13.7	D_1		Simulation
NF36	Palos Verdes 1	7.1	1.5	D_1		Simulation
NF37	Palos Verdes 2	7.1	1.5	D_1		Simulation
NF38	Palos Verdes 3	7.1	1.5	D_1		Simulation
NF39	Palos Verdes 4	7.1	1.5	D_1		Simulation
NF40	Palos Verdes 5	7.1	1.5	D_1		Simulation
D = soil site; D_1 = rock converted to soil						

Table 7.2 SAC Near Fault Records

PEER Near Fault Records		
Earthquake Station	Rupture Dist (km)	Site
One Sided Displacement Pulses		
1940 Imperial Valley El Cent #9	8.3	Soil
1992 Landers Lucerne	1.1	Rock
1994 Northridge Sylmar	6.1	Soil
Two Sided Displacement Pulses		
1978 Tabas, Iran	3	Soil
1992 Erzinkan	2	Soil
1995 Kobe Takaka	-	-
Multiple Sided Displacement Pulses		
1989 Loma Prieta Los Gatos	6.1	Rock
1992 Landers Joshua Tree	11.6	Soil
1994 Northridge Rinaldi RS	7.1	Soil
1995 Kobe KJMA	0.6	Rock

Table 7.3 PEER Near Fault Records

[ ] = RESULTING MAX. PLASTIC ROTATIONS BASED ON LOS GATOS RECORD
{ } = RESULTING MAX. PLASTIC ROTATIONS BASED ON RINALDI RECORD
( ) = RESULTING MAX. PLASTIC ROTATIONS BASED ON TAKATORI RECORD
< > = RESULTING MAX. PLASTIC ROTATIONS BASED ON JAMES ROAD RECORD

THREE STORY BUILDING - REVISED SIZES

Figure 7.23 Three Story Building Plastic Rotations from PEER Records

103

Figure 7.24 Twenty Story Building Plastic Rotations from PEER Records

were eventually strengthened with the energy procedure. However, the resulting plastic rotations in the beams were still in the range of .030 to .040 radians which is considered excessive as shown in Figure 7.26. Plastic rotations were successfully kept out of the columns. While the design procedure has not produced satisfactory plastic rotations for the twenty story building when subjected to a Near Fault record, the documentation of this iterative redistribution of energy is considered valuable. Possibly an iterative procedure such as has been undertaken here is required for a tall building. It is acknowledged taller buildings do require more extensive analysis. Also, it is possible that a multiple of the envelope of the final maximum energies for all iterations as shown in Figure 7.25 could be used as a distribution for design.

A final check of the iterative procedure for the twenty story building is to confirm the assumed strain hardening factor in the beams as described by Anderson and Gupta. In their paper, the increase on the column moment was suggested to be the inverse of $(1 - p\mu_G)$, where p is the ratio of the stain hardening modulus to the elastic modulus and μ_G is design girder rotational ductility. These values are assumed to be .030 for the strain hardening and the girder rotational ductility taken as 7 in the paper and were used here. The expression above calculates to be .79 or an increase in the required column moment of 1/.79 or 1.26. Considering an approximate expression given for the yield rotation for a beam member given in

FEMA 273 (FEMA-273 1997), $\theta_y = \dfrac{ZF_{ye}l_b}{6EI_b}$; where Z is the beam plastic section

modulus, F_{ye} is the expected yield stress, l_b is the beam length, E is the modulus of elasticity and I_b is moment of inertia of the beam. For the typical beam size of W36x150, θ_y was calculated to be .0044 radians. For the maximum plastic rotation in Figure 7.26 of .041 radians, the rotational ductility factor calculates to a figure of approximately 9. This compares favorably with the initial assumed value.

20 Story Building
Hysteretic Energy vs. Height
Iterative Results Using Record NF039
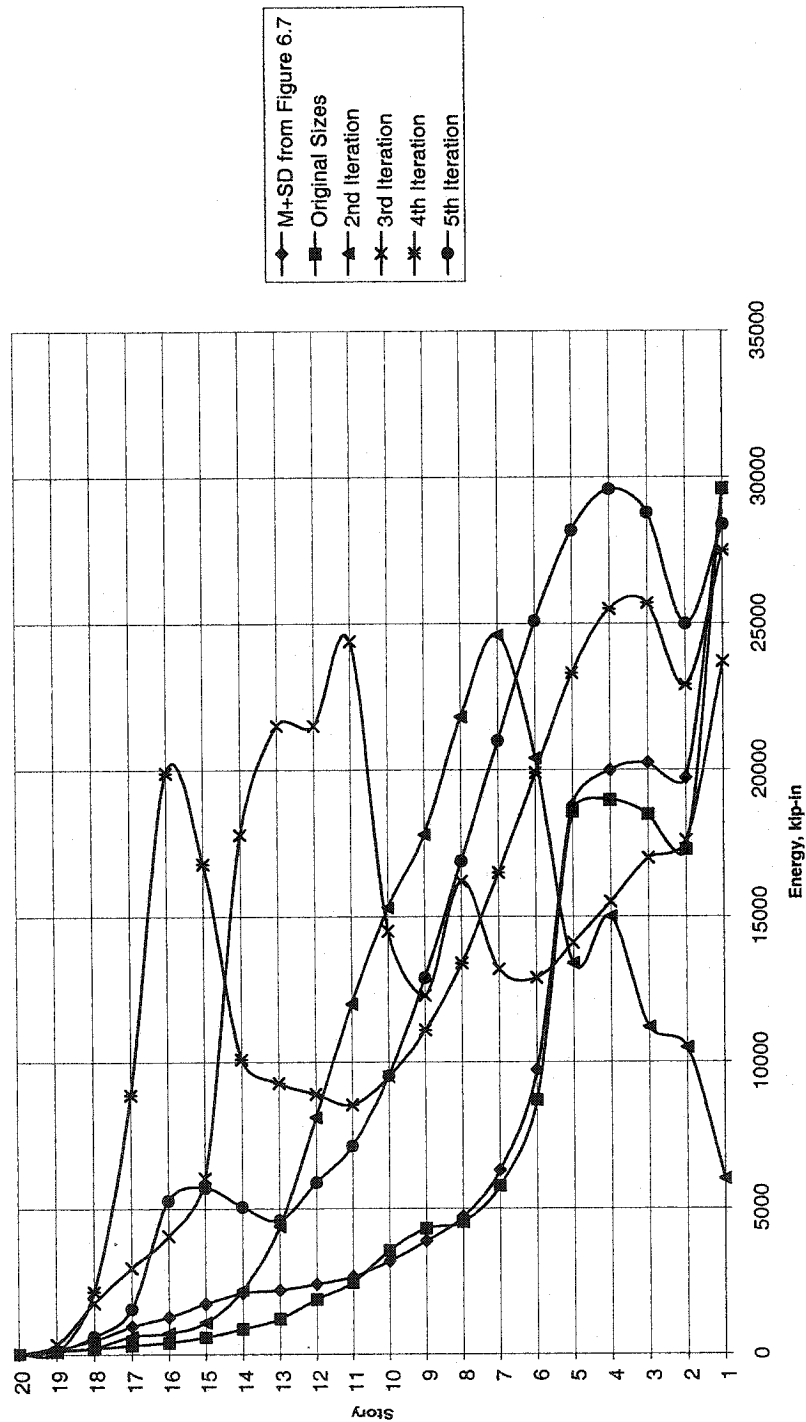
Figure 7.25 Twenty Story Building Energy Distribution from Successive Design Iterations

107

TYPICAL CORNER COLUMN

TYPICAL COLUMN UNO

[-]	Beam (W21x50)	Corner Column	Dimension
[.010]	W24x62	W24x84	15"[]x.5"
[.023]	W27x84	W24x84	15"[]x.5"
[.034]	W27x84	W24x117	15"[]x.75"
[.020]	W36x150	W24x117	15"[]x.75"
[.018]	W36x150	W36x527	15"[]x.75"
[.017]	W36x150	W36x527	24"[]x2"
[.017]	W36x150	W36x527	24"[]x2"
[.018]	W36x150	W36x527	24"[]x2"
[.016]	W36x150	W36x527	24"[]x2"
[.025]	W36x150	W36x527	24"[]x2"
[.029]	W36x150	W36x527	24"[]x2"
[.033]	W36x150	W36x527	24"[]x2"
[.036]	W36x150	W36x527	24"[]x2"
[.040]	W36x150	W36x527	24"[]x2"
[.041]	W36x150	W36x527	24"[]x2"
[.040]	W36x150	W36x527	24"[]x2"
[.036]	W36x150	W36x527	24"[]x2"
[.031]	W36x150	W36x527	24"[]x2"
[-]	W36x150	W36x527	24"[]x2"
	W30x99	W36x527	24"[]x2"
	W21X44	W36x527	
		W36x527	

[] = RESULTING MAX. PLASTIC ROTATIONS
BASED ON RECORD NF039
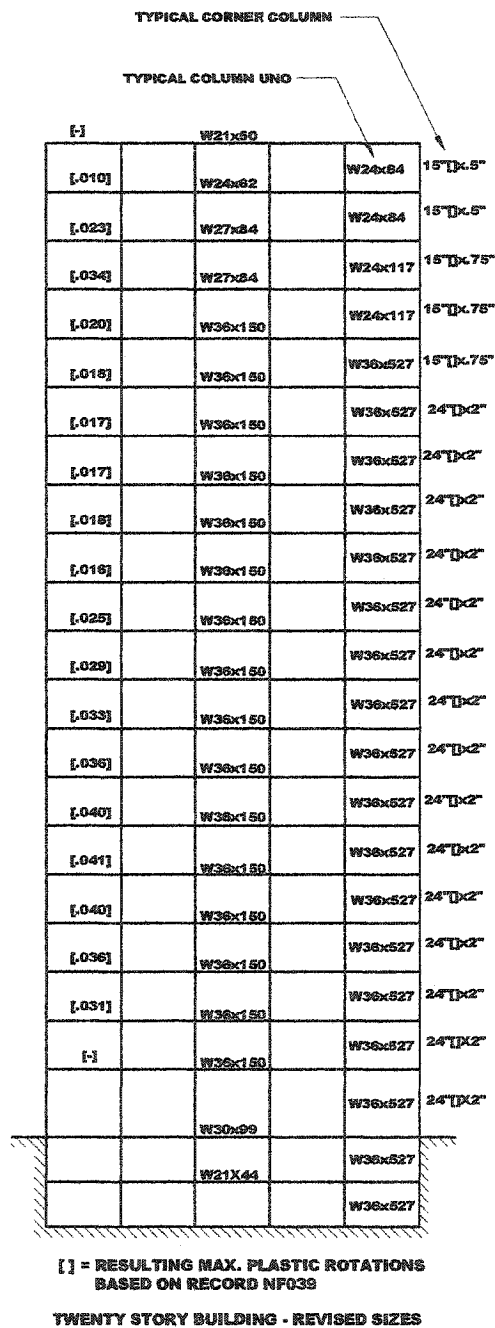
TWENTY STORY BUILDING - REVISED SIZES

**Figure 7.26 Twenty Story Building Sizes After Successive Design Iterations**

108

Chapter 8: The Use of Energy Demand Based on a Single Degree of Freedom System

The procedure outlined and demonstrated in this paper has used as the energy demand for the building frames a mean or mean plus one standard deviation from multiple nonlinear time history analyses of prototype buildings. As has been alluded to earlier in this work, it may be desirable to make use of energy spectra to derive the energy demand for any given building frame. In order to study the effect of the hysteretic energy of a multidegree of freedom (MDOF) system versus the hysteretic energy of a single degree of freedom (SDOF) system, generalized properties for each of the three SAC buildings were calculated using the first mode shape and the fundamental frequency from the DRAIN 2D+ analyses. These properties were input into the program NONLIN (Charney, 1996) which can perform some sophisticated analyses on SDOF systems. An inelastic analysis was performed on each equivalent SDOF building frame subjected to the same 10/50 earthquake records. The normalized hysteretic energy (energy/mass) from the SDOF analyses were then compared with the corresponding normalized hysteretic energies from the DRAIN 2D+ runs for each record. Results of this analysis are shown in Figures 8.1 and 8.2. An equal energy line is shown plus a "trendline" that shows the *linear* least squares fit of the data. For the three story building, the average MDOF normalized energy is approximately a constant 85% of the generalized SDOF normalized energy. The nine story building begins to show scatter in the data. The MDOF normalized hysteretic energy was still an average of 85% of the SDOF normalized energy. The

109

twenty story building indicated a general increase in this energy ratio. The MDOF normalized hysteretic energy averaged 105% of the SDOF energy. So it seems as a general trend that an estimate of hysteretic energy based on a SDOF system is a fair estimate for a MDOF system for the same period structure. Early researchers such as Housner (Housner, 1956) and Akiyama (Akiyama, 1985) made this same assertion. Uang and Bertero demonstrated the validity of this hypothesis generally by shake table test (Uang and Bertero,1988). It is believed that the results shown in the referenced figures demonstrate in a rigorous way that the energy from SDOF energy spectra can be used as the demand for a MDOF system.

3 Story Building
MDOF vs SDOF Hystertic Energy
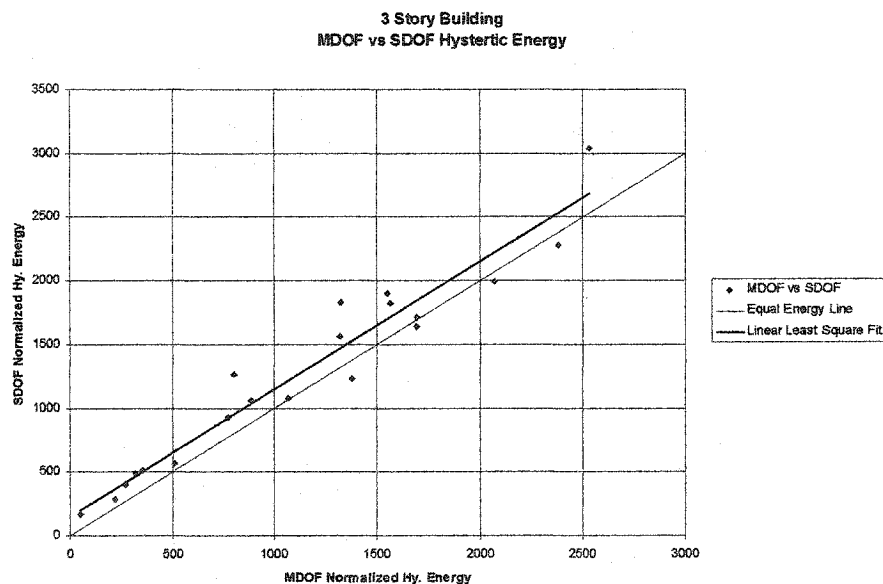
Figure 8.1 Three Story Building MDOF vs. SDOF Energies

110

9 Story Building
MDOF vs SDOF Hysteretic Energy

20 Story Building
MDOF vs. SDOF Hysteretic Energy
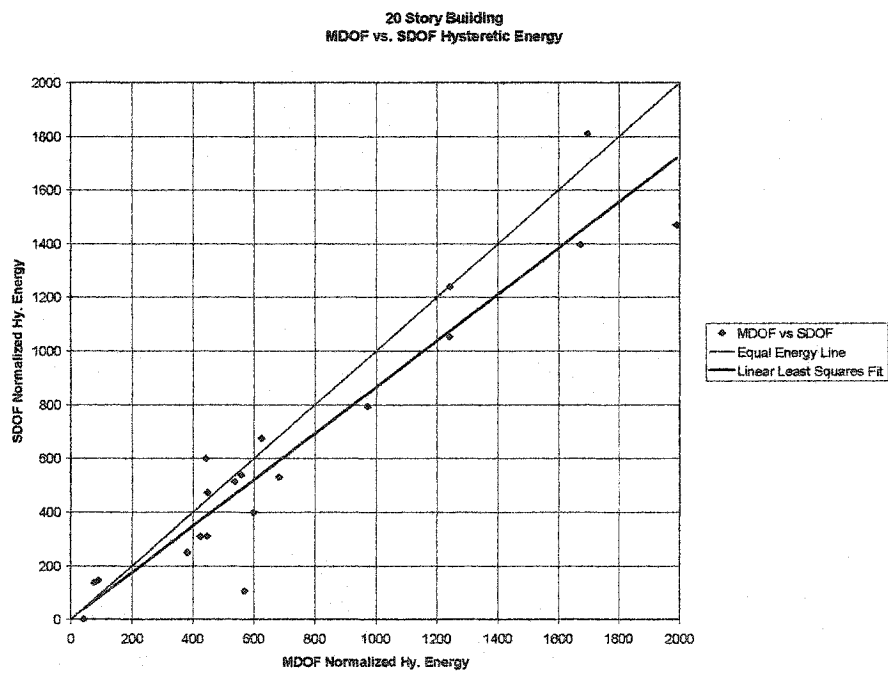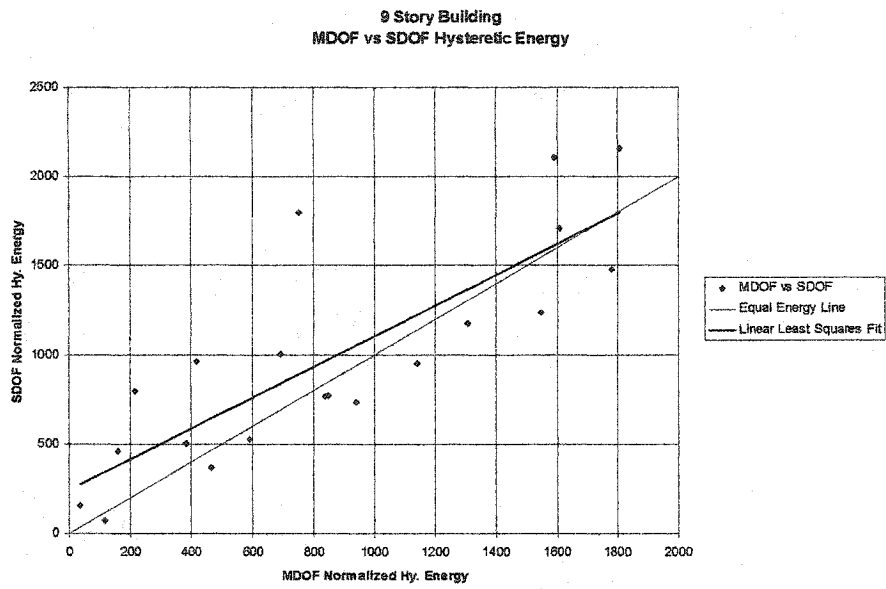
Figure 8.2 Nine and Twenty Story Buildings MDOF vs. SDOF Energies

111

As part of this analysis, a sample of energy spectra from those developed by Naiem and Anderson (Naiem and Anderson 1996) were examined. Shown in Table 8.1 is a comparison of hysteretic energy from various energy spectra for selected earthquake records. The normalized energy is read from the spectra using the fundamental period of each building. The total hysteretic energy is found by multiplying the normalized value by the mass that is tributary to each frame. It appears that the energy from the SAC mean plus standard deviation (M+SD) shown in the table generally is greater than the records shown. There is no comment regarding the level of risk or recurrence interval of the listed records. Clearly, one could establish the risk for each record to compare the energy level with the derived M+SD values from the SAC records. However, one could conclude that the energy from the spectra is definitely on the order of magnitude of the SAC records. The only exception is the well known Mexico City record, which is known to possess an extreme amount of energy due to its long duration.

Comparison of Calculated Hysteretic Energies vs. Energy Spectra			
Reference: Classification and Evaluation of Earthquake Records for Design by Naeim and Anderson (2000)			
Records are given in terms of yield coefficient, C_y, and Normalized Hysteretic Energy, E_h/m.			
Hysteretic Energy is obtained by E/m * mass			

Three Story Building T=1.10 sec; Use C_y = .10 (p. 122)
Total Building Mass (for one frame) = 8.42 kip-sec^2/in

Record	E_h/m	Total HE	
Mean + SD (SAC 10/50)	-	16030	k-in
1940 El Centro - COA**	500	4210	
1952 Taft - FOA	125	1052.5	
1966 Parkfield - 20A	750	6315	
1971 San Fernando - DOA	1200	10104	
1979 Imperial Valley - TAA	1500	12630	
1985 Mexico - T1B	4200	35364	
1989 Loma Prieta - 000	1200	10104	
1992 Landers - 000	800	6736	

Nine Story Building T = 2.19 sec; Use C_y = .05
Total Building Mass (for one frame) = 25.72

Record	E_h/m	Total HE	
Mean + SD (SAC 10/50)	-	38083	k-in
1940 El Centro - COA	290	7458.8	
1952 Taft - FOA	0	0	
1966 Parkfield - 20A	350	9002	
1971 San Fernando - DOA	700	18004	
1979 Imperial Valley - TAA	750	19290	
1985 Mexico - T1B	2300	59156	
1989 Loma Prieta - 000	250	6430	
1992 Landers - 000	600	15432	

Twenty Story Building T = 3.78 sec; Use C_y = .05
Total Building Mass (for one frame) = 31.60

Record	E_h/m	Total HE	
Mean + SD (SAC 10/50)	-	36900	k-in
1940 El Centro - COA	0	0	
1952 Taft - FOA	0	0	
1966 Parkfield - 20A	100	3160	
1971 San Fernando - DOA	500	15800	
1979 Imperial Valley - TAA	200	6320	
1985 Mexico - T1B	1000	31600	
1989 Loma Prieta - 000	0	0	
1992 Landers - 000	200	6320	

** Refers to identification designation in Naeim and Anderson (1993)

Table 8.1 Comparison of Derived Hysteretic Energies vs. Energy Spectra

113

Chapter 9: Conclusions and Recommendations

9.1 Conclusions

Based on the results of this study, the following conclusions are suggested:

1. For a multistory building, a story by story optimization procedure can be used to optimize an entire frame.

2. The internal work for a plastic mechanism can be set equal to a story hysteretic energy demand. It has been demonstrated that by limiting the plastic rotations, the member plastic capacities in a moment frame can be determined using an energy based procedure.

3. A minimum weight procedure has been developed using the Simplex method to optimize beam and column sizes. An interactive subroutine using Microsoft Excel has been developed to facilitate this process.

4. A design example using a two story moment frame building was demonstrated. The building frame was designed for the UBC and modified for the energy demands of a record from the Northridge earthquake, in addition to SAC 10/50 and Near Fault records.

5. Conducting inelastic time history analyses with DRAIN 2D+ for representative steel building frames and earthquake records, it is possible to study the distribution of derived hysteretic energy versus height. For building frames designed for the Los Angeles area the hysteretic energy is

114

not linearly decreasing with height for a tall building frame. The shape of the energy curve is variable and not necessarily a maximum at the base.

6. Various earthquake records were studied in this work. The primary records were scaled to provide a 10% probability of exceedance in 50 years. The effects of Near Fault records were also studied. There was large variability in the hysteretic energy demand for the various records with the pulse type earthquakes having the maximum hysteretic energy demand. The coefficient of variation in the Near Fault records was 33% higher than that for the SAC 10/50 records.

7. The hysteretic energies developed from the suite of Near Fault records for three, nine, and twenty story frames are approximately five times larger than those developed from the 10/50 records. This is 2 ½ to 3 times larger than the near source factors currently contained in the 1997 Uniform Building Code. Given the variability of these records, it is all the more difficult to capture their full effect with the Near Fault code factors.

8. The energy based design procedure was demonstrated on the representative buildings for the 10/50 and Near Fault SAC records using the energy distribution with height developed earlier. A distribution of energy for design that applied an equal amount of energy per story was found to produce the most consistent results.

115

9. In the procedure for storywise optimization, the actual column moment demand from the energy procedure was used as an external load to the story below. The actual member column plastic moment capacity be used. It was found that this can induce excessive amounts of energy demand that are, in fact, not present when checking an as-designed frame. For a design procedure check, it is recommended to use the actual column energy demand moment.

10. The proposed energy design procedure adequately checked the sizes for a twenty story building for the SAC 10/50 records. The Near Fault records proved to be more elusive. It appears that for a tall, flexible building frame the sizes are limited by drift and P-Δ effects. Designing tall buildings to the Near Fault records is a suggested area of future study. The Near Fault energy redistribution over several design iterations was studied and documented.

11. The normalized hysteretic energy for a Generalized Single Degree of Freedom system appears to be a good estimate of the energy demand for a Multi Degree of Freedom System, which is consistent with the observations of previous researchers such as Housner, Akiyama, Kato, Uang and Bertero. It therefore appears reasonable to use the hysteretic energy spectra as the hysteretic energy demand for a multistory building with the same fundamental period. This energy at the base can be distributed over the height of the building for design purposes.

116

9.2 Recommendations

1. The target plastic rotations are an area of ongoing research by FEMA. The proposed energy design procedure could be modified to incorporate this work.

2. There is a high degree of variability in the SAC Near Fault records. Their development and use for design is recommended for further study.

3. It is important as more researchers develop energy spectra to evaluate their applicability to the design procedure demonstrated in this paper. Energy spectra could be classified by specified level of risk and incorporated into performance based design methodologies, including the proposed energy design procedure contained in this work.

4. It is recommended that the Near Fault factors used in current building codes be reexamined. The increase in hysteretic energy for the Near Fault earthquake records versus the SAC 10/50 records is dramatic and may merit an increase in the code Near Fault factors.

5. The design of tall, flexible buildings subject to Near Fault records is a suggested area of future research.

References

Akiyama, Hiroshi (1985), Earthquake-Resistant Limit-State Design for Buildings, University of Tokyo Press.

Akiyama, H. and Kato B. (1982), Seismic Design of Steel Buildings, ASCE Journal of the Structural Division, Vol 108, No. ST8, pp. 1709-1721, Raston, Virginia.

Allahabadi, R. (1987), Drain-2DX, Seismic Response and Damage Assessment for 2D Structures, Ph.D. dissertation for U. C. Berkeley.

American Institute of Steel Construction (AISC 1997), LRFD Manual of Steel Construction, 2nd Edition.

American Society of Civil Engineers (1971), Plastic Design in Steel: A Guide and Commentary – 2nd Edition," ASCE Manuals and Reports on Engineering Practice No. 41.

Anderson, James C. and Bertero, Victelmo V. (1987), Uncertainties in Establishing Design Earthquakes, ASCE Journal of Structural Engineering, Vol 113, No. 8, August.

Anderson, James C. and Gupta, Raj P. (1972), Earthquake Resistant Design of Unbraced Frames, ASCE Journal of Structural Engineering, Vol. 98, No. ST11, November.

Anderson, Johnston, Partridge (1995), Post Earthquake studies of a Damaged Low Rise Office Building, University of Southern California Report CE 95-07, December.

Applied Technology Council (1996), ATC-40, Seismic Evaluation and Retrofit of Concrete Buildings.

Arya, Anand S. (1974), Inelastic and Reserve Energy Analysis of Multistory Buildings, Proceedings of the Fifth World Conference on Earthquake Engineering.

Baker and Heyman (1969, 1971), Plastic Design of Frames – Parts I and II, Cambridge University Press.

Beedle, Lynn and Galambos, T. V. (1969), Plastic Design of Steel Frames, Structural Engineering Handbook edited by Gaylord and Gaylord, McGraw-Hill.

118

Benioff, Hugo (1934), The Physical Destructiveness of Earthquakes, The Bulletin of the Seismological Society of America.

Berg, G. V. and Thomaides, S. S. (1960), Energy Consumption by Structures in Strong-Motion Earthquakes, The 2nd U.S. Conference on Earthquake Engineering.

Biot, M. A. (1940), A Mechanical Analyzer for the Prediction of Earthquake Stresses, The Bulletin of the Seismological Society of America.

Blume, John (1960), A Reserve Energy Technique for the Earthquake Design and Rating of Structures in the Inelastic Range, Proceedings of the Second World Conference on Earthquake Engineering, 1960.

Charney, F.A. (1996), NONLIN, Version 5.2, Nonlinear Dynamic Time History Analysis of Single Degree of Freedom Systems, Advanced Structural Concepts, Golden, Colorado, July.

Chou, Chung-Che and Uang, Chia-Ming (2002), Evaluation of Site-Specific Energy Demand for Building Structures, Proceedings of the 7th U.S. Conference on Earthquake Engineering, July.

Computers and Structures, Inc., ETABS – Three Dimensional Analysis of Building Systems, Version 6.21.

Earthquake Engineering Research Institute (1997), Connections – EERI Oral History Series – George Housner.

El Hafez, M. Bassam and Powell, Graham (1974), Preliminary Plastic Design of Tall Steel Frames, ASCE Journal of Structural Engineering, Vol 100, No. ST9, September 1974.

Emkin, Leroy and Litle, William (1970), Plastic Design of Multistory Steel Frames by Computer, ASCE Journal of Structural Engineering, Vol. 96, No. ST11, November.

Fajfar and Krawinkler (1992), Nonlinear Seismic Analysis and Design of Reinforced Concrete Buildings, Elsevier Applied Science.

Federal Emergency Management Agency (1997), FEMA-273 and 274, NEHRP Guidelines for the Seismic Rehabilitation of Buildings and Commentary, October.

FEMA (1997), Interim Guidelines Advisory No. 1, FEMA 267A, March.

119

Foulkes, J. (1953), Minimum Weight Design and the Theory of Plastic Collapse, Quarterly Applied Mathematics, Vol 10, p. 347.

Gerlein, Mauricio and Beaufait, Fred (1979), An Optimum Preliminary Strength Design of Reinforced Concrete Frames, Computers and Structures, Vol. 11, pp. 515-524.

Gluck, J (1974), An Energy Dissipation Factor as Structural Design Criterion for Strong Earthquake Motion, Proceedings of the Fifth World Conference on Earthquake Engineering.

Goel, S. and Leelataviwat, S. (1998), Seismic Design by Plastic Method, Engineering Structures, 20(4-6), 465-471.

Gupta, Akshay and Krawinkler, Helmut (2002), "Relating the Seismic Drift Demands of SMRFs to Element Deformation Demands", AISC Engineering Journal, Second Quarter.

Horne, M. R. and L. J. Morris (1982), Plastic Design of Low-Rise Frames, MIT Press, Cambridge.

Housner, George (1956), Limit Design of Structures to Resist Earthquakes, Proceedings of the First World Conference on Earthquake Engineering.

Housner, G. W. (1960), The Plastic Failure of Frames During Earthquakes, The 2nd U.S. Conference on Earthquake Engineering.

International Conference of Building Officials (1997), The 1997 Uniform Building Code.

Krawinkler, H. (2000), "New Recommended Seismic Design Criteria for Steel Moment Frame Buildings", SAC Seminar notes, September.

Leelataviwat, S., Goel, S., and Stojadinovic, B.(1999), Towards Performance Based Seismic Design of Structures, Earthquake Spectra, Volume 15, No. 3, August.

Leelataviwat, Sutat, Goel, Subhash, and Stojadinovic, Bozidar (2002), Energy-based Seismic Design of Structures using Yield Mechanism and Target Drift, ASCE Journal of Structural Engineering, August.

Leger, Pierre and Dussault, Serge (1992), Seismic-Energy Dissipation in MDOF Structures, ASCE Journal of Structural Engineering, Vol. 118, No. 5, May.

120

Mazzolani, F. and Piluso, V. (1997), Plastic Design of Seismic Resistant Steel Frames, Earthquake Engineering and Structural Dynamics, Vol. 26, 167-191.

Mazzolani, F.M. editor (2000), Moment Resistant Connections of Steel Frames in Seismic Areas, Chapter 8.2, Routledge mot E F & N Spon.

McKevitt, W. E. et al (1979), Towards a Simple Energy Method for Seismic Design for Buildings, Proceedings of the Second U.S. Conference on Earthquake Engineering.

Naeim, F. and Anderson, J. (1993), Classification and Evaluation of Earthquake Records for Design, The 1993 NEHRP Professional Fellowship Report, July.

RAM Xlinea, Version 3.0, Ram International

Riddell, R. and Garcia, J.E. (2002), Hysteretic Energy Spectrum and Earthquake Damage, Proceedings of the 7th U.S. Conference on Earthquake Engineering, July.

Ridha, R. and Wright, M (1967), Minimum Cost Design of Frames, ASCE Journal of the Structural Division, Vol. 93, August.

Rubenstein, Moshe and Karagozian, John (1966), Building Design Using Linear Programming, ASCE Journal of the Structural Division, Vol. 92, No. ST6, December.

SAC (1998), Update No 3, SAC Steel Project, April.

Salidi, Mehdi and Sozen, Mete (1981), Simple Nonlinear Seismic Analysis of R/C Structures, ASCE Journal of Structural Engineering, Vol 107, No. ST5, May.

Salmon, C. and Johnson, J., Steel Structures – Design and Behavior, Intext Educational Publishers.

Somerville, P., Smith, H., Puriyamurthala, S., Sun, J., (1997), "Development of Ground Motion Time Histories for Phase 2 of the FEMA/SAC Steel Project," SAC Joint Venture, SAC/BD-97/04, October.

Soni, R. Y. et al (1977), Energy Approach to Earthquake Resistant Design, Proceedings of the Sixth World Conference on Earthquake Engineering.

Structural Engineers Association of California (1999), Recommended Lateral Force Requirements and Commentary, 1999 Seventh Edition.

Tsai, K. C. and Li, J. (1994), Drain2D+ and View2D, Version 1.14, National Taiwan University, November.

Uang and Bertero (1988), Implications of Recorded Earthquake Ground Motions on Seismic Design of Building Structures, EERC Report No. UCB/EERC-88/13, November.

Uang and Bertero (1988), Use of Energy as a Design Criterion in Earthquake-resistant Design, EERC Report No. UCB/EERC-88/18, November.

White, D. and Chen, W. (1993), Plastic Hinge Based Methods for Advanced Analysis and Design of Steel Frames, Structural Stability Research Council, March.

Ziemian, R. D., McGuire, W., and Deierlein, G. (1992), Inelastic Limit States Design, Part I: Planer Frame Studies, ASCE Journal of Structural Engineering, Vol. 118, No. 9, September.